Biological Functions of Cytochrome P450 1A1 in the
Proliferation and Survival of Breast Cancer Cells

A DISSERTATION
SUBMITTED TO THE FACULTY OF
UNIVERSITY OF MINNESOTA
BY

Mariangellys Rodríguez Pantoja

IN PARTIAL FULFILLMENT OF THE REQUIREMENTS
FOR THE DEGREE OF
DOCTOR OF PHILOSOPHY

David A. Potter, M.D., Ph.D., Adviser

April 2013

ACKNOWLEDGEMENTS

My successes and my doctorate would not be possible without my mentor, David. I thank my adviser for being caring, supportive, and patient throughout my training. To past and current lab members, especially Monica, Ranjana, Zhijun, and Jill, who made the time spent in the lab so much better. Thank you all for helping me brainstorm about my research and troubleshoot countless experiments. I am also thankful to my thesis committee Jim, Carol, Kaylee, and David for their support and critical advice on my research. To my MICaB fellow students, thank you for your empathy and for reminding me that I am only human. Finally, thanks to all our collaborators for their expert advice, providing reagents and protocol, and sharing unpublished results for the advancement of our research. Their specific contributions are acknowledged throughout this dissertation.

DEDICATION

To my heavenly Father for the privilege of my education and

for surrounding me with caring family and friends.

ABSTRACT

Cytochrome P450 1A1 (CYP1A1) is an extrahepatic phase I metabolizing enzyme whose expression is suppressed under physiologic conditions, but can be induced by substrates via the aryl hydrocarbon receptor (AhR). Nonetheless, recent studies show that the majority of breast tumors constitutively express CYP1A1. These findings led us to test the hypothesis that CYP1A1 promotes breast cancer progression by evaluating the effects of CYP1A1 knockdown on the proliferation and survival of the MCF7 and MDA-MB-231 lines. Independent of estrogen receptor status, CYP1A1 knockdown decreases cell proliferation, decreases colony formation, blocks the cell cycle at G0/G1 associated with reduction of cyclin D1, and increases apoptosis associated with reduction of survivin. CYP1A1knockdown markedly increases phosphorylation of AMP-activated protein kinase (AMPK) and decreases phosphorylation of AKT, extracellular signal-regulated kinases (ERK)-1 and 2, and 70 kDa ribosomal protein S6 kinase (P70S6K). AMPK inhibition by compound C partially abrogates the proapoptotic effects of CYP1A1siRNA, suggesting that CYP1A1siRNA effects are mediated, in part, through AMPK signaling. Consistent with CYP1A1 knockdown results, pharmacologic reduction of CYP1A1 levels by the phytopolyphenol carnosol also correlates with impaired proliferation and induced AMPK phosphorylation. These results indicate that reduction of basal CYP1A1 expression is critical for inhibition of proliferation, which is neither affected by alpha-naphthoflavone–mediated inhibition of CYP1A1 activity nor modulated by AhR silencing. Growth complementation experiments were performed to identify the

exact mechanism by which CYP1A1 regulates these signaling pathways. Our results show that CYP1A1 regulates cell signal transduction through mechanisms other than synthesis of 8,9- epoxyeicosatrienoic acid, 11,12- epoxyeicosatrienoic acid, 14,15-epoxyeicosatrienoic acid, 20-hydroxyeicosatetraenoic acid, and 17,18-epoxyeicosatetraenoic acid or metabolism of all-*trans*-retinoic acid, 9-*cis* retinoic acid, 13-*cis* retinoic acid and pregnenolone. These studies support that CYP1A1 may promote breast cancer proliferation and survival, at least in part, through AMPK signaling and that reduction of CYP1A1 levels is a potential strategy for breast cancer therapeutics.

TABLE OF CONTENTS

LIST OF TABLES

LIST OF FIGURES

CHAPTER I

Introduction

PURPOSE AND RATIONALE

The body of evidence summarized in this chapter implicates cytochrome P450s (CYPs) in the biology and etiology of cancer. Nonetheless, little is known about the roles and mechanisms by which different CYPs may participate in cancer. Recent studies provide evidence that cytochrome P450 1A1 (CYP1A1) is expressed to various degrees in breast tumors and may be associated with breast cancer biology. However, whether CYP1A1 plays a biological role in breast cancer has not been determined. The **goal** of this dissertation is: (a) to determine whether CYP1A1 is important for breast cancer cells, (b) to determine the functional roles of CYP1A1 in breast cancer biology, and (c) to determine the mechanisms by which CYP1A1 promotes breast cancer progression. Toward this goal we tested the **hypothesis** that CYP1A1 promotes the proliferation and survival of breast cancer cells, in part, through signal transduction mechanisms. The studies performed to test this hypothesis are discussed in Chapter III and Chapter IV.

In this chapter we provide a literature review of our current state of knowledge as it pertains to this dissertation. This chapter is divided into three main sections:

(a) Breast Cancer- we provide an overview of the disease, current therapeutic strategies, and *in vitro* models used in these studies.

(b) Cytochrome P450 family- we discuss the overall structure and biochemistry of CYPs, their clinical relevance, and summarize known associations with cancer.

(c) Cytochrome P450 1A1- we discuss the structure and biochemistry of CYP1A1, mechanisms of transcriptional and post-transcriptional regulation, metabolic functions, polymorphic variants, and relevance of CYP1A1 in cancer etiology and progression.

BREAST CANCER

Breast cancer is a malignant tumor that arises from the uncontrolled proliferation of abnormal cells of the breast. Breast cancer may originate within the lobules, which are the milk production glands, or within the ducts that connect the lobules to the nipple. Of all localized breast cancers, 83% are of ductal origin (ductal carcinoma *in situ*), 11% are of lobular origin (lobular carcinoma *in situ*), and the remainder either share intermediate characteristics or are of unspecified origins (Fonseca et al. 1997). The incidence of new cases of invasive (metastatic) breast cancer is 4 times higher than localized breast cancer (226,870 invasive cases vs. 57,650 localized cases) (ACS 2012). The 5-year disease free survival is 99% for localized, 84% for regional and 23% for distant-metastatic breast cancer (Howlader N 2010). This statistics stress the need to improve and innovate current therapeutic strategies.

Current treatment strategies involve some form of surgery, radiation therapy, and systemic therapy alone or in combination. Systemic therapies include chemotherapy, hormone therapy (e.g. aromatase inhibitors or tamoxifen if estrogen receptor α positive), and targeted therapy (e.g. trastuzumab if Her2/neu positive). Targeted therapy has become increasingly recognized as the "ideal" therapeutic strategy because its specificity provides enhanced efficacy with (potentially) reduced adverse effects. The most successful strategy to date is the monoclonal antibody trastuzumab which targets the growth-promoting protein HER2/neu overproduced in 15-30% of breast cancers (Gennari et al. 2008). The need for additional targeted therapy is great and in these studies we evaluate CYP1A1 as a potential target for breast cancer therapeutics.

Breast cancers classification on the basis of expression of estrogen receptor alpha (ER), progesterone receptor (PR), and human epidermal growth factor receptor 2 (HER2) are important as they represent distinct biological and clinical outcomes. As previously mentioned, hormone therapy is the preferred treatment option for ERα+ and anti-HER2/new therapeutics is the preferred option for HER2+ breast cancers. However, triple-negative (ER-, PR-, HER2-) exhibit decreased survival and are therefore in great need for improved therapeutic strategies (Dunnwald et al. 2007; Onitilo et al. 2009). Moreover, while hormone therapy has proven successful in receptor positive tumors (ER+, PR+), patients that relapse often develop resistance to hormone therapy thus leaving these patients without efficacious treatment options (Dowsett et al. 2005). For the studies presented in this dissertation we chose to study ER+ and triple-negative breast cancers where the need for improved therapeutic strategies is greatest. Specifically, two *in vitro* models of breast cancer were used: estrogen-receptor positive MCF7 line (ERα+/PR+/HER2+) and triple-negative line MDA-MB-231 (ER-/PR-/HER2-).

CYTOCHROME P450 FAMILY

Structure and metabolism

Completion of the Human Genome Project in 2003 confirmed the presence of 57 functional cytochrome P450 genes and 58 pseudogenes (Nelson et al. 2004). The structural elements of cytochrome P450 (CYP) enzymes are highly conserved, especially those closer to the heme center. In contrast, the side chains, which control substrate specificity, vary substantially among CYPs. The center of these enzymes consists of an iron protoporphyrin IX center (i.e. heme b) coordinated to a cysteine thiolate. This structure is essential for the monooxygenation of a substrate through the redox catalytic cycle, illustrated in Figure I.1 (Ortiz de Montellano 2005). Briefly, the oxidation of heme iron(III) to a radical intermediate oxoiron(IV) results in a highly reactive complex of iron and molecular oxygen (O_2). One oxygen atom is protonated to form water and the other oxygen atom is transferred to the bound substrate. This redox cycle yields an oxygenated substrate that can be further processed by phase II metabolism and readily excreted from the body.
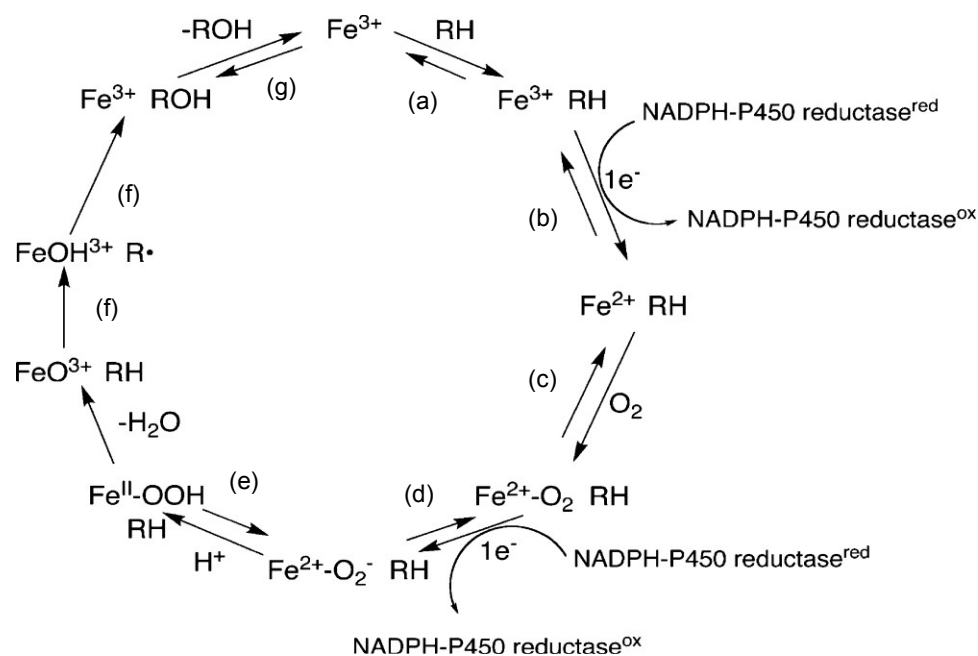
Figure I.1. Cytochrome P450 catalytic cycle.

(a) Binding of a substrate (R) to the active site generates a spin shift in the heme iron,

(b) an electron is transferred from NADPH to iron (III) via cytochrome P450 reductase

forming reduced iron (II), (c) molecular oxygen (O_2) binds to the heme iron and (d)

receives an electron from the cysteine ligand via the electron-transport system (e)

forming an unstable intermediate that is rapidly protonated to water, (f) the remaining

oxygen in the highly reactive oxoiron(IV) dissociates from the iron center and is

incorporated into a C-H bond of a substrate yielding an oxygenated substrate (R-OH)

and (g) the CYP enzyme returns to its original state with an iron(III) ready to perform

another catalytic cycle. Image modified and reprinted with permission from (Guengerich

2008); © 2008, American Chemical Society. Legend modified from (Ortiz de Montellano

2005) with kind permission from Springer Science+Business Media B. V.

Relevance of cytochrome P450 in clinical toxicity

Much attention is given to the study of CYP families 1-3 because of their pivotal role in xenobiotic metabolism. These CYP families mediate 70-80% of all phase I metabolism of the two hundred most prescribed drugs (Evans and Relling 1999; Ingelman-Sundberg 2004; Williams et al. 2004). The majority of this metabolism is catalyzed by CYP3A4/5/7 > CYP2C9 > CYP2C19 > CYP2D6 > CYP1A2 (Evans and Relling 1999; Williams et al. 2004). Therefore, it is not surprising that a common step during early drug development involves studying CYP induction and metabolism in order to predict the bioavailability of the drug candidate (Guengerich 2008). Additionally much effort has been allocated to understanding the different CYP expression patterns and polymorphism exhibited by individuals and populations because these differences not only impact drug bioavailability but also contribute to adverse drug effects (Guengerich 2008).

CYP1 family members (i.e. CYP1A1, CYP1A2, and CYP1B1) also play a significant role in the metabolic activation of procarcinogens. For this reason, pharmaceutical companies test the inducibility of CYP1 by the candidate drug (Sinz et al. 2008) and often regard the induction of CYP1 members as a liability; a viewpoint that has been argued against by (Nebert et al. 2004). Nonetheless, while CYP inducibility is associated with enhanced toxicity, it can also play an important role in the bioactivation of drugs for therapeutic purposes. Metabolism of a certain drug may yield a derivative with enhanced biological activity or an electrophilic drug metabolite that binds to and damages DNA thereby resulting in cancer cell death. Examples include the bioactivation

of tamoxifen to 4-hydroxy-tamoxifen catalyzed by CYP2D6 and the formation of benzothiazole electrophilic metabolites by CYP1A1 (Dehal and Kupfer 1997; Chua et al. 2000; Leong et al. 2003).

In summary, CYPs are largely involved in xenobiotic metabolism with important implications in drug bioavailability and bioactivation of pro-carcinogens and pro-drugs.

Relevance of cytochrome P450 in cancer

Cytochrome P450 enzymes constitute a large gene family thus exhibiting multiple and diverse metabolic impacts on cancer progression. Some cancer promoting effects mediated by CYPs are due to activation of carcinogens, while others involve the biosynthesis of growth promoting products. An example of the former is CYP1A1, which metabolizes polycyclic aromatic hydrocarbons, such as those present in cigarette smoke, to mutagenic products that are associated with increased bronchial carcinoma (Kellermann et al. 1973; Conney 1982; McLemore et al. 1989; McLemore et al. 1990). Examples of the latter includes, synthesis of estrogen by CYP19 (aromatase) promotes breast cancer progression and, similarly, synthesis of testosterone by CYP17 (17-lyase) promotes prostate cancer progression (Sikka et al. 1985; Trachtenberg and Zadra 1988; Sasano et al. 1996; Yue et al. 1998). Other CYPs such as CYP2J, CYP2C, and CYP3A synthesize eicosanoids that promote cancer progression (Jiang et al. 2005; Pozzi et al. 2010; Mitra et al. 2011).

Reports of CYP expression in the absence of xenobiotic induction have been reported for several types of cancer. CYP1A1 overexpression was found in 30 ovarian

8

tumor specimens (Leung et al. 2005). CYP1A and CYP3A were expressed in 60% of 50

oesophageal tumors while little or no expression was found in non-neoplastic

oesophageal epithelium (Murray et al. 1994). Analysis of a small sample (25 specimens)

of bladder cancer showed that CYP1A and CYP3A were expressed in 68% of tumors

while only in 1 of 5 non-neoplastic bladder tissues (Murray et al. 1995). A large study

(393 patients) by Hass et al. correlated CYP3A4/5 expression with breast cancer

metastasis to the lymph node (Haas et al. 2006). To date the most comprehensive study

of CYP expression correlating with breast cancer was published by (Murray et al. 2010).

This microarray study identified several CYPs expressed in the majority of breast tumors

(Protein, total % expression): CYP4X1 (100%), CYP2U1 (100%), CYP1A1 (90%),

CYP2E (90%), CYP2R1 (90%), CYP24 (90%), CYP38 (90%), CYP2C (80%), CYP2S1

(80%), CYP3A4 (80%), and CYP26A1 (80%). Of these, CYP4X1, CYP2S1 and CYP2U1

exhibited the highest expression levels in breast cancer. Additionally, CYP2U1, CYP4X1

and CYP4Z1 correlated with increased tumor grade and CYP2S1, CYP3A4 CYP4V2,

and CYP26A1correlated with decreased survival (Murray et al. 2010). Concurrent

studies found association of CYP26A1 expression with tumorigenesis and metastasis

(Osanai et al. 2010) and of CYP1A1expression with breast cancer progression (Vinothini

and Nagini 2010).

Together, these metabolism mechanisms and expression profiles implicate CYPs

in cancer. However, whether CYPs are directly involved in cancer etiology or

progression remains to be determined. Mechanistic studies that focus on understanding

the biological roles of specific CYPs are greatly needed. The focus of this thesis is to

characterize the functional roles of CYP1A1 in the biology of breast cancer.

CYTOCHROME P450 1A1

Gene structure

The human *CYP1A1* gene was sequenced for the first time in 1985 and since then it has been discovered to have seven exons and six introns spanning 5,995 base pairs (Jaiswal et al. 1985; Kawajiri et al. 1986; Corchero et al. 2001). Two negative regulatory elements, four enhancer sequences (i.e. xenobiotic regulatory elements) clustered in a stretch of about 500bp, and three protein-DNA binding G-rich domains located within the enhancer region have been identified (Hines et al. 1988; Boucher et al. 1993; Boucher et al. 1995; Kress et al. 1998). *CYP1A1* is located in chromosome 15q24.1 and shares a 23,306bp bidirectional 5' flanking promoter with *CYP1A2,* whose gene is oriented in opposite direction to CYP1A1 (Jaiswal et al. 1987). The overall gene structure, chromosomal localization, and common sites of polymorphisms are shown in Figure I.2.
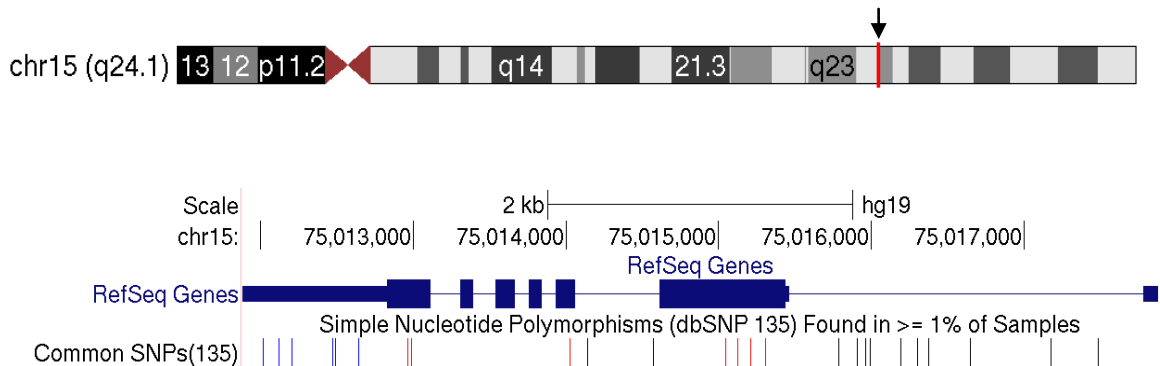
Figure I.2. Human CYP1A1 gene structure.

The position of human CYP1A1 in reference to chromosome 15 is highlighted in red (arrow). The structure of the CYP1A1 gene is shown: filled boxes indicate exons, the scale indicates specific position in chromosome 15, common single nucleotide polymorphisms (>1% of samples evaluated) are shown. Image generated through UCSC Genome, *http://genome.ucsc.edu* (Kent et al. 2002).

Protein structure

The human *CYP1A1* gene encodes a 512 amino acids protein which shares closest homology to CYP1A2 with 73% identity followed by CYP1B1 with 41% identity. A model of the 3D protein structure (PDB: 2hi4) of CYP1A1 is illustrated in **Figure I.3** and was generated utilizing CYP1A2 as template. Previous models and structural analyses of CYP1A1 with substrates 7-ethoxyresorufin and DF 203 docking in the active-site pocket of CYP1A1 are available (Lewis et al. 2007; Sangamwar et al. 2008). The most current model to date (PDB: 4i8V) was generated from the crystal structure of CYP1A1 bound to the inhibitor alpha-naphthoflavone (Walsh et al. 2013). These *in silico* structural analysis are important to identify potential pharmacologic inhibitors of this enzyme. The conserved heme b center surrounded by less conserved side chains important for substrate specificity can be appreciated.
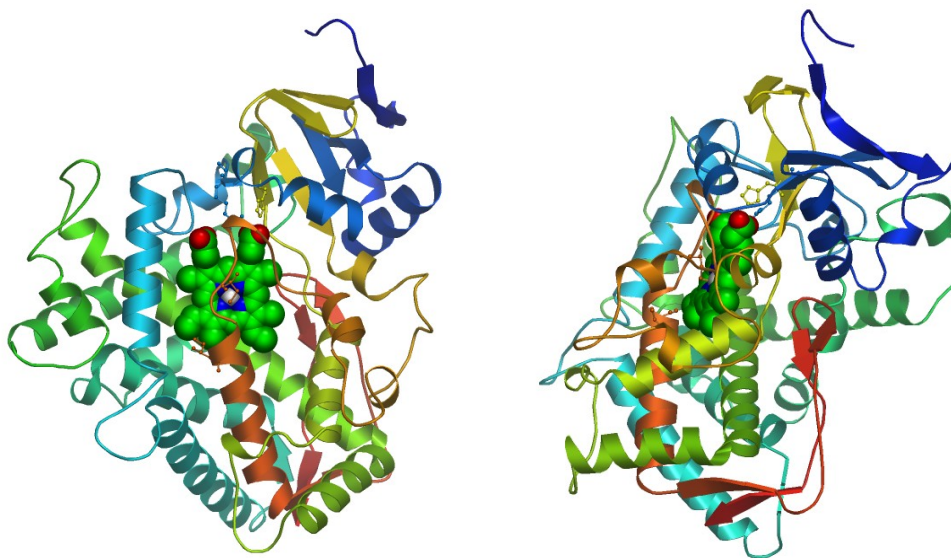
Figure I.3. CYP1A1 protein 3D structure model.

The structure model of CYP1A1 (residues 32-509) was generated by Swiss-Model

(Kopp and Schwede 2004; Kiefer et al. 2009) using the crystal structure of CYP1A2

[PDB ID: 2hi4] as template with root-mean-square deviation < 2Å. This structure was last

update by Swiss-Model on 09-12-2012.

Transcriptional, post-transcriptional, and post-translational regulation

In the absence of substrate, inactive aryl hydrocarbon receptor (AhR) remains in

the cytosol in a 280kDa complex that includes hsp90, hsp70, and ARA9/AP (Perdew and

Whitelaw 1991; Carver and Bradfield 1997; Ma and Whitlock 1997). In the presence of

substrate, the AhR complex translocates to the nucleus, dissociates from the 280kDa-

complex, and dimerizes with the AhR nuclear translocator protein (ARNT) (Pollenz et al. 1994). The AhR-ARNT dimer binds to the xenobiotic response element of *CYP1A1* (Shen and Whitlock 1992; Yao and Denison 1992; Lusska et al. 1993). In this manner the AhR-ARNT transcription factor increases the rate of transcription initiation and mRNA levels of *CYP1A1* (Gonzalez et al. 1984; Israel and Whitlock 1984; Fisher et al. 1989). In this manner CYP1A1 expression is said to be inducible and not constitutive. This increase in transcriptional rate of *CYP1A1* synthesis can occur in as early as 30min after exposure to substrate, and the induction response is substrate- and cell-type specific (Gonzalez et al. 1984; Israel and Whitlock 1984).

Another layer of regulation occurs at the post-transcriptional level (Silver and Krauter 1988; Xu et al. 1993). In contrast to other cytochrome P450s, CYP1A1 mRNA is short-lived exhibiting a half-life of 2.4 hours in the human hepatoma line HepG2 (Lekas et al. 2000). This rapid decay has been attributed to deadenylation of the poly (A) tail (Lekas et al. 2000). The molecular mechanisms and the significance of post-transcriptional regulation of CYP1A1 are still not fully understood, but in an effort to understand this mechanism, a recent study identified miR-892a as a negative post-transcriptional regulator of CYP1A1 (Choi et al. 2010).

Although CYP1A1 mRNA levels decline rapidly, the protein levels are sustained for at least 24 hours in the HepG2 line (Lekas et al. 2000). Similar transient mRNA induction accompanied by sustained protein stability has been observed in other inducible systems (Xu et al. 1993; Werlinder et al. 2001). This protein stability is achieved through post-translational regulation of CYP1A1 which involves protection from

13

degradation by substrate binding, but not by inhibition of lysosomal proteases (Werlinder et al. 2001).

Tissue-specific expression and subcellular localization

Human and murine studies show that in the absence of an inducer, only extrahepatic tissues may express low basal levels of CYP1A1. In contrast, both hepatic and extrahepatic tissues express CYP1A1 in the presence of an inducer (de Waziers et al. 1990; Ding and Kaminsky 2003; Galijatovic et al. 2004). The majority of CYP1A1 localizes to the endoplasmic reticulum (microsomal), the plasma membrane and the mitochondria (Niranjan et al. 1985; Raza and Avadhani 1988; Loeper et al. 1993). A 30-amino acid sequence in the NH2-terminal targets and anchors CYP1A1 to the endoplasmic reticulum and a 12-amino acid sequence in the COOH-terminal, exposed after proteolytic cleavage of the NH2-terminal, targets the enzyme to the mitochondria (Addya et al. 1997; Boopathi et al. 2008). Microsomal- and mitochondrial-CYP1A1 have distinct translation mechanisms and exhibit varying responses to xenobiotic exposure suggesting that distinct functional roles between these exist (Omura 2006; Dong et al. 2009). CYP1A1 has been observed in other subcellular compartments, including the nucleus, but whether this compartmentalization has any functional relevance remains unknown (Madra et al. 1996).

Substrates and mechanisms

Xenobiotics

CYP1A1 metabolizes several pro-carcinogens such as polycyclic aromatic hydrocarbons benzo[a]pyrene, 7,12-Dimethyl benzanthracene, the heterocyclic amine 2-Amino-1-methyl-6-phenylimidazo[4,5-b]pyridine, tobacco-related N-nitrosamines, as well as aflatoxin B1 (see **Table I.1**). These are ultimately metabolized to electrophilic compounds that bind to and consequently mutate DNA, thereby acting as potent carcinogens (Diamond et al. 1968; Gelboin 1969; Gelboin et al. 1969; Kinoshita and Gelboin 1972; Huberman et al. 1976; Soderkvist et al. 1983; Baertschi 1988; Kaderlik et al. 1994; Hammons et al. 1997; Fujita and Kamataki 2001).

While formation of DNA adducts by these metabolites exhibits detrimental effects, in the context of cancer cells this results in potent anti-cancer activity. For example, metabolism of the pro-drugs 2-(4-amino-3-methylphenyl)-5-fluorobenzothiazole and aminoflavone by CYP1A1 results in electrophilic species that bind to DNA and inhibit cancer growth (Kuffel et al. 2002; Hose et al. 2003; Leong et al. 2003). The natural phytochemical flavonoids eupatorin, cirsiliol, genistein, daidzein, and diosmetin, are CYP1A1 substrates that also exhibit anti-proliferative activity as shown in *in vitro* cancer models (Kupchan et al. 1965; Peterson and Barnes 1991; Ciolino et al. 1998; Androutsopoulos et al. 2009a). Most recently, the duocarmycin analogue chloromethylindoline (ICT2700) was shown to exhibit anti-tumor activity in *in vitro* bladder cancer model via CYP1A1-mediated bioactivation to seco-

chloromethylpyrroloindolone, which forms N^3-adenine covalent adduct with DNA (Pors et al. 2011; Sutherland et al. 2012).

Endobiotics

CYP1A1 catalyzes the 2-, 4- and to a lesser extent 16α-hydroxylation of the steroid hormone 17β-estradiol into 2-hydroxy-17β-estradiol, 4-hydroxy-17β-estradiol, and 16α-hydroxy-17β-estradiol, respectively (Badawi et al. 2001; Dawling et al. 2004). Although the effects of estrogen metabolism are not fully understood, it appears to correlate with increased risk of breast cancer (Lemon et al. 1992; Liehr and Ricci 1996).

Arachidonic acid (omega-6 fatty acid) and eicosapentaenoic acid (omega-3 fatty acid) have been shown to be metabolized by CYP1A1 forming a variety of eicosanoids including several epoxyeicosatrienoic acids and 17,18- epoxyeicosatetraenoic acid, as shown in **Table I.1** (Choudhary et al. 2004; Schwarz et al. 2004; Mitra et al. 2011; Panigrahy et al. 2012). Some epoxyeicosatrienoic acids have been shown to promote cancer, which implicates CYPs in cancer progression through eicosanoid mechanisms (Panigrahy et al. 2012).

Additionally, CYP1A1 catalyzes the oxidation of all-*trans*-retinoic acid, 9-*cis* retinoic acid, and 13-*cis* retinoic acid. While these exhibit anti-proliferative activity in breast cancer line MCF7, metabolism of retinoic acids is thought to abrogate their anti-tumor activity (Seewaldt et al. 1995; Van heusden et al. 1998).

CYP1A1 also catalyzes the 16α- and 17α- hydroxylation of pregnenolone to generate precursors of steroid hormones (Niwa et al. 1998). Breast tumors convert

pregnenolone to steroid hormones *in situ,* supporting the notion that tumors may rely on pregnenolone metabolism to maintain their supply of hormones (Abul-Hajj et al. 1979).

Little is known, however, in regards to the direct effects and biological relevance of CYP1A1-mediated metabolism of these endobiotic substrates in breast cancer. In **Chapter IV** we examine the roles of CYP1A1-mediated metabolism of eicosanoids, retinoic acids, and pregnenolone in the breast cancer line MCF7.

Substrate	Metabolite[1]	Effect	Reference
Benzo[a]pyrene	B[a]P-7,8-diol-9,10-epoxides	Carcinogenesis	(Gelboin et al. 1969; Huberman et al. 1976)
7,12-Dimethyl benzanthracene	7,12-DMBA-3,4-oxide-diol-1,2-epoxide	Carcinogenesis	(Diamond et al. 1968; Kinoshita and Gelboin 1972)
Aflatoxin B1	Aflatoxin B1-exo-8,9-epoxide	Carcinogenesis	(Soderkvist et al. 1983; Baertschi 1988)
2-Amino-1-methyl-6-phenylimidazo[4,5-b]pyridine	2-hydroxy-amino-2-Amino-1-methyl-6-phenylimidazo[4,5-b]pyridine[2]	Carcinogenesis	(Kaderlik et al. 1994; Hammons et al. 1997)
Tobacco N-nitrosamines	Multiple (see refs).	Carcinogenesis	(Fujita and Kamataki 2001)
2-(4-amino-3-methyl phenyl)-5-fluoro benzothiazole (NSC 703786)	Multiple (see (Chua et al. 1999))	Cancer growth inhibition	(Hose et al. 2003; Leong et al. 2003)
Aminoflavone (NSC 686288)	5-amino-2-(4-acetamido-3-fluorophenyl)-6,8-difluoro-7-methyl-4H-1-benzopyran-4-one	Cancer growth inhibition	(Kuffel et al. 2002)
Flavonoids	Multiple (see refs).	Cancer growth inhibition	(Kupchan et al. 1965; Peterson and Barnes 1991; Ciolino et al. 1998; Androutsopoulos et al. 2009a)
chloromethylpyrrolo-indoline	seco-chloromethylpyrroloindolone	Cancer growth inhibition	(Pors et al. 2011; Sutherland et al. 2012)
Estrogen	2-hydroxy-17β-estradiol 4-hydroxy-17β-estradiol 16α-hydroxy-17β-estradiol	↑ Cancer risk	(Badawi et al. 2001; Dawling et al. 2004)
Arachidonic acid	5,6-; 8,9-; 11,12-; and 14,15-epoxyeicosatrienoic acids 20-hydroxyeicosatetraenoic	Increased cancer growth	(Choudhary et al. 2004; Mitra et al. 2011; Panigrahy et al. 2012)
Eicosapentaenoic acid	17,18-epoxyeicosatetraenoic acid	Unknown	(Schwarz et al. 2004)
All-trans-retinoic acid 9-cis-retinoic acid 13-cis-retinoic acid	4-hydroxy-all-trans- retinoic acid, 4-hydroxy-9-cis-retinoic acid, 4-hydroxy-13-cis-retinoic acid	Increased cancer cell survival[?]	(Seewaldt et al. 1995; Van heusden et al. 1998)
Pregnenolone	16α-hydroxypregnenolone 17α-hydroxypregnenolone	Increased cancer cell growth[?]	(Abul-Hajj et al. 1979; Niwa et al. 1998)

Table I.1. Xenobiotic and endobiotic substrates of CYP1A1.

[1] The final metabolite is indicated, for brevity intermediate metabolites were omitted.

[2] The acetoxy and sulfonyloxy esters here are the ultimate carcinogenic metabolites catalyzed by N-acetyltransferase and sulfotransferase. [?]Proposed; no definitive evidence available.

Polymorphisms

We previously alluded to the idea that single nucleotide polymorphisms (SNPs) can affect the function of CYPs. For this reason, much effort has been made to discover CYP1A1 SNPs and to identify how these may affect its enzymatic function (**Table I.2** and (Landi et al. 1994; Bartsch et al. 2000)). Moreover, multiple studies have focused on determining associations between CYP1A1 SNPs and increased cancer incidence. For example, the A2455G allele has been implicated with increased breast cancer risk in Caucasian populations (Sergentanis and Economopoulos 2010). Nonetheless, lack of associations between SNPs and cancer have been reported and these discrepancies have been attributed to ethnic variations between populations, variation in sample size, and lack of confirmation of protein expression (Singh et al. 2008; Sergentanis and Economopoulos 2010). Therefore, with the current state of knowledge, CYP1A1 SNPs do not appear to play a major role in cancer progression and thus other possible mechanisms need to be examined. Comprehensive studies with larger population size are needed to draw definite conclusions of the functional roles of CYP1A1 SNPs.

Allele	Protein	Nucleotide change	Outcome
CYP1A1*1	CYP1A1.1	None	
CYP1A1*2A	CYP1A1.1	3798T>C (MspI)	
CYP1A1*2B	CYP1A1.2	2454A>G; 3798T>C (MspI)	I462V
CYP1A1*2C	CYP1A1.2	2454A>G	I462V
CYP1A1*3	CYP1A1.1	3204T>C	
CYP1A1*4	CYP1A1.4	2452C>A	T461N
CYP1A1*5	CYP1A1.5	2460C>A	R464S
CYP1A1*6	CYP1A1.6	1635G>T	M331I
CYP1A1*7		2345_2346insT	426Frameshift
CYP1A1*8	CYP1A1.8	2413T>A	I448N
CYP1A1*9	CYP1A1.9	2460C>T	R464C
CYP1A1*10	CYP1A1.10	2499C>T	R477W
CYP1A1*11	CYP1A1.11	2545C>G	P492R
haplotype not determined		-33T>C; 513A>C; 2216C>T; 2958C>T; 3324G>T; 3325G>C; 3422C>A	
haplotype not determined		233T>C	I78T
haplotype not determined		18C>G	T173R
haplotype not determined		2515G>A	V482M
haplotype not determined		322C>A	D108Y
haplotype not determined		262C>T	G88S
haplotype not determined		134C>T	G45D

Table I.2. CYP1A1 single nucleotide polymorphisms.

Summary of CYP1A1 single nucleotide polymorphisms (SNPs). Modified from *http:// www.cypalleles.ki.se/cyp1a1.htm* with permission (Sim and Ingelman-Sundberg 2010).

Phenotypes of mice CYP1A1 knock-out models

Dalton et al. published the first report of a Cyp1a1 knockout (Cyp1a1(-/-)) mice line using a Cre-lox system in a C57BL/6J background (Dalton et al. 2000). In the absence of exposure to xenobiotics, these mice developed without any apparent abnormal phenotype (grown up to 4months) and the levels of other AhR-regulated proteins were not affected. In **Figure** I.4 we summarize key findings of subsequent

CYP1 knockout mouse models exposed to B[a]P. To date the following mouse lines have been studied: Cyp1a1(-/-) , Cyp1a1/1b1(-/-) (i.e. double knockout), Cyp1a1/1a2/1b1(-/-) (i.e. triple knockout), and a humanized line hCYP1A1_1A2_Cyp1a1/1b1(-/-). These enhance our understanding of the role of CYP1a1 in tissue-specific toxicity mediated by pro-carcinogenic xenobiotics.

One would expect Cyp1a1(-/-) mice to be protected from B[a]P effects because of CYP1A1's role in catalyzing the biotransformation of this xenobiotic to a carcinogenic metabolite (Gelboin 1969; Gelboin et al. 1969; Huberman et al. 1976). However, Cyp1a1 knockout mice treated with B[a]P exhibited significantly enhanced toxicity compared to wild-type mice: Cyp1a1(-/-) > Cyp1a1/1b1(-/-) (**Figure** I.4, (Uno et al. 2004; Uno et al. 2006)). This result suggests that, at least in rodents, CYP1A1 plays a protective role rather than a procarcinogenic one. These effects were confirmed to be mediated specifically by CYP1a1 (Uno et al. 2004; Uno et al. 2006). Additional evidence for the protective role of CYP1A1 is provided by insertion of human CYP1A1/1A2 into the double knockout mice which partially restores the wild-type phenotype (Dragin et al. 2007). The Cyp1a1/1a2/1b1(-/-) mice exhibited increased risk of embryolethality and birth defects with incomplete penetrance. These abnormal effects were attributed to dysregulation of genes involved in biosynthesis of steroid, lipids (including eicosanoids) and cholesterol, protein translation, as well as other homeostatic processes (Dragin et al. 2008). Therefore, in light of these evidence, the authors concluded that CYP1a1 is more important in protection from B[a]P toxicity than in its metabolic activation. Observed proximal small intestine adenocarcinoma after B[a]P exposure was attributed to CYP1b1 and not CYP1a1 (Galvez-Peralta et al. 2012).

Cyp1a1 (-/-)	Cyp1a1 /1b1(-/-)	Cyp1a1 /1a2/1b 1(-/-)	h1A1/2 _1a1/2 (-/-)
↓ B[a]P clearance Restored by TCDD	↓↓ B[a]P clearance	↓↓↓ B[a]P clearance	Normal B[a]P clearance
↓ B[a]P-DNA adducts	inconsistency B[a]P-DNA adducts	↑ embryolethality (untreated)	Normal overall and spleen weight
↓ weight: overall, spleen and thymus	↓↓ weight: overall, spleen and thymus	↑ risk hemaphroitism	↓ thymus weight
Myelosuppression	No myelotoxicity	↑ risk cystic ovaries	↑ liver size
Adenocarcinoma	No adenocarcinoma	↑ risk hydrocephalus	Overall phenotype like wild-type
Death after 22days of B[a]P treatment	Immunesuppresion < Cyp1a1(-/-)	Immunesuppresion < Cyp1a1(-/-)	Rescued immunesuppresion
↑ liver size			

Figure I.4. Phenotypes of Cyp knockout mice exposed to benzo[a]pyrene (B[a]P).
Summary of phenotypes of mouse lines: Cyp1a1 single knockout [Cyp1a1(-/-)], Cyp1a1 and Cyp1b1 double knockout [Cyp1a1/1b1 (-/-)],Cyp1a1, Cyp1a2, and Cyp1b1 triple knockout, and humanized mouse line [hCYP1A1_1A2_Cyp1a1/1b1(-/-)]. (Uno et al. 2004; Uno et al. 2006; Dragin et al. 2007; Dragin et al. 2008)

Clinical relevance of CYP1A1

In the previous section we discussed the role of CYP1A1 in carcinogenesis upon exposure to pro-carcinogens. We also addressed CYP1A1 metabolizes pro-drugs to their bioactive form which results in inhibition of cancer growth. Evidence supporting a

potential cancer-promoting role of CYP1A1 via endobiotic metabolism was also provided. Furthermore, although the role CYP1A1 SNPs in the incidence of cancer is still largely debated, it is possible that future work confirm this involvement. We also cited evidence (on page 8) supporting the association of CYP1A1 expression with lung, ovarian, oesophageal, bladder, and breast cancers (Kellermann et al. 1973; McLemore et al. 1989; McLemore et al. 1990; Murray et al. 1994; Murray et al. 1995; Leung et al. 2005; Murray et al. 2010). Nonetheless, despite this combined evidence supports a functional role of CYP1A1 in cancer, the exact mechanisms remain to be determined.

To date the strongest supporting evidence of the involvement of CYP1A1 in breast cancer is reported by (Murray et al. 2010; Vinothini and Nagini 2010). Vinothini et al. reported on the expression levels of various xenobiotic-metabolizing enzymes, including CYP1A1, in 60 breast tumors from newly diagnosed patients who had not received prior adjuvant therapy. Their study showed that levels of CYP1A1: (a) were elevated in tumors compared to adjacent breast tissue, (b) were higher in premenopausal compared to post-menopausal patients, and (c) positively correlated with tumor grade (Vinothini and Nagini 2010). Murray et al. profiled the expression levels of twenty one CYPs in 170 breast tumors from patients that had not received prior adjuvant treatment. They found that CYP1A1 was expressed in about 90% of breast tumors but not correlation was found with estrogen receptor alpha levels, tumor grade, or clinical outcome (Murray et al. 2010). These studies provide evidence that CYP1A1 is expressed to various degrees in breast tumors and may be associated with breast cancer biology. But, does CYP1A1 play a functional role in breast cancer progression? And if so, what are the mechanisms? We address these questions in **Chapter III**.

23

CHAPTER II

Materials and Methods

COPYRIGHT DISCLOSURE

MATERIALS

Chemicals and reagents

IMEM MEM and cell culture supplements are from GIBCO/Invitrogen/Life Technologies (Carlsbad, CA). Charcoal/dextran-stripped serum and fetal bovine serum from HyClone (Logan, UT). ON-TARGET*plus* CYP1A1- and NTsiRNA pools (sequences below) are from Thermo Scientific Dharmacon (Lafayette, CO). Oligofectamine, Opti-MEM, SuperScript® III First-Strand synthesis system, and SYBR® GreenER™ qPCR SuperMixes for iCycler are from Invitrogen/Life Technology (Carlsbad, CA). All primers were purchased from Integrated DNA Technologies (Minneapolis, MN). The QiaShredder columns, RNeasy Mini Kit, QuantiTect Reverse Transcription Kit, and RNase-A are from Qiagen (Valencia, CA). The Wright-Giemsa was purchased from Thermo Fisher Scientific (Waltham, MA). Carnosol was purchased from Cayman Chemical (Ann Arbor, MI) and dissolved in DMSO to a final concentration of 40 mmol/L. The MG-132 and compound C are from Calbiochem/EMD Millipore (San Diego, CA). The tetrazolium salt, propidium iodide, NP-40, cell culture grade DMSO HYBRI-MAX, ethoxyresorufin, alpha-naphthoflavone, all-*trans*-retinoic acid, 9-*cis*-retinoic acid, 13-*cis*-retinoic acid, pregnenolone, DHE, DCFDA, and sodium citrate are from Sigma (St. Louis, MO). 2,3,7,8-tethachlorodibenzo-p-dioxin (TCDD) is from AccuStandard (New Haven, CT). Protease and phosphatase inhibitors are from Sigma (St. Louis, MO) and Roche (Indianapolis, IN). Human fibronectin (#356008) and the apoptosis detection kit are from BD Pharmingen (San Jose, CA). The ECL western blotting detection reagent

was purchased from GE Healthcare/Biocompare (South San Francisco, CA). The mineral oil is from Bio-Rad (Hercules, CA). CYP1A1 supersome was purchased from BD Biosciences (San Jose, CA). 20-HETE was purchased from Santa Cruz Biotechnology (Santa Cruz, CA). EETs and 17,18-EpETE were kind donations from Dr. J.R. Falck and also purchased from Cayman Chemical Co. (Ann Arbor, MI). The 12um pore polycarbonate membrane for the Boyden chamber was obtained from Neuro Probe, Inc. (Gaithersburg, MD).

Mass spectrometry reagents

Eicosanoid reagents (±)-8,9-(5Z,11Z,14Z)-EET, (±)-11,12-(5Z,8Z,14Z)-EET, and (±)-14,15- (5Z,8Z,11Z)-EET were purchased from Biomol International (Plymouth Meeting, PA). AA, (±)-15-(5Z,8Z,11Z,14Z)-HETE, 19-(R) -(5Z,8Z,11Z,14Z)-HETE, 20-(5Z,8Z,11Z,14Z)-HETE and d8-EETs were purchased from Cayman Chemical Co. (Ann Arbor, MI). Diisopropylethylamine (DIPE), 2,3,4,5,6-pentafluorobenzyl bromide (PFB-Br), 3-chloroperbenzoic acid (MCPBA), methylene chloride, NADPH, ethylenediamine tetraacetic acid (EDTA), HPLC-grade acetonitrile and diethyl ether were purchased from Sigma-Aldrich (St. Louis, MO). HPLC-grade hexane, isopropanol and ethanol were obtained from Fisher Scientific Co. (Fair Lawn, NJ). ACS-grade ethanol was obtained from Pharmco (Brookfield, CT). Soluble epoxide hydrolase inhibitor 1471 was a gift from Dr. Bruce Hammock, University of California, Davis.

Antibodies

Anti-actin antibody (HHF-35) from Calbiochem/EMD Millipore (San Diego, CA). Anti-phospho-p70S6 kinase (Thr421/Ser424) is from Millipore (Billerica, MA). Antibodies raised against total and phosphorylated forms of the following proteins were obtained from Cell Signaling Technology (Beverly, MA): mTOR (p-Ser2448/clone D9C2), phospho-p65NFKB (Ser536), IKBα, phospho-FOXO1 (Ser256), phospho-STAT3 (Tyr705 clone D3A7), NM-23 (H1/H2), phospho-Src (Tyr416 clone 100F9), JNK (total, p-Thr183/Tyr185), ERK1/2 (p-Thr202/Tyr204), Akt (total clone 40D4 and p-Ser473), LKB1 (total), AMPK (total clone F6 and p-Thr172/clone 40H9), P70S6K (total). Anti-CDK4, Jun (total, p-Ser63/73), and myc are from Santa Cruz Biotechnology, (Santa Cruz, CA). Anti-survivin antibody is from R&D systems (Minneapolis, MN). Antibodies against CYP1A1 (ab3568) and AhR (clone RPT1) were obtained from Abcam (Cambridge, MA). Anti-GAPDH antibody is from Research Diagnostics/Fitzgerald Industries (Concord, MA). Anti-phospho-GSK3β (Y216) is from BD Biosciences (San Jose, CA). Anti-PDK4 was a kind gift from Dr. Robert A. Harris (Indiana University School of Medicine, IN).

Cell culture

The lines MDA-MB-231 and MCF7 were purchased from American Type Culture Collection (Manassas, VA) and grown at $37^{o}C$ under 5% CO_2. Unless otherwise indicated, cells were grown and maintained in complete medium (MCF7: MEM, 10% FBS, 1% L-glutamine, 1% penicillin/streptomycin, and 1% HEPES; MDA-MB-231: MEM,

10% FBS, 1% L-glutamine, 1% penicillin/streptomycin, 1% sodium pyruvate, and 2 µg/mL insulin). Because antibiotics reduce transfection efficiency, for all siRNA transfection experiments cells were passaged once in antibiotic-free medium (AFM) prior to plating for the experiments and maintained in this medium throughout the duration of the experiment. MCF7: 10% charcoal/dextran-stripped serum, phenol-red free MEM, 1% HEPES, and 1% L-glutamine; MDA-MB-231: 10% FBS, phenol-red free MEM, 1% sodium pyruvate, 1% L-glutamine, and 2 µg/mL insulin).

METHODS

siRNA transfection

To knockdown CYP1A1 or AhR levels, cells were transfected with a pool of siRNA designed by Dharmacon (**Table II.2**). A detailed protocol in provided in **Appendix I**. Cells were seeded at 30% confluence on 6-well plate and incubated overnight. Prior to transfection cells were washed twice with phenol-red free MEM and 0.8mL of OptiMEM was added to each well. A transfection solution of 60 nmol/L siRNA suspended in 0.3% oligofectamine/OptiMEM was gently added to the cells (200uL/well). After overnight incubation, AFM medium was added to obtain 10% serum medium. For transfection quality purposes a separate well was transfected with siGLO green transfection indicator # D-001630-01.

Quantitative RT-PCR

To evaluate CYP1A1 mRNA knockdown efficiency, total RNA was collected in lysis (RLT) buffer and beta-mercaptoethanol, passed through a QiaShredder column, and purified using the RNeasy Mini Kit according to the manufacturer's protocol. First strand cDNA was made using the QuantiTect Reverse Transcription kit according to the manufacturer's protocol. The quantitative reverse transcriptase PCR (RT-PCR) reactions were prepared using SYBR® GreenER™ qPCR SuperMixes for iCycler and performed at as follow: $50^{o}C$ for 2 minutes, $95^{o}C$ for 8.5 minutes, 40 cycles of $95^{o}C$ for 15 seconds

and 60°C for 1 minute. The comparative Ct value method was used for data analysis (Schmittgen and Livak 2008). GAPDH was utilized for normalization. Primers are listed in **Table II.2**.

Semi-quantitative RT-PCR

To evaluate siRNA specificity for CYP1A1 compared to other CYPs, total mRNA was collected and purified as described above. The cDNA was prepared using the First Strand Synthesis Kit according to the manufacturer's protocol (Invitrogen). Semi-quantitative RT-PCR analysis of CYP1A1, CYP1A2, and CYP1B1 was performed using SuperScript® III Reverse Transcriptase (Invitrogen) and Taq Master Mix kit according to manufacturer's protocol (Qiagen) in a PX2 Thermal Cycler (Thermo) (94°C for 2 minutes, 50 cycles: 94°C/30sec, 55°C/30sec, 72°C/45sec, 72°C for 10 minutes and 4°C for 5 minutes). The PCR products were resolved in a 1.5% agarose gel and GAPDH was used to normalize samples. Primers are listed in **Table II.2**.

Western blot analysis

To evaluate protein levels, cell extracts were prepared using radioimmunoprecipitation assay extraction buffer (RIPA, described below) and processed to standard Western blot analysis. A total of 15-30 μg of protein were loaded onto an SDS-PAGE gel, transferred for 2 hours at 40V onto a 0.22microns nitrocellulose membrane, followed by 1 hour blocking in 5% milk/TBST and overnight incubation of

primary antibody at 4°C. GAPDH was used as loading control and relative protein amounts were quantified by densitometry of X-ray film exposures using an Alpha-Innotec densitometer. RIPA extraction buffer: 50 mmol/L Tris pH 7.5, 150 mmol/L NaCl, 1% NP-40, 0.5% DOC, 0.1% SDS, 2 mmol/L EDTA pH 8, 2 mmol/L EGTA pH 8, 1 mmol/L DL-dithiothreitol, 1 mmol/L phenylmethylsulfonylfluoride, 5 µmol/L phenylarsine oxide, 25 mmol/L NaF, 2 mmol/L Na$_3$VO$_4$, 100 µmol/L leupeptin, 2 µmol/L pepstatin, 2.8 µmol/L Tosyl-L-phenylalanyl-chloromethane, 2.7 µmol/L Tosyl-L-lysyl-chloromethane hydrochloride, 4.17 µmol/L 4-(2-Aminoethyl) benzenesulfonyl fluoride hydrochloride, 4.17 µmol/L chymostatin, 2 µmol/L aprotinin, 2 µmol/L antipain, 5 mmol/L N-ethyl-maliemide, 40 µmol/L MG-132.

MTT cell proliferation assay

To assess proliferation, cells were incubated with 0.1mg/mL of tetrazolium MTT (3, [4,5-dimethylthiazol-2-yl]-2,5-diphenyltetrazolium bromide) for 2 hours at 37°C under 5% CO$_2$. The supernatant was replaced with DMSO. Proliferating cells reduce the yellow tetrazolium into DMSO-soluble purple formazan which was read in a BioTek plate reader at an absorbance of 540 nm.

Anchorage-dependent clonogenic assay

To assess cell survival, 200 transfected cells were seeded onto fibronectin-coated 6-well plates and incubated for 14 days until visible colonies were observed.

Colonies were fixed and stained with Wright-Giemsa and total colony number was counted. Plate preparation: 1mL of fibronectin (10ug/mL in PBS) was incubated overnight at 4°C, then blocked with 3% BSA in PBS for 1 hour at room temperature, and rinsed with PBS prior to use.

Cell cycle assay

To evaluate the cell cycle distribution, cellular DNA content was measured by propidium iodide staining. Because MCF7 cells form clumps in the presence of ethanol, two different methods were utilized for fixing and staining. MDA-MB-231 method: cells were collected by trypsinization, washed with ice cold PBS, resuspended in 200 µL of ice cold 70% ethanol, incubated overnight at 4°C, centrifuged, washed with PBS, and finally resuspended in 0.5mL of Nicoletti buffer (50 µg/ml propidium iodide, 0.1% sodium citrate, 0.1% Triton X-100 and 1 mg/ml RNase-A in PBS). MCF7 method: cells were washed twice with PBS over ice, scraped off the plate with 1mL of PBS, collected and centrifuged for 5 minutes, resuspended in 0.5mL of staining solution (0.1% sodium citrate, 50 µg/mL propidium iodide, 0.01% NP-40, and 1 µg/mL RNase A in water), and incubated overnight at 4°C. Following the respective staining methods propidium iodide content was profiled using a FACScalibur flow cytometer (BD Bioscience). Cell cycle distribution was determined using the Watson Pragmatic algorithm in the FlowJo software.

Apoptosis assay

To evaluate cell death cells were collected by trypsinization, washed with PBS, and stained with propidium iodide and Annexin-V/FITC for 15 minutes at RT. Stained cells were evaluated using a FACScalibur flow cytometer (BD Bioscience) and the results were analyzed with FlowJo software (Tree Star).

Cell death measured by propidium iodide staining of culture medium

To assess cell death in an alternative way to FACS analysis, the amount of dead cells in the culture medium was measured by propidium iodide staining. Cells were plated and treated as desired. As positive control, cells were treated with 1 µmol/L staurosporine for 2 hours. The culture medium was collected, centrifuged at 2,000rpm for 10 minutes, and the supernatant was carefully removed and discarded. The remaining pellet was resuspended in 20 ug/mL propidium iodide in PBS, and incubated for 20 minutes in the dark at 37°C. Stained samples were transferred to a black 96-well plate and read in a fluorescent plate reader (BioTek Synergy HT) at excitation 540 nm and emission 600 nm. Staining solution alone was used as blank. For normalization purposes, the cultured cells were trypsinized and counted on a hemocytometer and fluorescence was normalized to the total cell number on each well. To visually confirm our observations, an aliquot of stained culture medium was observed under a fluorescent microscope.

Mitotic index assay

To assess changes in mitosis, cells were plated and treated as described, trypsinized, centrifuged, resuspended in 5mL of hypotonic solution (40% culture medium/60% H_2O) and incubated for ≤ 6 minutes to allow swelling of the cells. To fix the cells a fixative solution (10mL) consisting of 75% methanol and 25% glacial acetic acid was added. Cells were centrifuged and resuspended (by gentle taping) in the fixative solution. This step was repeated again for a total of three times. After the last centrifugation step, cells were resuspended in the fixation solution and kept overnight at 4^oC. Cells were centrifuged and all but 1mL of the supernatant was removed. The cells were resuspended in the remainder 1mL of supernatant.

Mounting: using a Pasteur glass pipette, aliquots were dropped on slides from 1 foot above to allow even spreading of the cells. The slides were air dried, dipped in 5% giemsa staining solution for 2 minutes, rinsed with dH_2O, air dried, mounted using mineral oil, and allowed to cure overnight at room temperature. Slides were visualized under 40X in a Zeiss Axio Plan II microscope V1.2 equipped with an Axio Cam miRC5 camera. Slides were scanned systematically and cells exhibiting mitosis (i.e. prophase, metaphase, anaphase, telophase) were recorded and normalized to the total number of cells (350 total cells/slides). Mitotic index = # mitotic cells/ total # cells.

Boyden chamber migration assay

To assess cell migration we utilized a Boyden chamber assay modified from Dr. Doug Yee's laboratory. A solution of IMEM supplemented with 2µg/mL of fibronectin, and 5% FBS was added to the bottom of each well of a 9-well Boyden chamber. A serum-free condition served as negative control (IMEM supplemented with fibronectin). A 12 µm pore polycarbonate membrane was placed on top of the solution, glossy-side up, and the top portion of the chamber was carefully mounted on top. Healthy cells at 70-80% confluence were trypsinized for 30-60 seconds, centrifuged, washed twice with IMEM, and resuspended to $5x10^5$cells/mL in IMEM medium supplemented with the desired treatment and 2 µg/mL of fibronectin (no serum added). This cell suspension (300uL) was gently added to the top portion of the chamber and incubated for 4-6h at $37^{o}C$ in a humidified container (plastic box with wet paper tissue underneath the chamber). After incubation the medium on the top portion of the chamber was carefully removed and, while still mounted, the membrane was gently and thoroughly cleaned (including the edges) with a sterile cotton swab to remove excess cells. The chamber was then disassembled, and the membrane was stained with HEMA 3 staining kit as follow: 2 minutes submerged in the fixative solution, 2 minutes in the eosin solution to stain cytoplasm, 2 minutes in the methylene blue solution. The membrane was rinsed with water and hanged to dry for 10-15 minutes. Mineral oil was used to mount the membrane onto glass slides. Cells were counted in at least 5 fields per well.

Scratch assay

The scratch assay was performed to complement the findings of the Boyden chamber migration assay. Cells were plated onto a 6-well plate (500,000cells/well) and grown overnight or until 100% confluence was reached. For the eicosanoid studies, cells were starved for 24 hours at this point. A scratch was done through the center of the well with pipette tip and pictures of the scratched area were immediately taken. The medium was replaced with for the desired treatment and incubated for 24 hours. Following treatment pictures of the scratched area were taken. The scratched area before treatment was subtracted from the area after treatment; this calculation provides the migration index.

LC-ESI/MRM/MS method for eicosanoid measurement

Samples were analyzed by LC-ESI/MRM/MS in a Thermo Electron Quantum Discovery Max triple quadrupole mass spectrometer (Thermo Finnigan, San Jose, CA) coupled with an Agilent 1100 HPLC (Santa Clara, CA), using argon as the collision gas. Negative ion monitoring was performed at the following diagnostic product ions: 317 m/z $\rightarrow$ 259 m/z for 17-EpETE; 339 m/z $\rightarrow$ 163 m/z for 8,9-[$^{13}C_{20}$]EET; 339 m/z $\rightarrow$ 233 m/z for 11,12-[$^{13}C_{20}$]EET; and 339 m/z $\rightarrow$ 259 m/z for 14,15-[$^{13}C_{20}$]EET. Base-line resolution of was achieved on a Phenomenex Luna C18 (2) reverse phase capillary column (250 $\times$ 0.5 mm, 5-μm particles) using the following mobile phase combinations: isocratic 5% B for 5 minutes, gradient 5–70% B for 5 minutes, hold at 70% for 30 minutes and then 95%

36

for 10 minutes; A: 0.01% acetic acid in water, B: 0.01% acetic acid in acetonitrile; 10 µl/min flow rate. Protocol design and experiment performed by Dr. Zhijun Guo.

Synthesis of 17,18-EpETE by CYP1A1 microsome

CYP1A1 and insect control Supersomes[TM] (BD Biosciences) were incubated at 37 °C for 30 minutes with eicosapentaenoic acid (30µM) in PBS in the presence or absence of NADPH (1 mmol/L). Reactions were terminated by adding CH_2Cl_2 (1 mL). After the addition of $[^{13}C_{20}]$EET labeled EET internal standards, brief vigorous vortexing and centrifugation at 3,000 rpm for 10 minutes, organic phases were separated and evaporated under nitrogen. Samples were reconstituted in 100 µl of methanol and analyzed by LC-ESI/SIM/MS method by Dr. Zhijun Guo.

Eicosanoid extraction protocol

A detailed protocol can be found in **Appendix II**. Briefly, cells grown to 50–75% confluence on 150 × 20-mm plates were washed twice with cold PBS and collected in cold PBS containing 2 µM soluble epoxide hydrolase inhibitor 1471 (a gift from Dr. Bruce Hammock, University of California, Davis) and, after the addition of $[^{13}C_{20}]$EET internal standards, extracted with a 2:1 mixture of chloroform/methanol. After saponification of the organic extracts, extraction of the resulting fatty acids into acidified ethyl ether, and evaporation under N_2, the samples were dissolved in methanol for mass spectrometric analysis.

Eicosanoid treatment

Treatment with EETs, HETEs, and EpETE were done using the following general protocol. Cells were plated at 30-50% confluence and culture overnight. To avoid confounding factors of lipids present in serum, cells were serum-starved for 24 hours prior to treatment and maintained under serum-free conditions throughout the duration of the experiments. A solution of vehicle (ethanol) or the indicated eicosanoid was prepared in serum-free medium and cells were treated for the indicated amounts of time. All EETs, HETEs, and EpETE were stored at $-20^{o}C$ or $-80^{o}C$ under nitrogen to prevent oxidation. For quality control purposes new vials of eicosanoids were routinely tested by MTT and when appropriate by mass spectrometry. Serum-free medium for MCF7 line consisted of MEM, L-glutamine, and HEPES and for MDA-MB-231 line of MEM, L-glutamine, and sodium pyruvate. No serum, antibiotics, or insulin were added to this media.

Reactive oxygen species (ROS) assay

Cells were plated onto 6-well plate (80,000cells/well) and treated as described. Following treatment, cells were incubated for 30min with either 2 µmol/L dihydroethidium (DHE, to monitor primarily superoxide production) or 10 µmol/L of 6-*carboxy*-2',7'-dichlorodihydrofluorescein diacetate (DCFDA, to monitor general oxidative stress indicator). Stained cells were trypsinized, centrifuged, washed twice with 1X PBS,

resuspended in PBS, and analyzed by flow cytometry. Treatment with 250 μmol/L H_2O_2

for 2 hours served as positive control.

Mitochondrial membrane potential

To evaluate changes in the mitochondrial membrane potential cells stained with

5,5',6,6'-tetrachloro-1,1',3,3'-tetraethylbenzimidazolcarbocyanine iodide (JC-1) were

assessed by fluorescent plate reader and by flow cytometry. In healthy cells exhibiting

high mitochondrial membrane potential, JC-1 forms red-fluorescent aggregates with

excitation at 560 nm and emission at 595 nm. In contrast, in unhealthy or apoptotic cells

JC-1 remains as monomers that exhibit green-fluorescence with excitation at 485 nm

and emission at 535 nm. Treatment with 100 μmol/L carbonyl cyanide m-

chlorophenylhydrazone (CCCP) for 15 minutes in a $37^{o}C$, 5% CO_2 incubator served as

positive control (reduces the mitochondrial membrane potential). The change in the

mitochondrial membrane potential was determined by the ratio between JC-1

aggregates to monomers (red/green) as measured by the plate reader and FACS

methods.

Plate reader method: Cells were plated onto black plates and after desired

treatment were stained in the dark at room temperature for 15 minutes with 2.5ug/mL of

JC-1 dissolved in warm medium. Following staining cells fluorescence plates were read

in a fluorescence plate reader.

FACS method: Cells were plated in regular 6-well plates and treated as desired.

Cells were stained with JC-1 as indicated above for 30 minutes in a $37^{o}C$, 5% CO_2

incubator. Following staining, cells were trypsinized, centrifuged, resuspended in culture medium and analyzed by flow cytometry (red, FL-2; green, FL-1).

Ethoxyresorufin-O-deethylase (EROD) assay

To assess CYP1A1 activity, an EROD assay adapted from (Sinal and Bend 1997; Yu et al. 2004) was utilized. Cells were plated onto 6-well plates, treated as desired, washed 2x with 1xPBS, then incubated at 37°C for 60 minutes with 2 mmol/L ethoxyresorufin in buffer (50 mmol/L Tris, 0.1M NaCl, 6.25 mmol/L $MgCl_2$, pH 7.8, warmed to 37°C). A 100uL aliquot of the assay supernatant was transferred to a black-wall clear bottom 96-well plate and fluorescence was read in a BioTek fluorescence plate reader at excitation λ (530 nm)/emission λ (590 nm). When necessary fluorescent counts were normalized to total cell number.

Statistics

All experiments were reproducible and performed at least in triplicate. Statistical significance (p values) was calculated using 2-tailed Student *t* test. Equality of variance was determined by *F* test.

Non-targeting siRNA ON-TARGET plus # D-001810-10
UGGUUUACAUGUCGACUAA
UGGUUUACAUGUUGUGUGA
UGGUUUACAUGUUUUCUGA
UGGUUUACAUGUUUUCCUA
Human CYP1A1siRNA ON-TARGETplus SMARTpool #L-004790-00-0005
UCGACAAGGUGUUAAGUGA
AAAUGCAGCUGCGCUCUUA
CUACAGGUAUGUGGUGGUA
GAACUGCUUAGCCUAGUCA
Human AhRsiRNA ON-TARGETplus SMART pool # L-004990-00-0005
GCAAGUUAAUGGCAUGUUU
GAACUCAAGCUGUAUGGUA
GCACGAGAGGCUCAGGUUA
GCAACAAGAUGAGUCUAUU

Table II.1. Sequences of siRNA pools.

Sequences designed by Thermo Scientific Dharmacon (Lafayette, CO).

Gene	Amplicon	Forward primer (5'-3')	Reverse primer (5'-3')
CYP1A1	qPCR	GCT GAC TTC ATC CCT ATT CTT CG	TTT TGT AGT GCT CCT TGA CCATCT
GAPDH	qPCR	GGG AAG GTG AAG GTC GGA GT	GAG TTA AAA GCA GCC CTG GTG A
GAPDH	609 bp	CAC AGT CCA TGC CAT CAC TGC	GGT CTA CAT GGC AAC TGT GAG
CYP1A1	294 bp	CTT CAT CCT GGA GAC CTT CC	AAG ACC TCC AGC GGG CA A
CYP3A4	187 bp	GCC TGG TGC TCC TCT ATC TA	GGC TGT TGA CCA TCA TAA AAG
CYP2C9	104 bp	AGG AAA AGC ACA ACC AAC CA	TCT CAG GGT TGT GCT TGT C
CYP1A2	371 bp	CAA TCA GGT GGT GGT GTC AG	GCT CCT GGA CTG TTT TCT GC
CYP1B1	350 bp	TCA ACC GCA ACT TCA GCA ACT T	ATA GGG CAG GTT GGG CTG GTC A
CYP2C8	158 bp	AGA TCA GAA TTT TCT CAC CC	AAC TTC GTG TAA GAG CAA CA
CYP2J2	126 bp	GCC CGG GAG TCC ATG CCC TA	GGG CAG GTG GTA CCC AGC CA

Table II.2. Primers for quantitative and semi-quantitative RT-PCR.

Primers were designed by Ranjana Mitra or found through the published literature.

CHAPTER III

Cytochrome P450 1A1 Regulates Breast Cancer Cell Proliferation and Survival

COPYRIGHT DISCLOSURE

INTRODUCTION

Cytochrome P450 1A1 (CYP1A1) is an extrahepatic phase-I enzyme that metabolizes endogenous and xenobiotic substrates. Prior studies implicating CYP1A1 in cancer have dealt primarily with the metabolic activation of pro-carcinogens including polycyclic aromatic hydrocarbons and estradiol (van Cantfort and Gielen 1981; Asokan et al. 1986; Das et al. 1986; Spink et al. 1992). Other studies have focused on associations between CYP1A1 single nucleotide polymorphisms (SNPs) and increased cancer incidence. For example, the A2455G allele has been implicated with increased breast cancer risk in Caucasian populations (Sergentanis and Economopoulos 2010). Nonetheless, lack of associations between SNPs and cancer have been reported and these discrepancies have been attributed to ethnic variations between populations, variation in sample size, and lack of confirmation of protein expression (Singh et al. 2008). However, little is known about the roles of CYP1A1 in cancer biology in the absence of xenobiotic exposure.

Under physiological conditions, CYP1A1 expression is suppressed but it is induced in the presence of substrates via the transcriptional regulation of the aryl hydrocarbon receptor (AhR) (Androutsopoulos et al. 2009b) In recent years studies have shown that breast tumors constitutively express CYP1A1 (Murray et al. 2010; Vinothini and Nagini 2010). Murray et al. profiled the expression levels of twenty one CYPs in 170 breast tumors from patients who had not received prior adjuvant treatment. This profiling revealed that CYP1A1 was expressed in about 90% of breast tumors. Even so, the degree of CYP1A1 expression varied among tumors and did not correlate with estrogen

44

receptor alpha levels, tumor grade, or clinical outcome (Murray et al. 2010). Vinothini et al. reported on the expression levels of various xenobiotic-metabolizing enzymes, including CYP1A1, in 60 breast tumors from newly diagnosed patients who had not received prior adjuvant therapy. Their study showed that CYP1A1 levels were: (a) elevated in tumors compared to adjacent breast tissue, (b) higher in premenopausal compared to post-menopausal patients, and (c) positively correlated with tumor grade (Vinothini and Nagini 2010). These studies provide evidence that CYP1A1 is expressed to varying degrees in breast tumors and may be associated with cancer biology. Moreover, because of its ubiquitous expression in breast cancer and its ability to metabolize xenobiotics, interest has been shown to exploit CYP1A1 activity for breast cancer therapeutics (Chua et al. 2000; Bradshaw et al. 2001; Hose et al. 2003; Monks et al. 2003; Trapani et al. 2003; Brantley et al. 2004). Nonetheless, little is known about the activities of CYP1A1 that may participate in breast cancer progression. Therefore, better understanding the function of CYP1A1 in breast cancer will assist in the development of targeted therapy and improve treatment strategies.

The purpose of this study was to determine the biologic functions and roles in signal transduction of CYP1A1 in breast cancer cells. Toward this goal we utilized small interfering RNA (siRNA) to knockdown CYP1A1 in the breast cancer lines MCF7 (estrogen receptor positive; ER+) and MDA-MB-231 (triple negative; ER-/PR-/HER2-). We determined that CYP1A1 knockdown decreases proliferation, decreases colony formation, blocks the cell cycle at G0/G1 associated with reduction of cyclin D1, and increases apoptosis associated with reduction of survivin. CYP1A1 silencing reduces proliferation and survival, at least in part, through increased phosphorylation of AMP-

activated protein kinase (AMPK) and reduced phosphorylation of AKT, extracellular signal-regulated kinases 1 and 2 (ERK1/2), and 70kDa ribosomal protein S6 kinase (P70S6K). Consistent with CYP1A1siRNA results, pharmacologic reduction of CYP1A1 levels by carnosol also impairs proliferation and induces AMPK phosphorylation. Together, these results implicate CYP1A1 in cell proliferation and survival pathways. Additionally, modulation studies of CYP1A1 activity via 2,3,7,8-tethachlorodibenzo-p-dioxin (TCDD, inducer) and alpha-naphthoflavone (inhibitor) indicate that reduction of CYP1A1 expression levels is critical for these biologic effects and cannot be substituted by modulation of its activity alone. The evidence presented here suggests that CYP1A1 silencing is a potential therapeutic strategy for breast cancer independent of estrogen receptor status.

RESULTS

CYP1A1 knockdown impairs cell proliferation and survival.

The purpose of this study was to understand the biological roles of CYP1A1 in MCF7 and MDA-MB-231 breast cancer lines. We chose ER+ and triple-negative breast cancer because there is a significant unmet need for new treatments for metastatic hormone therapy refractory and triple negative breast cancer. To achieve the goal of defining the role of CYP1A1 in breast cancer growth, pooled siRNA was utilized to knockdown CYP1A1 mRNA and protein. To validate the knockdown efficiency, CYP1A1 mRNA and protein levels were measured by quantitative RT-PCR and by Western blot, respectively. Significant reductions of CYP1A1 mRNA and protein levels were observed between 48 hours and 120 hours. CYP1A1 mRNA levels were reduced by 53% (p = 0.002) in the MCF7 line and by 70% (p = 6×10^{-6}) in MDA-MB-231 line (**Figure III.1 A**). CYP1A1 protein levels were reduced by 64% (p = 0.02) in the MCF7 line and by 52% (p = 0.04) in the MDA-MB-231 line (**Figure III.1 B**). Because CYP1A1 shares 73% identity with CYP1A2 and 41% identity with CYP1B1, we also evaluated by semi-quantitative RT-PCR whether CYP1A1siRNA alters the mRNA levels of these CYP1 family members. No change was observed in the levels of these CYPs indicating that the biological effects observed are due specifically to reduction of CYP1A1 (**Figure III.1 C-D**).

To investigate the functional roles of CYP1A1 in breast cancer, we determined the effects of CYP1A1 knockdown on two "hallmarks of cancer": uncontrolled cell

proliferation and loss of inhibition of cell death. First, we examined the effects of CYP1A1 knockdown on the ability of MCF7 and MDA-MB-231 cells to proliferate. After transfection for 48 hours, 72 hours, and 96 hours, viable cells were measured by MTT assay. CYP1A1siRNA reduces the proliferation of both lines. At 96 hours of transfection with CYP1A1siRNA, proliferation was reduced by ~40% for the MCF7 and MDA-MB-231 lines (**Figure III.2 A**).

To determine the effects of CYP1A1 knockdown on cell survival we performed a clonogenic assay to count cells able to survive and proliferate to form visible colonies. MCF7 and MDA-MB-231 cells were transfected for 48 hours, seeded at low density onto fibronectin-coated plates, and colonies were counted after two weeks of culture. Compared to NTsiRNA control, CYP1A1siRNA inhibited colony formation of MCF7 line by 82% ($p = 4 \times 10^{-6}$) and of MDA-MB-231 line by 56% ($p = 0.03$) (**Figure III.2 B**). Together these results indicate that CYP1A1 silencing impairs proliferation and survival of breast cancer cells.

The aryl hydrocarbon receptor (AhR) localizes to the cytosol of MCF7 cells and translocates to the nucleus upon ligand activation. In contrast, MDA-MB-231 cells display primarily nuclear AhR expression. In both lines, nuclear AhR is responsible for the inducible transcriptional regulation of CYP1A1. Given the important role of AhR in the regulation of CYP1A1, it is possible that the biological functions of CYP1A1 may be affected by or be dependent on the AhR status. To determine whether AhR is required for the roles of CYP1A1 on cell proliferation, we investigated the impact of siRNA-mediated knockdown of AhR on basal CYP1A1 expression and cell proliferation. While AhRsiRNA reduces AhR levels by at least 70% ($p < 0.05$) in both lines, the levels of

CYP1A1 remain unaffected (**Figure III.8 A**). Therefore, this system allows us to distinguish AhR-specific effects. As assessed by MTT assay, the proliferation of these lines is not impaired by AhR knockdown (**Figure III.8 B**), suggesting that the effects of CYP1A1 knockdown on cell proliferation and survival (**Figure III.2**) may be independent of the AhR expression status of these lines.

CYP1A1 knockdown blocks the cell cycle.

The ability of cells to proliferate depends on the balance between cell growth, division and death. For this reason we investigated the effect of CYP1A1 knockdown on the ability of MCF7 and MDA-MB-231 lines to progress through the cell cycle. To achieve this goal, cells were transfected for 48 hours, permeabilized, stained with propidium iodide, and cell cycle distribution was analyzed by flow cytometry. The G0/G1 populations of MCF7 and MDA-MB-231 lines increased by 37% ($p = 0.001$) and 20% ($p = 0.003$) respectively, consistent with a block in the cell cycle at G0/G1 (**Figure III.3 A**).

Because the cyclin D1/CDK4 complex regulates the G1-S transition of the cell cycle (Lukas et al. 1996), we investigated the effects of CYP1A1 knockdown on these regulatory proteins. Cyclin D1 levels were reduced by 74% ($p = 0.001$) in MCF7 line and by 36% ($p = 0.001$) in MDA-MB-231 line (**Figure III.3 B**). CDK4 levels were not significantly reduced in both lines, although a trend toward reduction is observed. These results suggest that CYP1A1 knockdown may block the cell cycle, at least in part, through downregulation of cyclin D1.

CYP1A1 knockdown increases cell death.

To further understand the anti-proliferative effects of CYP1A1 silencing, apoptosis was measured by flow cytometry. In this assay, cells were transfected for 48 hours, stained with propidium iodide and Annexin-V/FITC, and analyzed by flow cytometry. CYP1A1 silencing of the MCF7 line correlated with a 50% increase in the early (lower right) and late (upper right quadrant) apoptotic populations ($p < 0.05$; **Figure III.4 A**). CYP1A1 silencing of the MDA-MB-231 line correlated with a 50% increase in the late apoptotic population ($p = 0.006$; **Figure III.4 A**).

Survivin is an anti-apoptotic protein of the inhibitor of apoptosis (IAP) family whose importance in breast cancer, including MCF7 and MDA-MB-231 lines, has been established (Tanaka et al. 2000; Yang et al. 2003). Therefore, to further understand the role of CYP1A1 in apoptosis, we measured the effects of CYP1A1 knockdown on the levels of survivin. Consistent with increased apoptosis, we observed that CYP1A1 knockdown was associated with an 80% reduction of survivin ($p = 0.003$) in MCF7 line and a 56% reduction ($p = 0.04$) in MDA-MB-231 line (**Figure III.4 B**).

CYP1A1 knockdown inhibits the ERK1/2 and AKT pathways

Because the MEK/ERK and PI3K/AKT signaling pathways promote the growth of breast cancer (Sivaraman et al. 1997; Xing and Imagawa 1999; Sun et al. 2001a; Sun et al. 2001b), we determined whether CYP1A1 knockdown inhibits ERK1/2 and/or AKT phosphorylation in these lines (**Figure III.5**). CYP1A1 knockdown reduced

phosphorylation of ERK in both lines, most notably by 45% (p = 0.001) in the MCF7 line. CYP1A1 knockdown resulted in reduction of AKT phosphorylation by 45% (p = 0.02) in MCF7 line and by 65% in MDA-MB-231 line (p = 0.004). These reductions in phosphorylation correlate with downstream inhibition of the protein synthesis regulator P70S6K (Fingar et al. 2004; She et al. 2010). Phosphorylation of P70S6K was reduced by 53% (p = 0.001) in the MCF7 line and by 37% (p = 0.03) in the MDA-MB-231 line. These results implicate CYP1A1 upstream of the ERK and PI3K/AKT pathways.

CYP1A1 knockdown induces the AMPK pathway

While reduction of P70S6K phosphorylation caused by CYP1A1 silencing could be related to loss of ERK1/2 and PI3K/AKT signaling, this inhibition could also be due to activation of AMPK, a major regulator of cellular bioenergetics and metabolic tumor suppressor (Luo et al. 2010). CYP1A1 knockdown increases phosphorylation of AMPK 5.6-fold (p = 0.01) in the MCF7 line and 2.4-fold (p = 0.02) in MDA-MB-231 line (**Figure III.5**). The activation of AMPK phosphorylation by CYP1A1 silencing in conjunction with concomitant down-regulation of ERK1/2 and AKT phosphorylation is consistent with known crosstalk with AMPK (Kovacic et al. 2003; Du et al. 2008; Kim et al. 2010) and potentially places CYP1A1 as a candidate upstream regulator of these kinases. The levels of LKB1, a known regulator of AMPK (Hawley et al. 2003), were determined by Western blot in the MCF7 line. Although an initial marginal reduction of LKB1 by CYP1A1siRNA was observed (48 hours transfection fold change = 0.70; p = 0.047), this reduction was not sustained at longer time points (72-96 hours; 96 hours transfection

fold change= 1.01; p = 0.98). This suggests that LKB1-dependent and LKB1-independent mechanisms of AMPK activation may be involved. A possible model summarizing these mechanisms is presented in **Figure III.11**.

AMPK inhibition partially abrogates CYP1A1siRNA-mediated apoptosis

We hypothesized that if AMPK signaling is necessary for the biological effects of CYP1A1 knockdown, then blocking AMPK activation should abrogate these effects. To test this hypothesis MCF7 cells were transfected for 24 hours with CYP1A1siRNA, followed by treatment for 24 hours with either vehicle (DMSO) or the AMPK inhibitor compound C (6-[4-(2-Piperidin-1-yl-ethoxy)-phenyl)]-3-pyridin-4-yl-pyyrazolo[1,5-a] pyrimidine; from now on abbreviated as CC). The reverse order of treatment (i.e. 24 hours treatment with DMSO or CC followed by NT/CYP1A1siRNA transfection) was also performed, leading to similar results. Following treatment, apoptosis was measured by flow cytometry and the percentage of overall cell death was calculated as follow: ΣDead= % early apoptotic + % late apoptotic + % necrotic populations. It should be noted that, because compound C induces cell death in MCF7 line (ref. (Jin et al. 2009) and confirmed in **Figure III.6**), the results are interpreted only within the context of treatment (i.e. DMSO or CC) as shown in the diagram on **Figure III.6**. Therefore, within the context of vehicle treatment CYP1A1siRNA increases cell death (ΣDead (NTsi+DMSO) = 27% *vs.* ΣDead (1A1si+DMSO) = 44%; p = 0.01; **Figure III.6**). This pro-apoptotic effect of CYP1A1siRNA in the presence of vehicle is consistent with our results

in **Figure III.4** and confirms that these effects are due to CYP1A1siRNA and not vehicle treatment.

Within the context of CC treatment two potential outcomes could be expected depending on whether AMPK is necessary for the pro-apoptotic effects of CYP1A1siRNA (**Figure III.6**; diagram): (a) if AMPK is necessary, then inhibition of AMPK would prevent CYP1A1siRNA-induced apoptosis and thus less cell death would be observed with "1A1si + CC" treatment compared to "NTsi + CC" treatment; (b) on the other hand if AMPK in not necessary, then inhibition of AMPK would not abrogate the pro-apoptotic effects of CYP1A1siRNA but would instead add to the pro-apoptotic effects of CYP1A1siRNA, thus resulting in an increase in cell death when treated with "1A1si + CC" compared to "NTsi + CC". Our results agree with the first scenario, 72% total cell death is observed with "NTsi + CC" while 46% total cell death is observed in "1A1si + CC" ($p = 0.003$; **Figure III.6**). This reduction of cell death observed for CYP1A1 knockdown cells treated with the AMPK inhibitor (CC) indicates that AMPK is necessary for the effects of CYP1A1siRNA and agrees with our findings showing that CYP1A1siRNA induces AMPK signaling (**Figure III.5**). Together, these results suggest that AMPK phosphorylation may be repressed by CYP1A1 and reduction of CYP1A1 levels promotes AMPK phosphorylation. In this manner AMPK may be required for the effects of CYP1A1siRNA on cell death (**Figure III.11**).

Carnosol impairs proliferation, in part, via reduction of CYP1A1 and activation of AMPK

To further test whether CYP1A1 signals, in part, through AMPK, we sought a pharmacologic approach to reduce CYP1A1 levels (Mohebati et al. 2012). Carnosol inhibits the aryl hydrocarbon receptor (AhR), a transcription factor that regulates the inducible and basal expression of CYP1 family members including CYP1A1 (Mohebati et al. 2012). Carnosol has been shown to reduce basal CYP1A1 expression in pre-malignant tongue and bronchial lines and in prostate cancer lines (Offord et al. 1995; Johnson et al. 2008; Mohebati et al. 2012). Treatment with carnosol inhibits the proliferation of the MCF7 and MDA-MB-231 lines exhibiting IC_{50} values of ~40 µmol/L for both lines ($p < 0.001$; **Figure III.7 A**). We performed time course experiments to investigate early effects (i.e. 2-12 hours) of carnosol treatment on CYP1A1 expression and determined that the optimal time for CYP1A1 reduction is 8 hours ($p < 0.05$; **Figure III.7 B**). Carnosol treatment reduces AhR levels in both lines by over 50% ($p < 0.05$; **Figure III.7 B**). In agreement with CYP1A1siRNA results (**Figure III.5**), treatment of the MCF7 and MDA-MB-231 lines with 40 µmol/L carnosol for 8 hours results in the activation of AMPK ($p < 0.01$; **Figure III.7 B**). This suggests that CYP1A1 reduction, whether by siRNA or carnosol, is associated with inhibition of proliferation mediated, in part, through activation of AMPK signaling.

Because carnosol inhibits both AhR and CYP1A1 levels, we tested whether the anti-proliferative effects of carnosol were mediated through AhR-dependent mechanisms. As previously shown, knockdown of AhR does not reduce basal CYP1A1

levels (**Figure III.8**), suggesting that carnosol inhibits basal CYP1A1 through an AhR-independent mechanism. Therefore, to better understand these mechanisms, we tested whether AhR is required for the therapeutic effects of carnosol. If so, we would expect AhR knockdown to shift the dose-response curve of carnosol. Treatment of AhR knockdown cells with carnosol does not result in a shift of the dose response curve (**Figure III.8 C**), further supporting that carnosol's effects may be independent of AhR. Therefore, together these results suggest that carnosol's anti-proliferative effects are primarily due to CYP1A1 reduction, AMPK activation, and potentially other yet unidentified mechanisms.

CYP1A1 targeting: expression versus activity

To this point we have focused on the impact of CYP1A1 levels in the biology of breast cancer cells. Nonetheless, for therapeutic development purposes we should distinguish between the expression levels and the enzymatic activity of CYP1A1. To address this issue we tested whether inhibition and/or induction of CYP1A1 activity affects breast cancer cell proliferation.

First, the effects of inhibiting CYP1A1 activity on cell proliferation were determined. To achieve this we first evaluated whether CYP1A1siRNA affects the activity of CYP1A1. To test this, cells were transfected with CYP1A1siRNA for 48 hours and TCDD-induced CYP1A1 activity was measured by EROD assay. CYP1A1 knockdown reduces CYP1A1 EROD activity by 38% ($p = 0.04$) in MCF7 line, but it is unaffected ($p = 0.52$) in MDA-MB-231 line (**Figure III.9 A**). These results led us to

hypothesize that, while reduction of CYP1A1 levels is necessary for impaired proliferation (**Figure III.2**), this effect on proliferation may not be dependent on the inhibition of CYP1A1 activity. To further test this hypothesis, we measured the effects of inhibiting CYP1A1's activity on cell proliferation. Cells were treated with 1 μmol/L of alpha-naphthoflavone, an inhibitor of CYP1A1 activity that does not affect CYP1A1 levels (**Figure III.9 B** and data not shown). Inhibition of CYP1A1 activity by alpha-naphthoflavone does not affect cell proliferation (**Figure III.9 C**), supporting the hypothesis that reduction CYP1A1 levels, but not its activity, is required for impairment of proliferation and survival (**Figure III.2**).

Secondly, the effects of inducing CYP1A1 activity on cell proliferation were determined. Cells were treated with the CYP1A1 inducer 2,3,7,8-tetrachlorodibenzo-p-dioxin (TCDD), which results in increased CYP1A1 levels and activity. Treatment with 5-20 nmol/L TCDD induces CYP1A1 activity, but does not stimulate cell proliferation (10 nmol/L shown in **Figure III.9 D-E**). It is noteworthy that the induction of CYP1A1 activity is greatest in the MCF7 line, when compared to MDA-MB-231, which is likely attributable to differences in AhR status in these lines (**Figure III.9 D**). These results suggest that breast cancer lines MCF7 and MDA-MB-231 have an optimal amount of CYP1A1 protein and further increasing its level or activity may not enhance the proliferative capability of these lines.

Together, our findings suggest that the development of therapeutic strategies to target CYP1A1 should consider the expression levels of the protein and not just its activity. Nonetheless, it remains to be determined whether CYP1A1's enzymatic activity

or a yet unidentified function(s) is mechanistically responsible for the proliferative and survival cell signaling identified in the present studies.

CYP1A1 knockdown does not affect ROS production or the mitochondrial membrane potential.

To gain more insight into the exact mechanism by which CYP1A1 regulates downstream signaling pathways, we determined the effects of CYP1A1 knockdown on reactive oxygen species (ROS) production and mitochondrial membrane potential (MΦ). ROS production as measured by DHE and DCFDA staining, two markers of superoxide and hydrogen peroxide formation. Even though it has been suggested that CYP1A1 promotes ROS production (Nebert et al. 2000), under the conditions tested we did not observe any changes in ROS production (**Figure III.10**). Because of CYP1A1 localization to the mitochondria (Addya et al. 1997), we tested whether CYP1A1 silencing affects the MΦ. Two independent methods were utilized to measure the MΦ, a plate reader assay and flow cytometry assays as described in Chapter II. Under the context of these experiments, CYP1A1 silencing does not result in changes to the mitochondrial membrane potential (**Table III.1**). Together, these results suggest that under these conditions CYP1A1 regulates ERK1/2, AKT, AMPK, and P70S6K through mechanisms other than affecting ROS production or the mitochondrial membrane potential.

57

DISCUSSION

CYP1A1 in breast cancer biology

Recent studies showing that CYP1A1 is expressed in breast tumors (Murray et al. 2010; Vinothini and Nagini 2010) led us to investigate the functional roles of CYP1A1 in the proliferation, survival, and signal transduction of breast cancer cells. Although CYP1A1 has been extensively studied in context of extrahepatic drug metabolism, little is known about its roles in cancer progression and cancer cell signal transduction in the absence of xenobiotics. In this study we provide evidence that CYP1A1 silencing impairs proliferation and survival, in part, through activation of AMPK phosphorylation and reduction of AKT, ERK, and P70S6K signaling. These results mean that CYP1A1 is not only involved in the metabolism of xenobiotics, but has its own role in breast cancer progression.

The PI3K/AKT and the MEK/ERK pathways are critical for breast cancer progression (Sivaraman et al. 1997; Xing and Imagawa 1999; Sun et al. 2001a; Sun et al. 2001b). Knockdown of CYP1A1 correlates with decreased phosphorylation of AKT (Ser473) and ERK1/2 (Thr202/Tyr204). CYP1A1 silencing also correlates with induction of AMPK tumor suppressor via phosphorylation of Thr172 in the catalytic subunit alpha. The AKT oncogene promotes proliferation via inhibition of the TSC1/TSC2 complex upstream of the mTOR/P70S6K pathway (Manning et al. 2002). In contrast, AMPK activates the TSC1/TSC2 complex thereby inhibiting protein synthesis and growth (Inoki

et al. 2003; Corradetti et al. 2004). In this manner AKT and AMPK signaling converge on P70S6K to regulate cell proliferation (Fingar et al. 2004; Zhao et al. 2010).

The effects of CYP1A1 knockdown on cell proliferation correlate with cell cycle arrest and increased apoptosis. Our results indicate that cyclin D1 is suppressed by CYP1A1 knockdown and correlates with a decrease in G1 to S cell cycle progression. In contrast, in the absence of TCDD induction, AhR knockdown does not appear to significantly affect basal CYP1A1 expression (**Figure III.8 A**), cyclin D1 or cell cycle profile (Abdelrahim et al. 2003). AKT and ERK1/2 promote G1-S transition of the cell cycle by stabilizing cyclin D1, while AMPK activation inhibits this transition by decreasing cyclin D1 levels, (Lavoie et al. 1996; Diehl et al. 1998; Meloche and Pouyssegur 2007; Zhuang and Miskimins 2008). Additionally, AKT and ERK1/2 regulate apoptosis through the anti-apoptotic protein survivin (Fornaro et al. 2003; Asanuma et al. 2005). Other feedback regulations between AKT, ERK1/2, and AMPK have also been described (Kovacic et al. 2003; Du et al. 2008; Kim et al. 2010; Tao et al. 2010). Therefore, based on these previous findings, the effects of CYP1A1 silencing on proliferation, cell cycle, and apoptosis are consistent with inhibition of AKT, ERK1/2, and P70S6K and activation of AMPK signaling. Moreover, our results showing that AMPK inhibition by compound C abrogates CYP1A1siRNA-mediated apoptosis further suggest that CYP1A1 signals through AMPK.

In light of previous findings and the evidence presented in this study we propose a model where CYP1A1 silencing inhibits AKT and ERK phosphorylation, thereby activating AMPK signaling (**Figure III.11**; steps 1-4). AMPK activation and concurrent loss of AKT signaling results in the inhibition of mTOR/P70S6K signaling (**Figure III.11**;

steps 5-8) which consequently decreases synthesis of proliferative and pro-survival proteins such as cyclin D1 and survivin (**Figure III.11**; step 9). These findings differ from other cytochrome P450 enzymes, such as CYP3A4, which may act primarily through activation of STAT3 and regulation of the G2-M checkpoint (Mitra et al. 2011). Our model, however, presents its limitations as it remains to be determined the CYP1A1 functions that affect these signaling pathways. The results presented suggest that CYP1A1 expression is critical for these biological functions and the roles of CYP1A1 in cancer cell growth may not be abrogated by inhibition of its measurable (EROD) enzymatic activity alone. Moreover, it is possible that CYP1A1 may be carrying functions distinct from its canonical metabolic functions. Novel hypotheses regarding non-enzymatic and enzymatic functions of CYP1A1 in cancer cell growth remain to be investigated.

Clinical impact

Inhibition of the PI3K/AKT and MEK/ERK pathways correlating with CYP1A1 silencing is important because cross talk between these pathways displays synergistic effects when combined inhibition is utilized for cancer therapeutics (She et al. 2010). The involvement of CYP1A1 in both pathways suggests that CYP1A1 may be a promising target for cancer therapeutics. Furthermore, because CYP1A1 silencing significantly inhibits proliferation and survival of ER+ and triple-negative breast cancer lines, the results presented in this study may have therapeutic implications for breast cancer independent of ER status. The effect of CYP1A1 knockdown on cell death appears to be

greater in ER+ MCF7 line than in triple-negative MDA-MB-231 line, whereas both lines appear to be strongly inhibited at the G1/S checkpoint. Whether strategies to inhibit CYP1A1 would be more effective in ER+ compared to triple-negative breast cancer or effective in both remains to be determined.

The widespread expression of CYP1A1 in breast cancer has been exploited as a strategy to activate pro-drug compounds to cytotoxic intratumoral metabolites. For example, drugs of the 2-(4-aminophenyl)benzothiazole class such as 5F 203 (Phortress) (Leong et al. 2003) and aminoflavone drugs (McLean et al. 2008) exhibit potent anti-tumor properties in xenograft models and have been moved forward to clinical trials (Chua et al. 2000; Leong et al. 2003; Fichtner et al. 2004; Nandekar and Sangamwar 2012). The proposed mechanism of action is that these agents induce and are activated by CYP1A1 into electrophilic metabolites that bind to and damage DNA, thus resulting in tumor growth arrest. Of considerable interest, the benzothiazoles and aminoflavone appear to be active in ER+ but not triple negative breast cancer (Leong et al. 2003; Trapani et al. 2003). Our results suggest that an alternative approach to exploit CYP1A1 expression in breast cancer through reduction of basal levels may extend the range of CYP1A1 targeted approaches to triple negative breast cancer.

Consistent with observations in other cell types (Johnson et al. 2008; Johnson et al. 2010; Mohebati et al. 2012), our results indicate that carnosol treatment inhibits breast cancer cell proliferation. This inhibition of proliferation in breast cancer lines is associated with reduced CYP1A1 expression and activation of AMPK, which has not been previously described in breast cancer. While the activation of AMPK phosphorylation by carnosol may be part of a generalized stress response, these results

provide new mechanistic information that carnosol is likely to affect bioenergetics in breast cancer in addition to exhibiting antioxidant properties. Our results suggest that the relevant target of carnosol in breast cancer may be reduction of CYP1A1 levels, resulting in AMPK phosphorylation, rather than modulation of AhR. The studies presented here suggest that reduction of CYP1A1 levels is a potential therapeutic strategy for breast cancer and that carnosol may be an approach to actualize this strategy.

In summary, we show that the basal level of CYP1A1, independent of measurable enzymatic (EROD) activity and AhR status, is important for breast cancer proliferation and survival. The identification of widespread expression of CYP1A1 in breast cancer suggests that its therapeutic potential could be exploited, either by induction followed by metabolism of pro-drugs to DNA damaging agents (Chua et al. 2000; Bradshaw et al. 2001; Leong et al. 2003) or by a new approach of CYP1A1 reduction. Our study suggests that strategies that directly lower CYP1A1 levels using RNA silencing or carnosol may be a potential new approach for breast cancer therapeutics.

FIGURES

A)
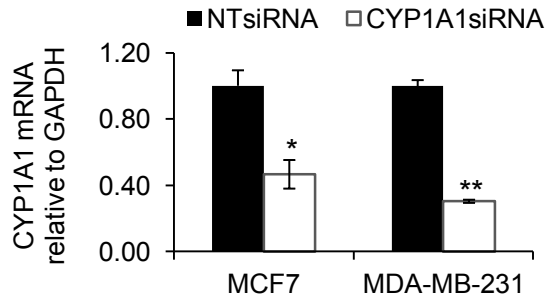
B)
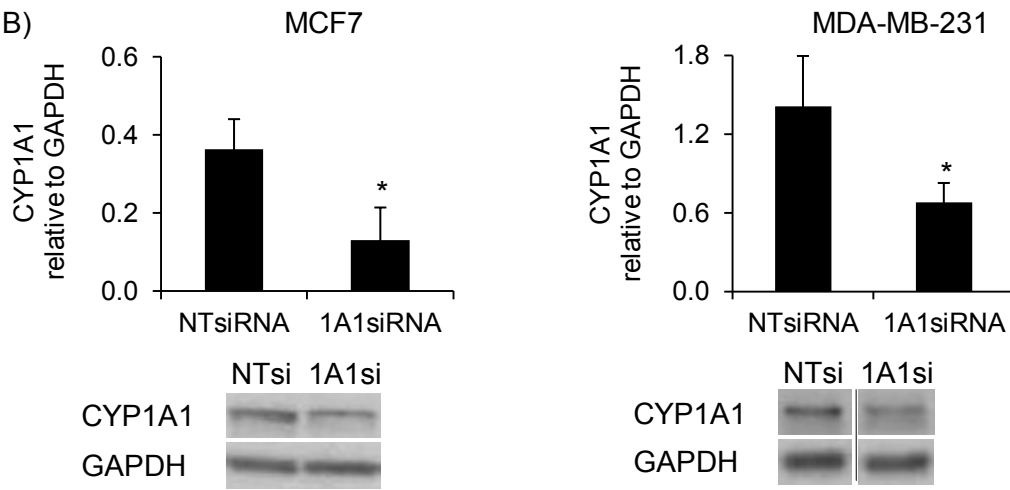
C) MCF7
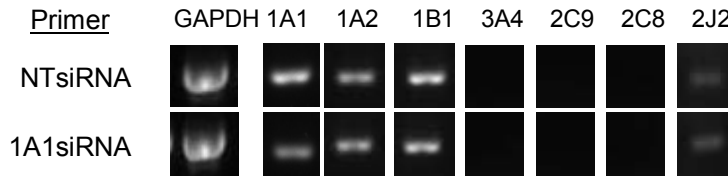
D) MDA-MB-231
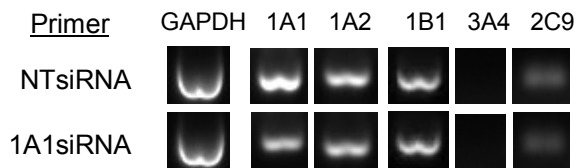
Figure III.1. CYP1A1siRNA knockdown efficiency and specificity.

CYP1A1siRNA knockdown in MCF7 and MDA-MB-231 cells was evaluated by quantitative RT-PCR (A) and by western blot (B). To evaluate siRNA specificity semi-quantitative RT-PCR was performed with the indicated primers and the products were run in 1.5% agarose gel (C-D). (n = 3, * $p < 0.05$, ** $p < 0.001$)
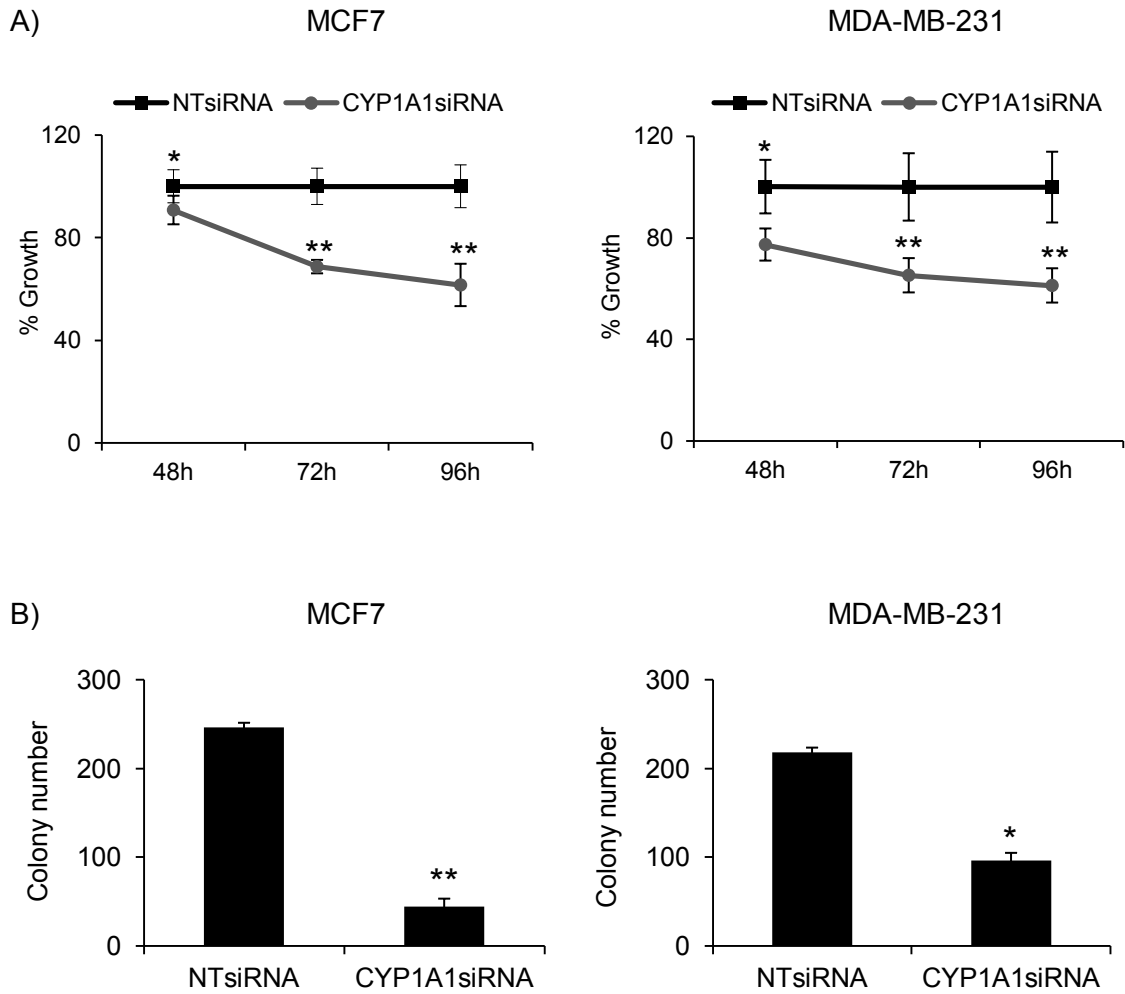
Figure III.2. CYP1A1 knockdown impairs breast cancer cell proliferation and survival.

(A) MTT proliferation experiments for lines MCF7 and MDA-MB-231 after transfection with CYP1A1siRNA for the indicated times. (B) Clonogenicity was evaluated by transfection for 48 hours followed by seeding of two-hundred transfected cells onto fibronectin-coated 6-well plates. Visible colonies were stained and counted after 14 days of culture. (n = 3, *p < 0.05, ** p < 0.001)

A) MCF7
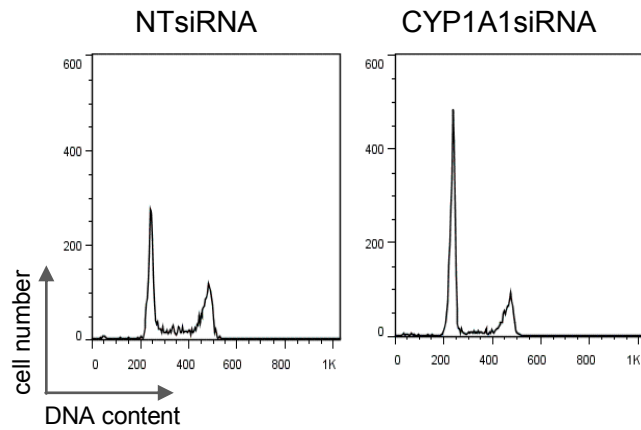
	G0/G1	S	G2/M
NTsiRNA	40.01	28.79	34.55
1A1siRNA	63.51	18.22	22.11
% Difference	37%	-58%	-56%
P	0.001*	0.011*	0.009*

B) MDA-MB-231
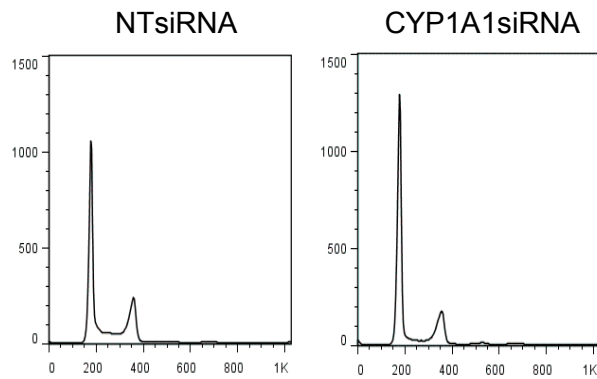
	G0/G1	S	G2/M
NTsiRNA	49.36	28.03	16.40
1A1siRNA	62.01	18.60	12.65
% Difference	20%	-51%	-30%
P	0.003*	0.001*	0.002*

C)
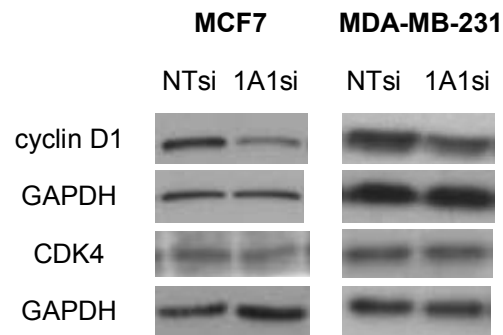
MCF7   MDA-MB-231

	MCF7		MDA231	
	Fold change	*P*	Fold change	*P*
Cyclin D1	0.26	0.001*	0.64	0.001*
CDK4	0.51	0.136	0.75	0.162

Figure III.3. CYP1A1 knockdown blocks the cell cycle.

(A-B) Cell cycle distribution was assessed by flow cytometry of MCF7 and MDA-MB-231 cells transfected for 48 hours and stained with propidium iodide. (C) Cyclin D1 and CDK4 proteins were visualized by western blot. Fold changes are expressed relative to CYP1A1siRNA knockdown (n = 3, p values shown, * indicates statistical significance).

A)

MCF7   MDA-MB-231

NTsiRNA   CYP1A1siRNA   NTsiRNA   CYP1A1siRNA

PI

AnnexinV-FITC
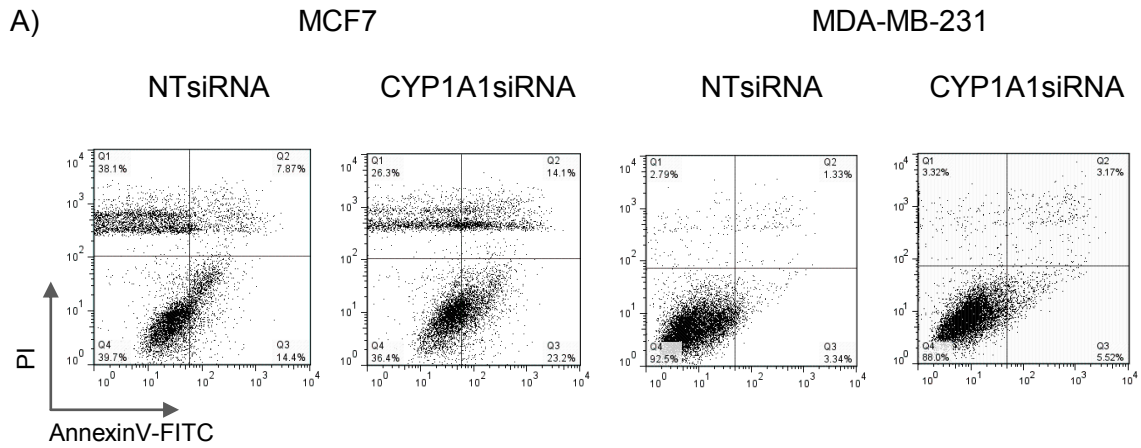
MCF7	Early	Late	Necrotic	Viable
NTsiRNA	12.40	7.68	32.73	47.23
CYP1A1siRNA	24.97	14.90	22.77	37.37
% Difference	50%	48%	-44%	-26%
P	0.043*	0.004*	0.154	0.067

MDA-MB-231	Early	Late	Necrotic	Viable
NTsiRNA	3.71	1.47	2.58	92.23
CYP1A1siRNA	5.47	3.07	2.92	88.53
% Difference	32%	52%	12%	-4%
P	0.142	0.006*	0.401	0.070

B)

MCF7   MDA-MB-231
NTsi 1A1si   NTsi 1A1si

survivin

GAPDH
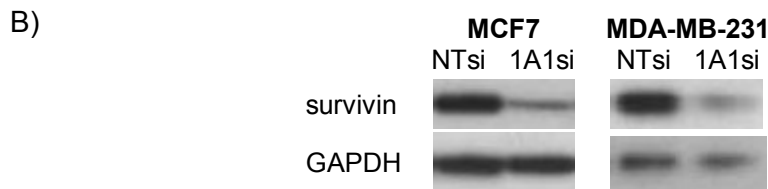
	MCF7		MDA231	
	Fold change	*P*	Fold change	*P*
survivin	0.19	0.003	0.44	0.041

68

Figure III.4. CYP1A1 knockdown increases cell death.

(A) Apoptosis was assessed by flow cytometry of MDA-MB-231 or MCF7 cells

transfected for 48 hours and stained with propidium iodine and Annexin V-FITC. (B)

Survivin protein was visualized by western blot. Fold changes are expressed relative to

CYP1A1siRNA knockdown (n = 3, p values shown, * indicates statistical significance).

Legend: Early, early apoptotic population in the lower right quadrant; Late, late apoptotic

population in the upper right quadrant; Necrotic, necrotic population in the upper left

quadrant; Viable, alive population in the lower left quadrant.

A) Western blot

	MCF7		MDA-MB-231	
	NTsi	1A1si	NTsi	1A1si

phospho AKT

total AKT

GAPDH

phospho ERK1/2

total ERK1/2

GAPDH

phospho AMPK

total AMPK

GAPDH

phospho P70S6K

total P70S6K

GAPDH
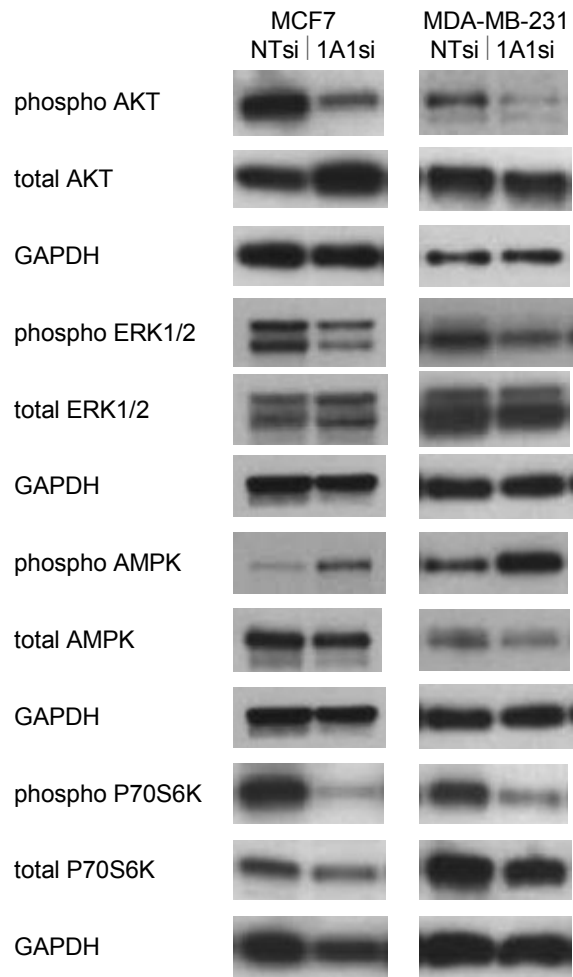
B) Quantification

	MCF7		MDA-MB-231	
	Fold change	P	Fold change	P
p- AKT	0.55	0.02*	0.37	0.004*
t- AKT	1.61	0.04*	1.27	0.41
Fractional-phospho	*0.39*	*0.01**	*0.33*	*0.02**
p- ERK1/2	0.55	0.001*	0.71	0.02*
t- ERK1/2	1.22	0.18	1.01	0.93
Fractional-phospho	*0.45*	*0.002**	*0.71*	*0.05**
p- AMPK	5.64	0.01*	2.42	0.02*
t- AMPK	1.00	0.99	0.98	0.97
Fractional-phospho	*5.62*	*0.003**	*3.30*	*0.01**
p-P70S6k	0.47	0.001*	0.63	0.03*
t-P70S6K	0.96	0.88	0.84	0.37
Fractional-phospho	*0.57*	*0.02**	*0.72*	*0.02**

Figure III.5. CYP1A1 knockdown inhibits ERK1/2 and AKT and activates AMPK.

(A) The effects of CYP1A1siRNA on downstream signaling were evaluated by western blot of cells transfected for 72-120 hours. (B) Fold changes are expressed relative to CYP1A1siRNA knockdown (n = 3, p values shown, * indicates statistical significance). Fractional phosphorylation results are included (*Fractional-phospho*= phosphorylated / total protein).

NTsi + DMSO   1A1si + DMSO   NTsi + Comp C   1A1si + Comp C
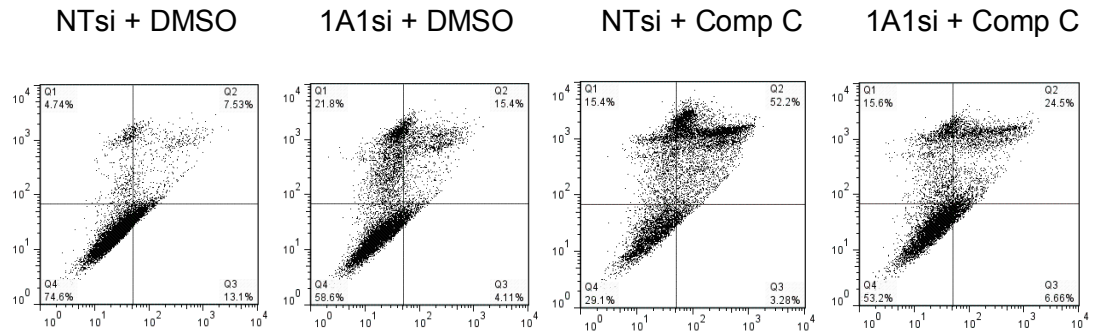
siRNA	→	Treatment	Σ Dead	Early	Late	Necrotic	Viable
NTsi	→	DMSO	27.3	13.2	9.8	4.2	72.7
NTsi	→	Comp C	71.7**	3.1**	49.2**	19.4*	28.3**
1A1si	→	DMSO	43.7	5.5	20.1	18.2	55.6
1A1si	→	Comp C	46.4	6.7	25.5	14.3	53.6

Diagram of potential outcomes:

NTsiRNA
- DMSO ⟶ Basal cell death
- CC ⊣ AMPK ⟶ Cell death induced by CC

1A1siRNA
- DMSO ⟶ Cell death induced by 1A1si
- CC ⊣ AMPK ⟶ Outcome 1: ↔ or ↓ cell death than 1A1si + DMSO
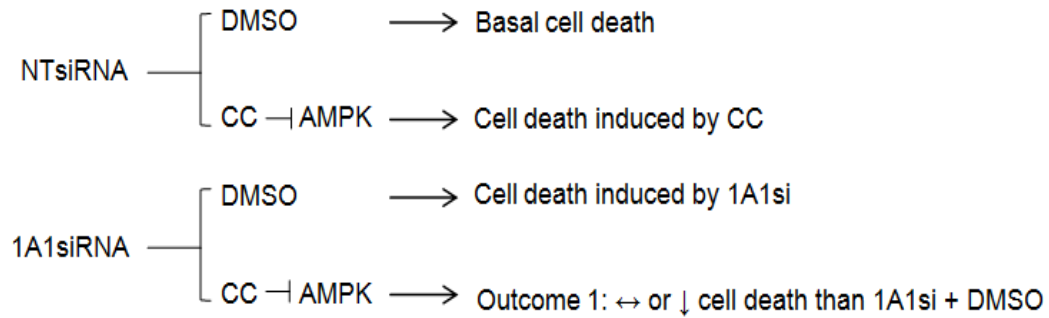
OR

Outcome 2: ↑↑ cell death due to CC plus 1A1siRNA pro-apoptotic effects

72

Figure III.6. AMPK inhibition partially abrogates CYP1A1siRNA-mediated apoptosis.

To support the hypothesis that the pro-apoptotic effects of CYP1A1siRNA require AMPK, MCF7 cells were transfected for 24 hours and then treated with 10 μmol/L of the AMPK inhibitor compound C for 24 hours. Cells were collected, stained with propidium iodide and Annexin V-FITC, and analyzed by flow cytometry. A diagram of expected outcomes is included, outcome 1 was observed in our experiments. (n = 3, * $p < 0.01$, ** $p < 0.001$, comparison between DMSO and compound C treatment)

A)

MCF7

MDA-MB-231

B)
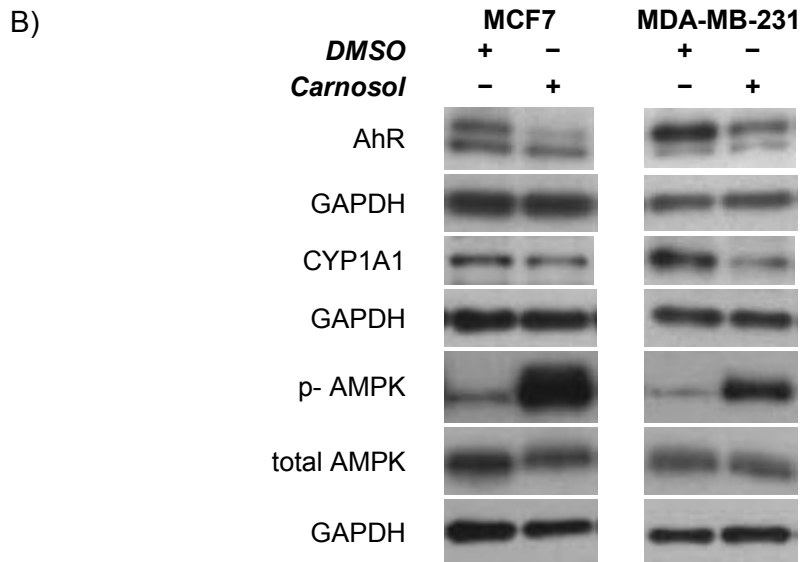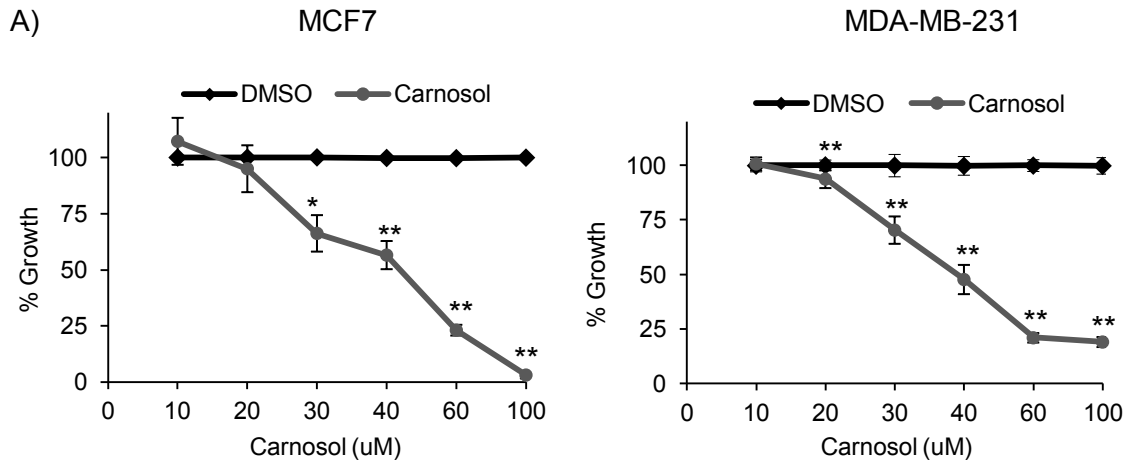
	MCF7		MDA-MB-231	
	Fold change	*P*	Fold change	*P*
CYP1A1	0.72	0.03*	0.40	2.5E-4**
AhR	0.34	0.03*	0.43	2.2E-4**
p- AMPK	4.57	8.5E-5**	5.20	0.01*
t- AMPK	0.78	0.10	0.77	0.56

74

Figure III.7. The AhR inhibitor carnosol impairs proliferation, in part, via reduction of CYP1A1 and activation of AMPK.

Carnosol treatment was used as an independent method to reduce CYP1A1 levels and evaluate downstream signaling. (A) The IC$_{50}$ of carnosol was determined by MTT assay. (B) Cell extracts were collected after treatment with 40 µmol/L carnosol for 8 hours the indicated proteins were evaluated by western blot. Fold changes are expressed relative to CYP1A1siRNA knockdown (n = 3, * $p < 0.05$, ** $p < 0.001$).

A)

MCF7

MDA-MB-231

← AhR (95kDa)

B)

MCF7

MDA-MB-231

76
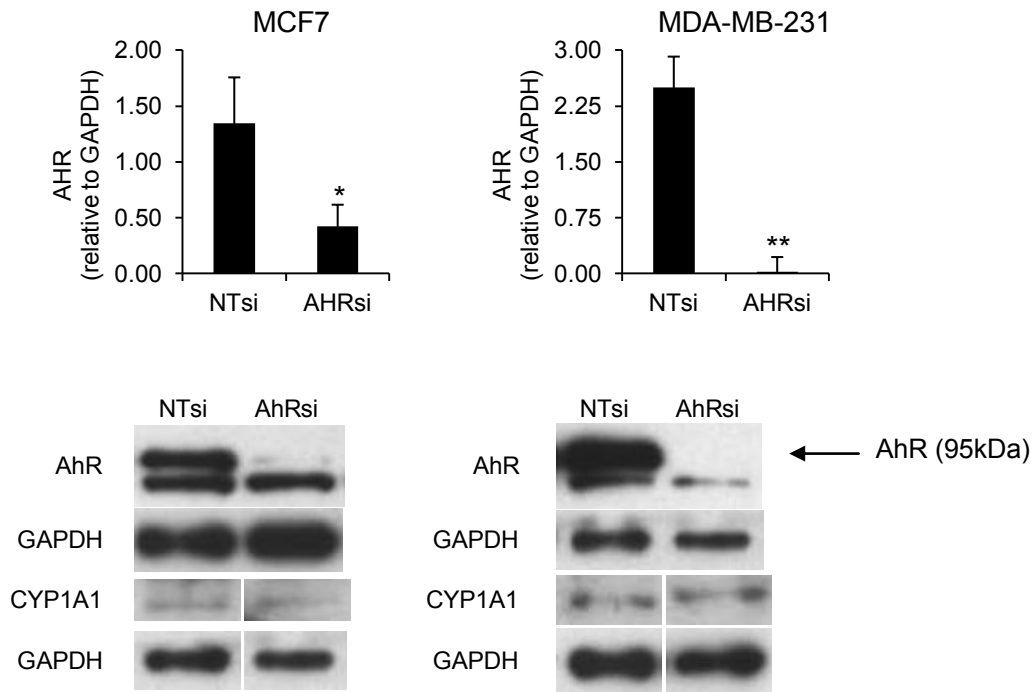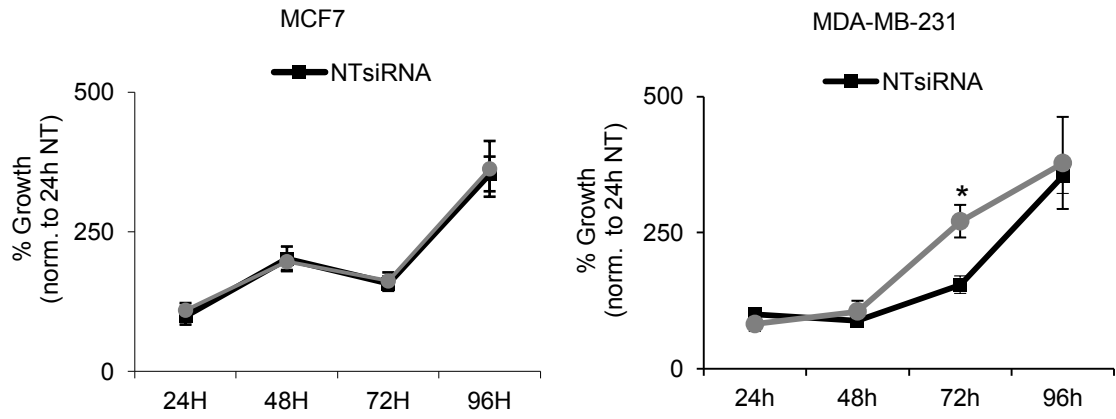
C
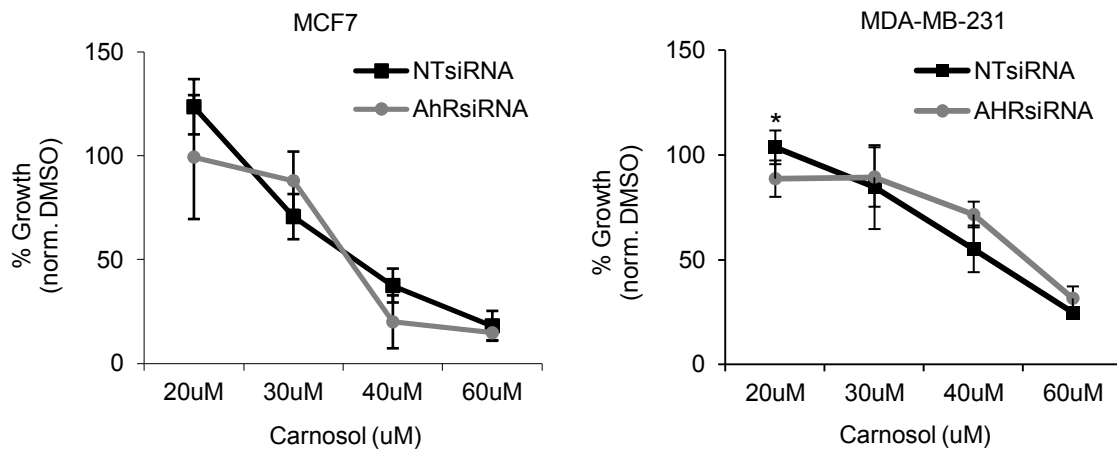
Figure III.8 Effect of AhRsiRNA on the growth of breast cancer cells.

(A) Cells were transfect with AhRsiRNA for 96 hours and the protein levels of AhR and

CYP1A1 were assessed by Western blot. The white lines indicate the blot was cut, the

lanes shown are representative of triplicates and each GAPDH corresponds to the same

lane of the protein probed. (B) Cells were transfected with AhRsiRNA and cell viability

was measured by MTT assay at the indicated times; % growth was normalized to vehicle

treatment at 24 hours. (C) Cells were transfected with NTsiRNA or AhRsiRNA for 48

hours and then treated with 20-40 μmol/L carnosol for 48 hours. Cell viability was

measured by MTT assay and % growth was normalized to vehicle treatment. (n = 3, * $p < 0.05$)
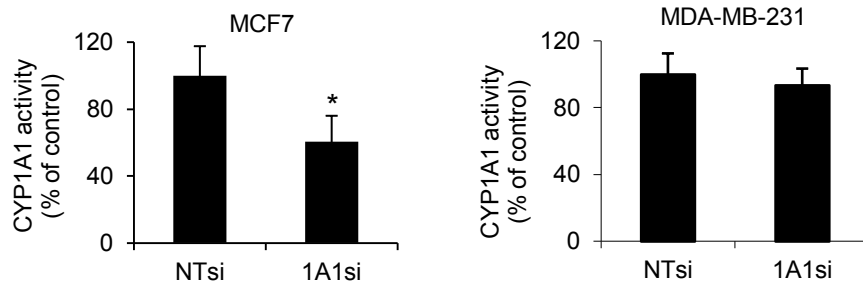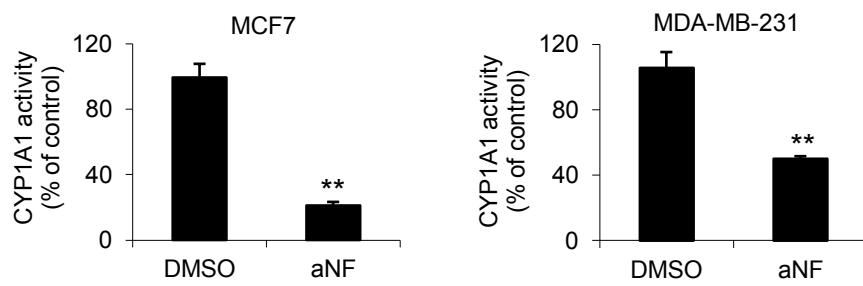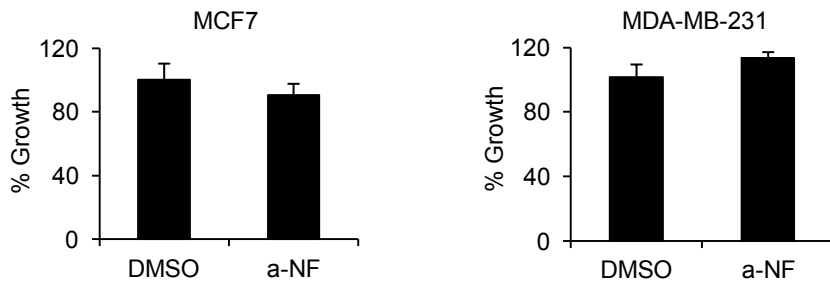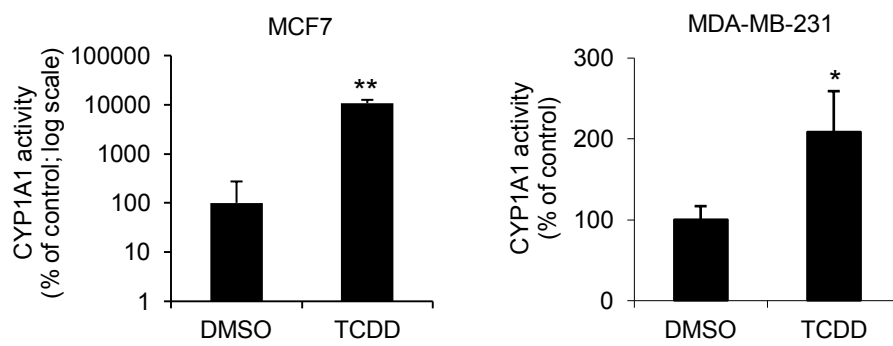
E
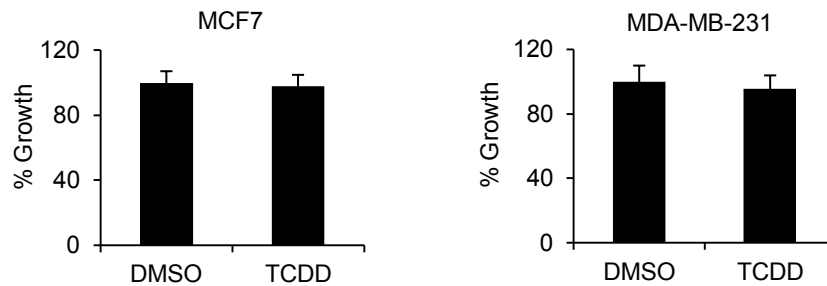
Figure III.9 Effect of modulation of CYP1A1 activity on the growth of breast cancer cells.

CYP1A1 activity was measured by EROD assay after treatment with (A) CYP1A1siRNA for 48 hours, (B) 1 μmol/L alpha-naphthoflavone for 72 hours or (C) 10 nmol/L TCDD for 24 hours. Cells were co-treated with 10 nmol/L TCDD for 24 hours prior to EROD assay. For (A), EROD fluorescence was normalized to total cell number. Activity is displayed as % of control; n = 3. Cells viability was measured by MTT assay after treatment with (C) 1 μmol/L alpha-naphthoflavone or (E) 10 nmol/L of TCDD for 72 hours. The % growth was normalized to vehicle treatment; n = 7. (* $p < 0.05$, ** $p < 0.001$)

DHE   DCFDA
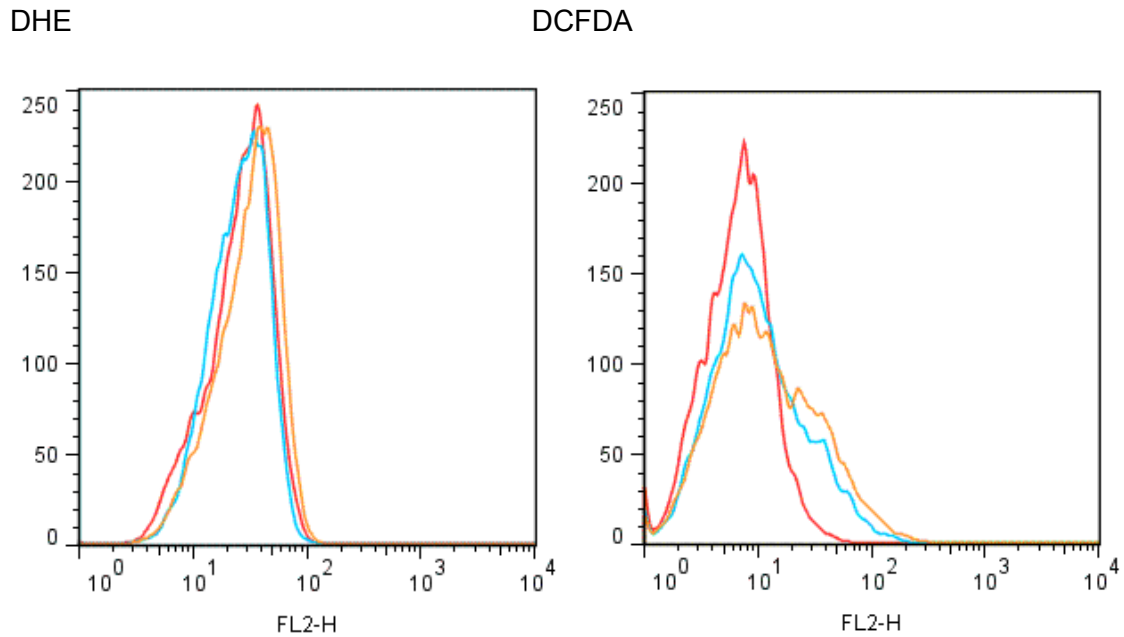
Figure III.10. CYP1A1 knockdown does not affect ROS production.

MCF7 cells were transfected for 48 hours, collected and stained with 2 µmol/L DHE or

10 µmol/L DCFDA, and analyzed by flow cytometry. MCF7 cells treated with 250 µmol/L

hydrogen peroxide for 2 hours served as positive control. A shift to the right and an

increase in the peak intensity indicate increase in ROS production. Experiment

performed in triplicate, representative samples are shown above. Legend: red, hydrogen

peroxide; blue, NTsiRNA; orange, CYP1A1siRNA

A) Plate reader assay

	Replicate 1			Replicate 2		
	AVG	Fold change	p value	AVG	Fold change	p value
NTsiRNA	0.15	1.27	0.176	0.375	0.74	1.5E-14
CYP1A1siRNA	0.19			0.279		
NT+CCCP	0.17	1.14	0.219	0.428	1.14	3.8E-12

B) FACS

	Healthy	Depolarized
NTsiRNA	45.5	47.9
CYP1A1siRNA	42.3	49.4
CCCP	30.8	64.5
Fold change	0.93	1.03
p value	0.690	0.822

Table III.1. CYP1A1 knockdown does not affect mitochondrial membrane potential.
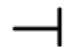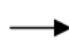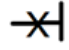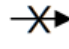
MCF7 cells were transfected with CYP1A1siRNA for 48 hours and mitochondrial membrane potential was assessed as follow. A) Fluorescent plate reader measurements of JC-1 aggregates at excitation 485 nm and emissions 528 nm and 600 nm. The average and fold change indicate the normalized loss of mitochondrial membrane potential (arbitrary units). B) Transfected cells were treated with JC-1, collected and analyzed by flow cytometry. Depolarized refers to the population with loss of mitochondrial membrane potential.
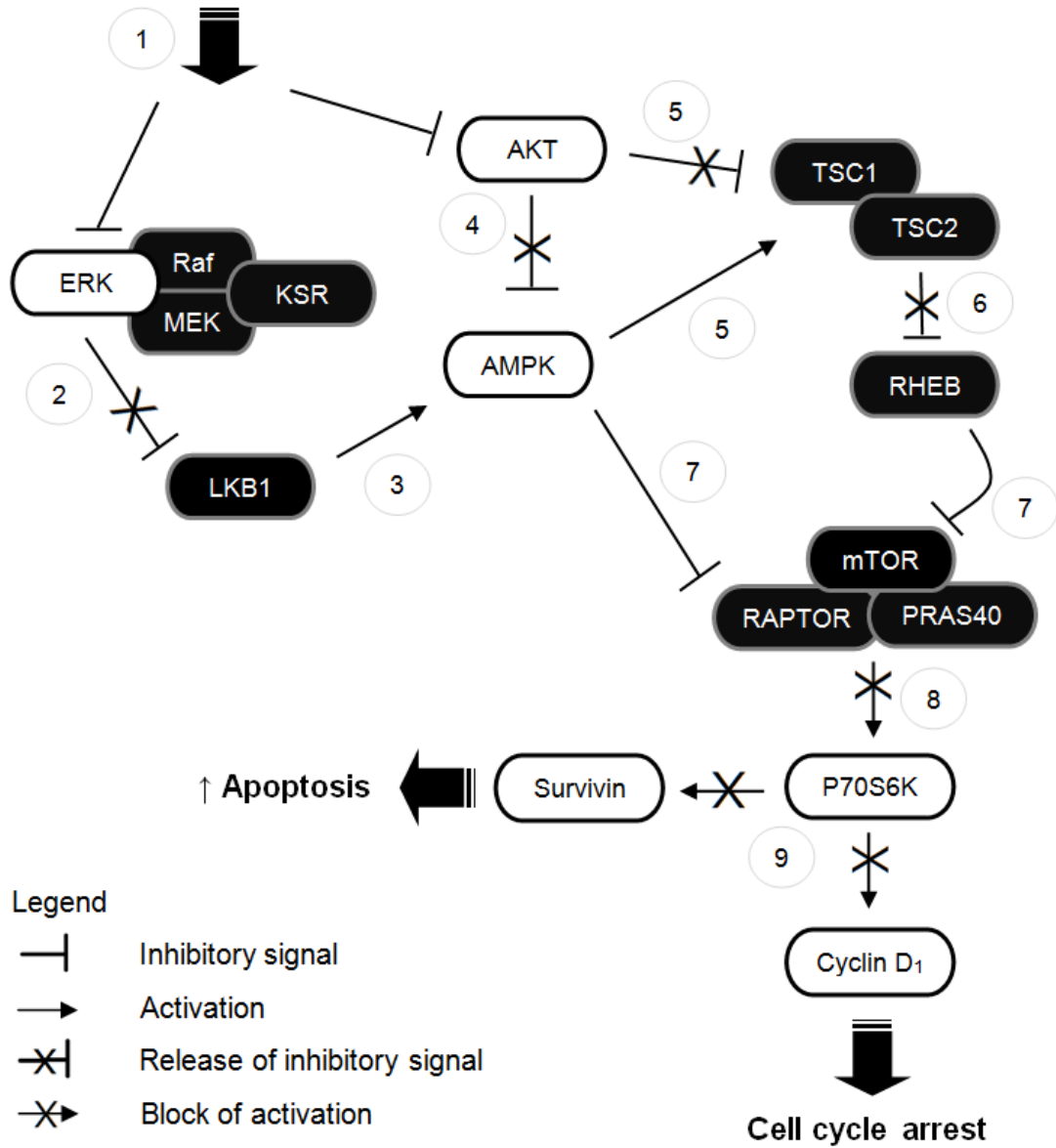
Figure III.11. Possible mechanisms of action of CYP1A1 knockdown.

CYP1A1 knockdown by siRNA results in the dual inactivation ERK and AKT (1). Inactivation of ERK could presumably remove the suppressive pressure that this exerts on LKB1 (2), thereby allowing activation of AMPK (3). LKB1-independent mechanisms may also be possible. In addition, inhibition of AKT could result in the release of its suppressive effect on AMPK (4). Alternatively, inhibition of AKT by CYP1A1siRNA could result in the release of the TSC1/2 complex from suppression(5), followed by release of Ras homolog enriched in brain (RHEB) (6), and subsequent inhibition of mTOR signaling (7). Alternatively, AMPK could directly activate TSC2 (5) and inhibit RAPTOR (7), thereby inhibiting mTOR signaling (8). In this manner CYP1A1siRNA treatment results in cell-cycle arrest and increased apoptosis (9). In summary, we propose that CYP1A1siRNA-mediated inhibition of ERK1/2 and/or AKT results in AMPK activation, thereby inhibiting the mTOR/P70S6K pathway and thus resulting in cellular death.

CHAPTER IV

Potential Metabolite Mechanisms
of CYP1A1 Function

INTRODUCTION

In Chapter II we showed that CYP1A1 contributes to breast cancer progression via regulation of proliferation and survival signaling pathways (Rodriguez and Potter 2013). We propose that CYP1A1 may potentially mediate these effects in two ways: (a) the metabolic activation of a substrate and/or (b) the metabolic inactivation of an anti-proliferative or pro-apoptotic substrate. In our attempt to identify such substrate, we investigated whether CYP1A1-mediated metabolism of retinoic acid, arachidonic acid, eicosapentaenoic acid, and pregnenolone may play a role in breast cancer.

The present chapter is divided into two main sections. **Section 1** addresses the general hypothesis that specific substrates and metabolites of CYP1A1 can complement the effects of CYP1A1 knockdown. Specifically, we investigated (a) known CYP1A1 substrates: all-*trans*-retinoic acid, 9-*cis* retinoic acid, 13-*cis* retinoic acid and pregnenolone and (b) known CYP1A1-derived metabolites: 5,6- epoxyeicosatrienoic acid, 8,9- epoxyeicosatrienoic acid, 11,12- epoxyeicosatrienoic acid, 14,15- epoxyeicosatrienoic acid, 20-hydroxyeicosatetraenoic acid, and 17,18-

epoxyeicosatetraenoic acid. **Section 2** addresses the hypothesis that CYP1A1's proliferative and survival effects on breast cancer could potential be mediated by 17,18-EpETE.

Retinoic acids

Retinoic acids (RAs) are products of vitamin A (retinol) metabolism by several dehydrogenases and cytochrome P450 enzymes. The growth inhibitory mechanisms of RA in cancer have been studied extensively (Tang and Gudas 2011). Most relevant to our study, all-*trans*-retinoic acid (ATRA), 9-*cis* retinoic acid (9-*c*RA) and 13-*cis* retinoic acid (13-*c*RA) have been shown to inhibit the proliferation of breast cancer line MCF7 (Seewaldt et al. 1995; Van heusden et al. 1998). It has been proposed that the metabolism of RA protects from its intrinsic growth-inhibitory effects. For example, CYP26 has been shown to protect cells from excess RA by metabolizing it primarily to 4-OH-*trans*RA (White et al. 1996; Sonneveld et al. 1998).

CYP1A1 metabolizes retinol to ATRA and further metabolizes ATRA by catalyzing a 4-hydroxilation to form all-*trans*-4-hydroxy retinoic acid (4-OH-tRA) (Chen et al. 2000; McSorley and Daly 2000; Zhang et al. 2000). CYP1A1 also catalyses the oxidation of 9-*c*RA, and 13-*c*RA (Zhang et al. 2000). Therefore, we propose that CYP1A1 protects breast cancer cells from death by metabolizing RA to non-cytotoxic metabolites. We tested the hypothesis that silencing of CYP1A1 abrogates its protective effects on MCF7 cells, consequently sensitizing the cells to RA treatment.

Pregnenolone

Pregnenolone (3α,5-tetrahydroprogesterone) is the precursor of steroid hormones such as androgens, estrogens, and progestogens relevant to hormone-dependent cancers (Ryan and Engel 1957; Neher and Wettstein 1960; West and Naville 1962; Kuhn and Briley 1970; Thibier-Fouchet et al. 1976). Although little is known regarding the direct role of pregnenolone in breast cancer, evidence showing that breast tumors convert pregnenolone to steroid hormones *in situ*, supports the notion that tumors may rely on pregnenolone metabolism to maintain their hormone supply (Abul-Hajj et al. 1979).

CYP1A1 catalyzes the 16α- and 17α- hydroxylation of pregnenolone to 16α-hydroxypregnenolone and 17α-hydroxypregnenolone (Niwa et al. 1998), which are precursors of steroid hormones. We propose that CYP1A1 may promote breast cancer progression, in part, through metabolism of pregnenolone. Therefore we hypothesized that CYP1A1 silencing results in an excess supply of pregnenolone thereby inhibiting proliferation of breast cancer cells.

Eicosanoids

Epoxyeicosatrienoic acids (EETs), such as 5,6-EET, 8,9-EET, 11,12-EET and 14,15-EET, are eicosanoids derived from arachidonic acid metabolism by cytochrome P450 epoxygenases and are known mediators of multiple cellular processes. Of particular interest is 14,15-EET which has been shown to stimulate proliferation of

epithelial (Chen et al. 1998; Chen et al. 1999) and breast cancer cells (Mitra et al. 2011).

Moreover, *in vivo* carcinoma models demonstrated that EETs promote tumor growth and

metastasis (Panigrahy et al. 2012).

The eicosanoid 20-hydroxyeicosatetraenoic acid (20-HETE) exhibits biological

effects that appear to be cell-context dependent. Effects of exposure to 20-HETE range

from proliferative effects (Lin et al. 1995; Yu et al. 2012), to growth-inhibitory effects

(Liang et al. 2008), and even lack of effects has been reported (Chen et al. 1998).

Metabolism of eicosapentaenoic acid (commonly found in fish oil) by CYP1A1

selectively results is synthesis of 17,18-epoxyeicosatetraenoic acid (17,18-EpETE)

(Schwarz et al. 2004). Although 17,18-EpETE has been largely understudied and the

few known functions involve anti-inflammatory activity, for example in lung and heart

tissues (Morin et al. 2009; Schmelzle et al. 2011).

CYP1A1 metabolizes arachidonic acid to 5,6-EET, 8,9-EET, 11,12-EET, 14,15-

EET, and 20-HETE and eicosapentaenoic acid to 17,18-EpETE (**Figure IV.6** and

(Choudhary et al. 2004; Schwarz et al. 2004; Bui et al. 2011)). We hypothesized that if

CYP1A1 promotes breast cancer proliferation through synthesis of any of these

eicosanoids, treatment with these eicosanoids should rescue the cells from the growth-

inhibitory effects of CYP1A1 silencing.

RESULTS- SECTION 1

Effects of retinoic acid on CYP1A1siRNA-transfected MCF7 cells

We tested the hypothesis that CYP1A1 silencing sensitizes MCF7 cells to RA treatment. To test this, MCF7 cells were cultured in 6-well plates, transfected with NTsiRNA or CYP1A1siRNA for 48 hours, and treated with 3 µmol/L of ATRA, 9-cRA, 13-cRA, or vehicle (DMSO) for 48 hours. Cell viability was assessed by MTT assay and proliferation (% growth) was calculated relative to DMSO-treated NTsiRNA cells. Surprisingly, none of the retinoic acids showed inhibition of proliferation of the NTsiRNA-transfected MCF7 cells. Similarly, no sensitization to RA retreatment was observed by CYP1A1 silencing (**Figure IV.1**). This suggests that the RA effects may be context dependent and that CYP1A1 metabolism of RA Is not required for the role of CYP1A1 in growth regulation.

Effects of pregnenolone on CYP1A1siRNA-transfected MCF7 cells

We hypothesized that cells transfected with CYP1A1siRNA will result in an excess supply of pregnenolone, thereby inhibiting the proliferation of breast cancer cells. The rationale is that cells with reduced expression of CYP1A1 will not be able to metabolize pregnenolone thus resulting in decreased production of steroid hormones that promote growth. To test this hypothesis we examined the ability of CYP1A1siRNA-transfected cells to proliferate in the presence of increasing doses of pregnenolone (i.e.

3 µmol/L and 40 µmol/L). We anticipated that CYP1A1siRNA-transfected cells to exhibit

enhanced growth inhibition when treated with pregnenolone in a dose-dependent

manner. As anticipated, pregnenolone inhibits proliferation of control (NTsiRNA) MCF7

cells in a dose-dependent manner. However, pregnenolone treatment did not enhance

the growth-inhibitory effects of CYP1A1siRNA (**Figure IV.2**). These results indicate that

metabolism of pregnenolone is not the primary mechanism by which CYP1A1 promotes

breast cancer proliferation and survival.

Effects of eicosanoids and CYP1A1 silencing on MCF7 cells

We hypothesized that treatment with eicosanoids restores the proliferation of

CYP1A1siRNA-transfected cells. To test this hypothesis, MCF7 cells were transfected

with CYP1A1siRNA for 48 hours, serum-starved for 24 hours, and treated with 1 µmol/L

of 8,9-, 11,12-, 14,15-EETs, 0.1-3 µmol/L 20-HETE, 3 µmol/L 17,18-EpETE, or vehicle

for 48 hours-72 hours. Following treatment, cell viability was assessed by MTT assay

and proliferation (% growth) was calculated relative to NTsiRNA-transfected cells treated

with vehicle.

In agreement with prior studies (Mitra et al. 2011), 11,12- and 14,15-EET

promotes proliferation of NTsiRNA-transfected MCF7 cells (**Figure IV.3 A**). Treatment

with 8,9-, 11,12-, and 14,15-EET increased the proliferation of CYP1A1siRNA-

transfected MCF7 cells (**Figure IV.3 A**). Albeit EETs partially restored the anti-

proliferative effects of CYP1A1 silencing, the magnitude of these effects were marginal

suggesting that EET synthesis may not be the primary mechanism by which CYP1A1 regulates breast cancer cell proliferation.

To investigate this further, we examined whether EET levels were affected by CYP1A1 silencing. We would expect EET levels to go down upon CYP1A1 silencing if EET synthesis is necessary for CYP1A1 proliferative effects. MCF7 cells transfected with NTsiRNA or CYP1A1siRNA for 72 hours and the levels of 8,9-, 11,12-, and 14,15-EETs were measured by mass spectrometry. CYP1A1 silencing modestly induced 8,9-EET levels but no change was observed in the levels of 11,12- and 14,15-EETs (**Figure IV.4 A**).

Treatment with 20-HETE induced proliferation of NTsiRNA-transfected cells but did not restore the proliferation of CYP1A1siRNA-transfected cells (**Figure IV.3 B**), indicating that it is not a primary mediator of CYP1A1 function. We and other have shown that CYP1A1 selectively metabolizes eicosapentaenoic acid to 17,18-EpETE (Morin et al. 2009) and Table IV. 1. These results led us to examine whether 17,18-EpETE complements CYP1A1 silencing. Treatment with 17,18-EpETE did not complement CYP1A1 silencing (**Figure IV.3 C**). However, CYP1A1 knockdown decreases synthesis of 17,18-EpETE in MCF7 line (**Figure IV.4 B**) which suggests that 17,18-EpETE may potentially have some relevance in the context of cancer biology. We explore this possibility in **Section 2**.

Taken together, in the context of these studies CYP1A1 promotes proliferative and survival signaling in breast cancer cells through mechanisms other than synthesis of 8,9-EET, 11,12-EET, 14,15-EET, 20-HETE, or 17,18-EpETE.

RESULTS- SECTION 2

Hypothesis and experimental approach

CYP1A1 selectively metabolizes eicosapentaenoic acid to 17,18-EpETE (**Table IV.1** and (Morin et al. 2009)). Mass spectrometry analysis of MDA-MB-231 and MCF7 cells revealed that these lines synthesize 17,18-EpETE (**Figure IV.6**). Furthermore, CYP1A1 knockdown in MCF7 line reduces the levels of 17,8-EpETE (**Figure IV.4 B**). Together, this evidence suggests that 17,18-EpETE may play a role in breast cancer biology. To test this hypothesis we purchased commercially available racemic 17,18-EpETE (Cayman Chemical Company, MI) to investigate the impact of treatment with exogenous 17,18-EpETE on various cell capabilities: cell proliferation, survival, migration, cell death, and cell signaling (Hanahan and Weinberg 2000). To avoid confounding effects of lipids in the serum medium, cells were serum-starved for 24 hours prior to treatment and maintained in serum-free conditions throughout the duration of the experiments, unless otherwise indicated (see **Chapter II** for specific methodology).

Limitations of this study

The series of experiments presented here were conducted over the course of two-years (2008-2010) utilizing multiple supplies of commercial 17,18-EpETE carrying the same lot number (Catalog No. 50861, Lot No. 0400015, various aliquot numbers, Cayman Chemical Company, MI). For quality assurance purposes these purchased

17,18-EpTE was routinely tested for biological activity (i.e. MTT assays and mass spectrometry analysis to confirm lipid identity). However, after approximately two years into this study, subsequent supplies of 17,18-EpETE purchased from Cayman Chemical failed to exhibit biological activity. In order to validate our previous results, Dr. J.R. (Camille) Falck, Ph.D., D.I.C. at the University of Texas South Western Medical Center kindly provided (R,S) and (S,R) stereoisomers of 17,18-EpETE. Proliferation studies performed with Dr. Falck's 17,18-EpETEs failed to reproduce previous results obtained with Cayman's 17,18-EpETE.

The two principal explanations for these discrepancies are: (a) 17,18-EpETE does exhibit biological effects but molecular changes in the cells have occurred (e.g. shift in lipid biosynthesis profile) thus making the cells less sensitive or dependent of 17,18-EpETE and/or (b) the commercial 17,18-EpETE supplies purchased contained a contaminant that was not detected through our quality control testing (e.g. *trans* lipids) but was responsible for the biological effects observed. With the technology and resources available to us at this time we are not able to distinguish between these or other possible explanations, nor can we validate or disprove our results.

Nevertheless, despite this major pitfall, we believe that it is necessary to make these results available to the scientific community in order to encourage future collaborations that can assist in overcoming these limitations. In Chapter V (*Future Directions*, page 132) we propose several approaches to characterize the exact role of 17,18-EpETE in breast cancer biology.

IMPORTANT NOTE: Throughout the remainder of this thesis we will refer to commercial 17,18-EpETE as *EpETE (Cayman Chemical Company, MI).

Quality control tests

In **Figure IV.5 A** we show a representative mass spectrometry spectrum of commercial 17,18-EpETE (i.e. *EpETE, Cayman Chemical) which exhibits the expected peak confirming that these samples do contain 17,18-EpETE. Samples provided by Dr. Falck were similarly validated by mass spectrometry (data not shown). We also routinely tested the biological effects of *EpETE (discussed below). To further validate that these effects are exclusive to *EpETE treatment, we performed a control experiment where *EpETE was hydrolyzed by acidifying an aliquot of *EpETE in water (pH < 3.0, HCl) and incubating it at $37^{o}C$ for 1 hour to accelerate the reaction. The acidified *EpETE solution was then brought to a concentration of 3 μmol/L with serum-free culture medium and to an alkaline pH suitable for cell culture. This hydrolysis destroys the activity of the epoxide ring and should abrogate the proliferative effects of *EpETE. As positive control, the integrity of the epoxide ring was protected by addition of an epoxide hydrolase inhibitor (1 μmol/L EHI 1471, gift from Dr. Hammock), thereby sustaining the proliferative effects of *EpETE. In this experiment MDA-MB-231 cells were subject to three types of treatment: a) 3 μmol/L *EpETE, b) 3 μmol/L hydrolyzed *EpETE, or c) 3 μmol/L *EpETE plus EHI. As shown in **Figure IV.5 B**, treatment with *EpETE or *EpETE+EHI promotes the proliferation of MDA-MB-231 line. In contrast hydrolysis of *EpETE abrogates these effects. Treatment with EHI alone partially promotes proliferation, presumably through protection of growth-promoting eicosanoids in the cell. However, the magnitude of the effect is smaller than treatment with *EpETE+EHI indicating that most of the proliferation is due to *EpETE. Together, these results indicate that *EpETE, whether because of

17,18-EpETE or a contaminant within, promotes the proliferation of MDA-MB-231 cells (further discussed below). Given that Dr. Falck's 17,18-EpETE does not promote proliferation, it is possible that these effects are due to a bioactive contaminant present in the *EpETE sample. This putative contaminant may also be sensitive to hydrolysis thus exhibiting the proliferative effects observed.

Effect of *EpETE on breast cancer cell proliferation and survival

To determine the role of 17,18-EpETE in the proliferation of breast cancer cell, MDA-MB-231 and MCF7 lines were serum-starved for 24 hours and then treated (still in the absence of serum) with increasing concentrations of *EpETE or vehicle (see **Chapter II** for treatment conditions). To determine whether the effects are specific to breast cancer, immortalized but non-transformed breast epithelial line MCF10A was utilized as control. Treatment with *EpETE results in increased proliferation of breast cancer lines in a concentration-dependent fashion with threshold effects at 1 μmol/L ($p < 0.05$) and continued effects observed up to of 6 μmol/L ($p < 0.001$) which was the highest concentration tested (**Figure IV.7 A, B, D**). In contrast, treatment with *EpETE does not promote the proliferation of breast epithelial line MCF10A (**Figure IV.7 E**). Furthermore, treatment with *EpETE increases colony formation by 63% ($p = 0.002$) in MDA-MB-231 line (**Figure IV.7 C**). Together these results suggest that *EpETE plays a role in the proliferation and survival of breast cancer cells, but not of healthy breast epithelial cells. Because the magnitude of the proliferative effects of *EpETE are greater in MDA-MB-231 compared to MCF7 line (i.e. 250% vs. 50%, $p < 0.001$), subsequent

studies were performed with the MDA-MB-231 line. Again, it is possible that these and subsequent results are not due to 17,18-EpETE per se, but to an unidentified contaminant in the commercial sample.

Effect of *EpETE on MDA-MB-231 cell death

Effects on cell proliferation depend on the balance between cell death and mitogenesis. In **Figure IV.8** we show the effects of *EpETE treatment on cell death and in **Figure IV.9** we show the effects on mitogenesis. To evaluate the effects of *EpETE on cell death two independent approaches were utilized. First, MDA-MB-231 cells were treated with 3 µmol/L *EpETE or vehicle for 48 hours and the amount of dead cells in the culture medium was assessed by propidium iodide staining. Treatment with *EpETE reduces cell death (induced by the lack of serum in the culture medium) of MDA-MB-231 line by 62% (p = 0.03; **Figure IV.8 A**). To confirm this result, cells were treated with 3 µmol/L *EpETE or vehicle for 48 hours, stained with propidium iodide and Annexin V-FITC, and analyzed by flow cytometry. Treatment with *EpETE reduces the early apoptotic population (lower right quadrant) by 64% (p = 0.001) and the necrotic population by 31% (p = 0.02) (**Figure IV.8 B**). Together these results suggest that *EpETE, compared to vehicle control, promotes survival leading to increased cell number.

Effect of *EpETE on MDA-MB-231 mitogenesis

To determine whether *EpETE promote proliferation through mitogenic mechanisms, we examined the effects of *EpETE treatment on the cell cycle and the mitotic index. First we measured the mitotic index by counting the number of cells undergoing mitosis. Treatment with *EpETE slightly increases mitogenesis but the effects are not statistically significant (n = 3; p = 0.237; **Figure IV.9 A**). Secondly, we determined the short-term (2-8 hours) and long-term (48 hours) effects of *EpETE on the cell cycle. Treatment with *EpETE does not affect the cell cycle short-term and only a marginal effect in the S-phase is observed long-term (**Figure IV.9 B**). These results indicate that the proliferative effects of *EpETE are due primarily to protection from cell death rather than increased mitogenesis.

Effect of *EpETE on MDA-MB-231 cell migration

Cancer metastasis accounts for the majority of cancer-related deaths (Sporn 1996), and this "hallmark of cancer" primarily occurs because of the ability of cancer cells to migrate and invade. Given the significance of metastasis in cancer therapeutics and previous associations of eicosanoid with metastasis (Panigrahy et al. 2012), we examined the effects of *EpETE on cell migration by two independent approaches. To assess migration and invasion traits we performed a Boyden chamber assay. In this assay cells treated with *EpETE in serum-free conditions were placed on the top chamber and were allowed to migrate through a porous membrane towards a serum-rich

96

medium. Surprisingly, cells treated with *EpETE exhibit 50% less migration than vehicle treated cells (p = 0.01; **Figure IV.10 A**). Cell migration was also assessed by a scratch assay (or wound-healing assay). In this assay cells were grown to confluence, a scratch was introduced with a pipette tip and cells were treated with *EpETE or vehicle. Images were taken of the area immediately after introducing the scratch (time 0 hours) and 24 hours after treatment (time 24 hours). The area fold change was calculated by subtracting average area at time 24 hours from time 0 hours. Consistent with results of the Boyden chamber assay, treatment with *EpETE reduced cell migration (**Figure IV.10 B**). Nonetheless, the results were not statistically significant due to an outlier in the *EpETE sample (table in **Figure IV.10 B**). These results suggest that *EpETE inhibits cell migration and indicates that different eicosanoids exhibit distinct biological roles in cancer.

Effect of *EpETE on MDA-MB-231 cell signaling pathways

In our attempt to characterize the mechanisms by which *EpETE promotes proliferation and survival of breast cancer line MDA-MB-231, we examined by western blot several growth-related signaling pathways. Of all the pathways examined, only GSK3-beta reproducibly appears to be affected by *EpETE treatment (**Table IV.2**; 2-fold induction; p < 0.05). Albeit GSK3 levels were induced, other PI3K/AKT signaling members were unaffected. Therefore, we decided to take a broader approach and look at other signaling pathways by microarray analysis. To determine early effects of *EpETE, MDA-MB-231 cells were serum starved overnight and treated for 1 hour with 3

µmol/L *EpETE (catalog no. 50861, lot no. 0400015-17, Cayman Chemical Company, MI). The samples were processed and analyzed by microarray and the exact methodology and relevant results are shown in **Appendix III**. The microarray array study showed that pyruvate hydrogenase kinase 4 (PDK4) was induced by 2-fold. To validate this result, the effects of *EpETE treatment for 2-4 hours on PDK4 protein levels were analyzed by western blot. Earlier time point studies (2-3.5 hours) revealed that *EpETE induces PDK4 (50% increase at 2 hours; p = 0.03; **Table IV.2**). In contrast, latter time point studies (4 hours) show a ~50% reduction in PDK4 levels (p = 0.0002; **Table IV.2**). These results show that *EpETE may play a role in the cyclic regulation of PDK4 expression and further implicates *EpETE in breast cancer cell bioenergetics. Interestingly, the cycling expression of PDK4 regulated by *EpETE resembles that of finely-tuned genes involved in cell development and the circadian clock (Jouve et al. 2000; Li et al. 2011).

Effect of *EpETE on MDA-MB-231 ROS production

It has been suggested that eicosanoids reduce production of reactive oxygen species (ROS) (Liu et al. 2011). For this reason we examined the effects of *EpETE on ROS production. Cells were treated with *EpETE for 2 hours, 4 hours, and 24 hours and stained with DHE to monitor superoxide production or with DCFDA to monitor general oxidative stress indicator. Samples were analyzed by flow cytometry. Our results indicate that *EpETE does not play a major role in ROS homeostasis (**Table IV.3**).

DISCUSSION SECTION 1

We previously showed that CYP1A1 is required for the proliferation and survival of breast cancer lines MCF7 and MDA-MB-231 (**Chapter III** and (Rodriguez and Potter 2013)). Nonetheless, the exact mechanism by which CYP1A1 regulates cell proliferation was not identified. We hypothesized that CYP1A1 may directly contribute to cancer progression in two ways: (a) the metabolic activation of a substrate and/or (b) the metabolic inactivation of an anti-proliferative or pro-apoptotic substrate. In our attempt to identify the putative substrate we searched the literature to identify known substrates of CYP1A1 that may account for the observed functions. In a comprehensive compendium of cytochrome P450 substrates, Niwa et al. reported that CYP1A1 metabolizes several retinoic acids, and pregnenolone (Niwa et al. 2009). A study by Schwarz et al. demonstrated that CYP1A1 metabolizes eicosapentaenoic acid to 17,18-EpETE (Schwarz et al. 2004). Our studies and others show that CYP1A1 synthesizes arachidonic acid to EETs (Choudhary et al. 2004). Therefore, we tested retinoic acids (i.e. ATRA, 13-cis RA, and 9-cis RA), pregnenolone, and eicosanoids (i.e. 14,15-EET, 11,12-EET, 8,9-EET, 20-HETE, and 17,18-EpETE) for their ability to complement CYP1A1 knockdown.

In our studies we did not observe substantial complementation of CYP1A1siRNA-mediated growth inhibition by any of these compounds. These results however, do not mean that CYP1A1 is not promoting breast cancer progression through metabolism of an endogenous substrate, but instead, our results leave open the possibility to identify the putative substrate in the future. It is possible that other

endogenous substrates of CYP1A1 remain to be discovered. Studies are underway to further investigate this hypothesis. Furthermore, whether such substrates could mediate the biological effects of CYP1A1 should also be investigated.

It is noteworthy that other alternative interpretations to these results exist. Examples include: (a) the intracellular system may already be saturated with the optimal amount of substrate/metabolite needed and therefore increasing the supply of such metabolite will not enhance the biological outcome; (b) other enzymes (including other CYPs) may be unregulated thereby compensating for the knockdown of CYP1A1. In conclusion, the exact mechanisms by which CYP1A1 regulates signaling through AKT, ERK1/2, AMPK and P70S6K remain to be elucidated.

These results differ from other CYPs that exhibit biological effects through substrate metabolism. For example, CYP3A4 promotes breast cancer growth through 14,15-EET-dependent activation of STAT3 (Mitra et al. 2011). Synthesis of estrogen by CYP19 (aromatase) promotes breast cancer progression and synthesis of testosterone by CYP17 (17-lyase) promotes prostate cancer progression (Sikka et al. 1985; Trachtenberg and Zadra 1988; Sasano et al. 1996; Yue et al. 1998). Additionally, CYP2J and CYP2C synthesize eicosanoids or steroidal products that promote cancer progression (Jiang et al. 2005; Pozzi et al. 2010). The effects of these and other CYPs are not mutually exclusive and much is needed to be learned about how individual CYP enzymes promote cancer progression and whether redundant mechanisms may allow these enzymes to complement each other.

DISCUSSION SECTION 2

In our studies we show for the first time that 17,18-EpETE is synthesized in cells, more importantly in breast cancer cells, and that these levels can be measured by mass spectrometry methods described in Chapter II. In contrast, previous studies have focused on *in vitro* systems (e.g. CYP supersome), rather than biological systems. Moreover, we show that genetic manipulation of cells (i.e. CYP1A1 knockdown in MCF7 line) results in measurable changes of 17,18-EpETE levels which are likely to have biological relevance. Therefore, these studies implicate 17,18-EpETE in breast cancer biology and provide a feasible system and methodology to further study the biological roles of 17,18-EpETE in cell biology.

Nonetheless, as discussed under *Results Section 2*, we acknowledge the limitations of our studies and thus interpret these results only within these boundaries. Whether 17,18-EpETE promotes breast cancer progression remains to be determined. On one hand, lack of proliferative effects of Dr. Falck's 17,18-EpETE suggests that this metabolite does not play a role in breast cancer proliferation. In contrast, results with Cayman's 17,18-EpETE (herein referred to as *EpETE) suggest that it does play a major role in proliferation and survival of breast cancer cells. These discrepancies may be the result of cellular changes or contamination of the commercial source of 17,18-EpETE.

First, let me explain the former possibility: cellular changes. It is possible that molecular changes within the cell line may have occurred. For example, increased expression of CYPs may alter the supply of 17,18-EpTE available. If so, the needs for 17,18-EpETE may have been met and additional 17,18-EpETE will not contribute any

further to their biology. In fact, we have observed that stocks of the same line exhibit different profiles of CYP expressions, indicating that cell lines are constantly evolving and adjusting their CYP profile. Another possibility is that cells have shifted their dependence to other metabolites and thus no longer rely on 17,18-EpETE for proliferation and survival. Dr. Potter refers to these mechanisms as "metabolite addiction", which defines the concept of cancer cells becoming dependant on specific metabolites (rather than oncogenes) for their progressions and/or maintenance. The concept of "metabolite addiction" has major implications for cancer progression as proposed by two independent studies (Mitra et al. 2011) and (Panigrahy et al. 2012).

Let me expand on the second possibility: contamination present in the commercial 17,18-EpETE. In spite of our routinely quality control procedures, it is possible that the commercial 17,18-EpETE (i.e. *EpETE) purchased may have been contaminated with a compound that (1) has growth-promoting capabilities in breast cancer, (2) it's activity is sensitive to hydrolysis (**Figure IV.5 B**) and (3) either has a mass distinct from that of 17,18-EpETE or is a *trans* version of 17,18-EpETE or EPA (because it was not detected by mass spectrometry analysis).

Nonetheless, should our results be validated or the putative contaminant be identified, our findings have significant implications for breast cancer biology because of the effects observed in proliferation, survival, and bioenergetics (through fine-tuning of PDK4 expression).

102
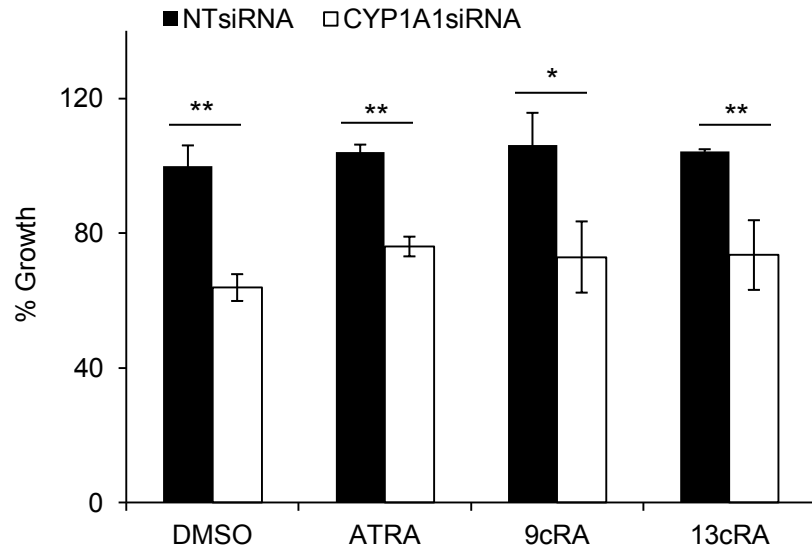
Figure IV.1. Effect of retinoic acid treatment on CY1A1siRNA-transfected MCF7 cells.

MCF7 cells were transfected with CYP1A1siRNA or NTsiRNA for 48 hours, re-plated onto 96-well plates, cultured overnight, and treated with 1μmol/L of the indicated retinoic acids for 48 hours. Cells were maintained in charcoal-stripped serum media throughout the duration of the experiment. Proliferation was assessed by MTT assay and % growth was calculated using NTsiRNA + DMSO treated cells as reference. As expected, CYP1A1siRNA shows growth inhibition, n = 3, * $p < 0.05$ and ** $p < 0.001$.
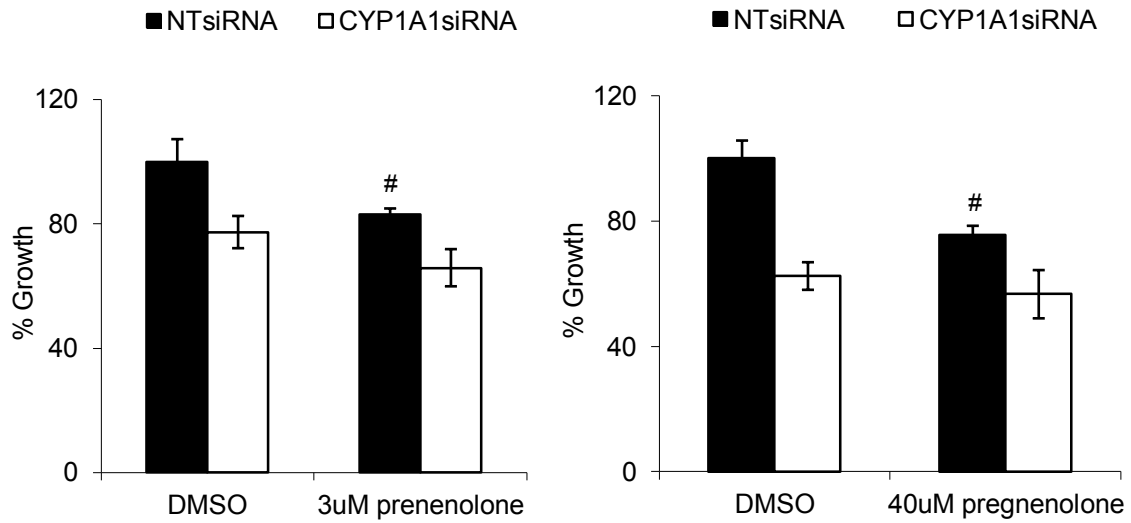
Figure IV.2. Effect of pregnenolone on CY1A1siRNA-transfected MCF7 cells.

A complementation assay was performed by transfecting MCF7 cells with

CYP1A1siRNA for 48 hours and treating with the indicated amounts of pregnenolone for

72 hours. Cells were maintained in charcoal-stripped serum media throughout the

duration of the experiment. Proliferation was assessed by MTT assay and % growth was

calculated using NTsiRNA + DMSO as reference. Experiments performed in at least

triplicate, [#]$p < 0.05$ when comparing NTsiRNA-transfected cells treated with vehicle vs.

pregnenolone. CYP1A1siRNA-transfected cells treated with pregnenolone were not

significantly different. As expected, CYP1A1siRNA shows growth inhibition ($p < 0.05$).

A) EETs
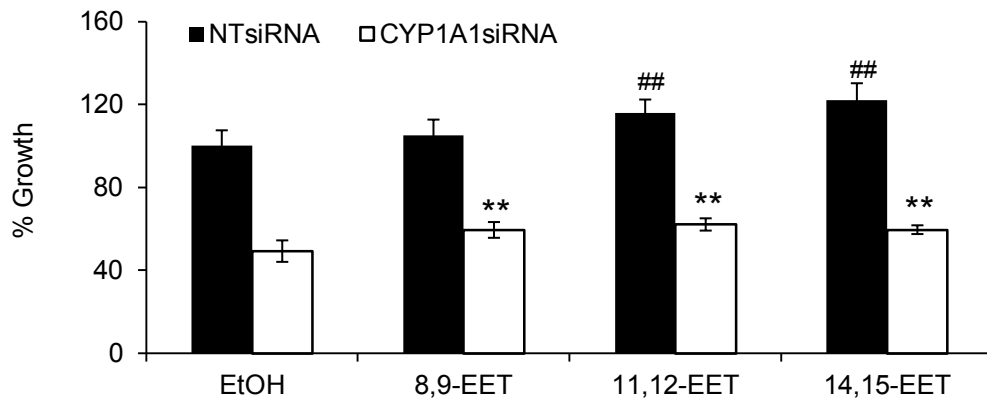
B) 20-HETE
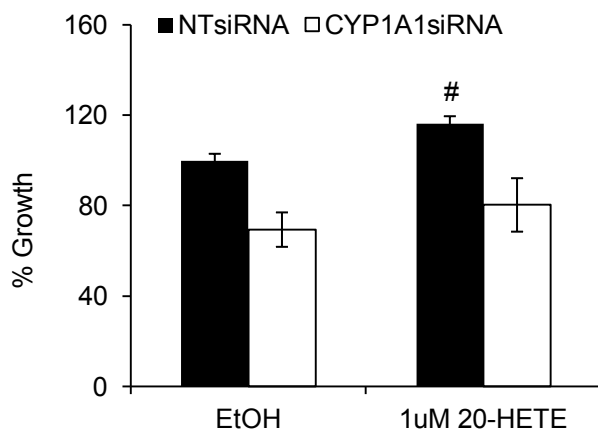
C) 17,18-EpETE (Dr. Falck source)
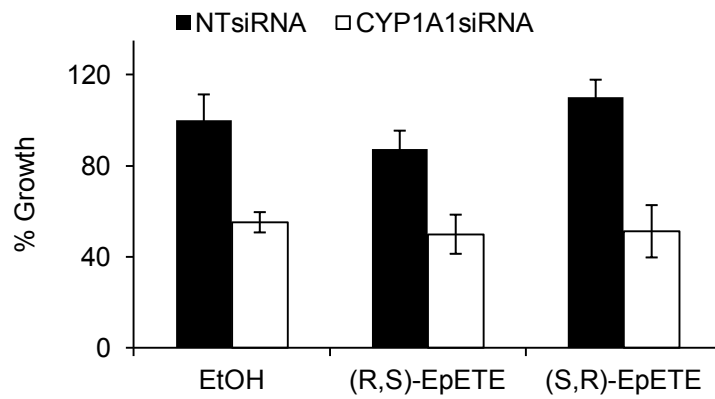
Figure IV.3. Effect of eicosanoid treatment on CY1A1siRNA-transfected MCF7 cells.

(A) MCF7 cells were transfected with CYP1A1siRNA or NTsiRNA for 72 hours, re-plated onto 96-well plates and cultured overnight, serum starved for 24 hours, and treated with 1 μmol/L of the indicated EETs for 48 hours. (B) MCF7 cells were transfected with CYP1A1siRNA or NTsiRNA for 48 hours, serum starved for 24 hours, and treated with 1 μmol/L 20-HETE for 72 hours. (C) MCF7 cells were transfected with CYP1A1siRNA or NTsiRNA for 48 hours, serum starved for 24 hours, and treated with 3 μmol/L of 17,18-EpETE for 72 hours. Proliferation was assessed by MTT assay and % growth was calculated using NTsiRNA cells treated with vehicle as reference. * $p < 0.05$ and ** $p < 0.001$ comparison of CYP1A1siRNA-transfected cells treated with vehicle vs. eicosanoid; [#]$p < 0.05$ and [##]$p < 0.001$ comparison of NTsiRNA-transfected cells treated with vehicle vs. eicosanoid. As expected, CYP1A1siRNA shows growth inhibition ($p < 0.01$). For all experiments n = 3.

A)
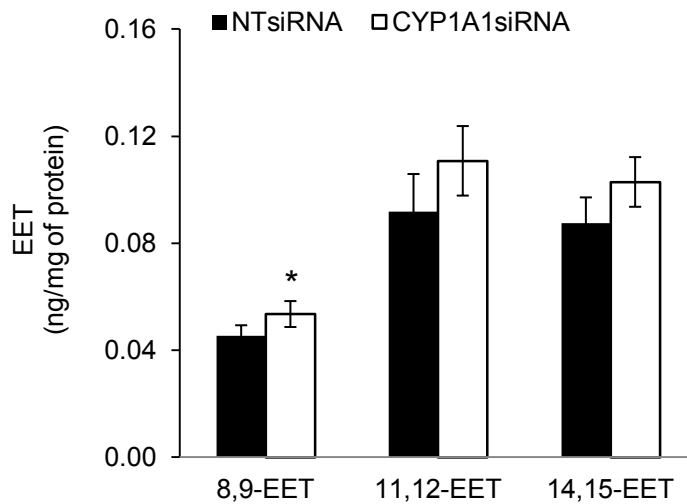
B)
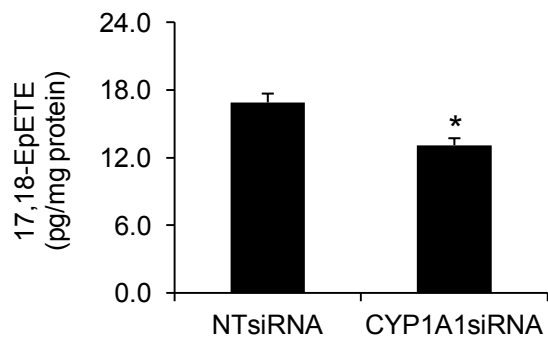
Figure IV.4. Effect of CYP1A1 silencing on eicosanoid levels in MCF7 line.

MCF7 cells transfected with CYP1A1siRNA or NTsiRNA for 72 hours and eicosanoids

were extracted and analyzed by LC-ESI/MRM/MS according to methodology described

in **Appendix II** and **Chapter II**. Protein content of transfected cells was utilized for

normalization. (n = 3, * $p < 0.05$)

	Unit	Average	StDev
Amount of 17,18-EpETE	pg EpETE/pmol CYP/min	215.66	39.43
Turn over	1/min	0.68	0.12

Table IV.1. CYP1A1 synthesizes 17,18-EpETE from eicosapentaenoic acid.

CYP1A1 insect microsomes were incubated with EPA for 30 minutes in the presence of

NADPH and the products were resolved by LC-ESI/MRM/MS. Levels of 17,18-EpETE

were normalized to internal standards.

A)   Cayman's 17,18-EpETE (*EpETE)
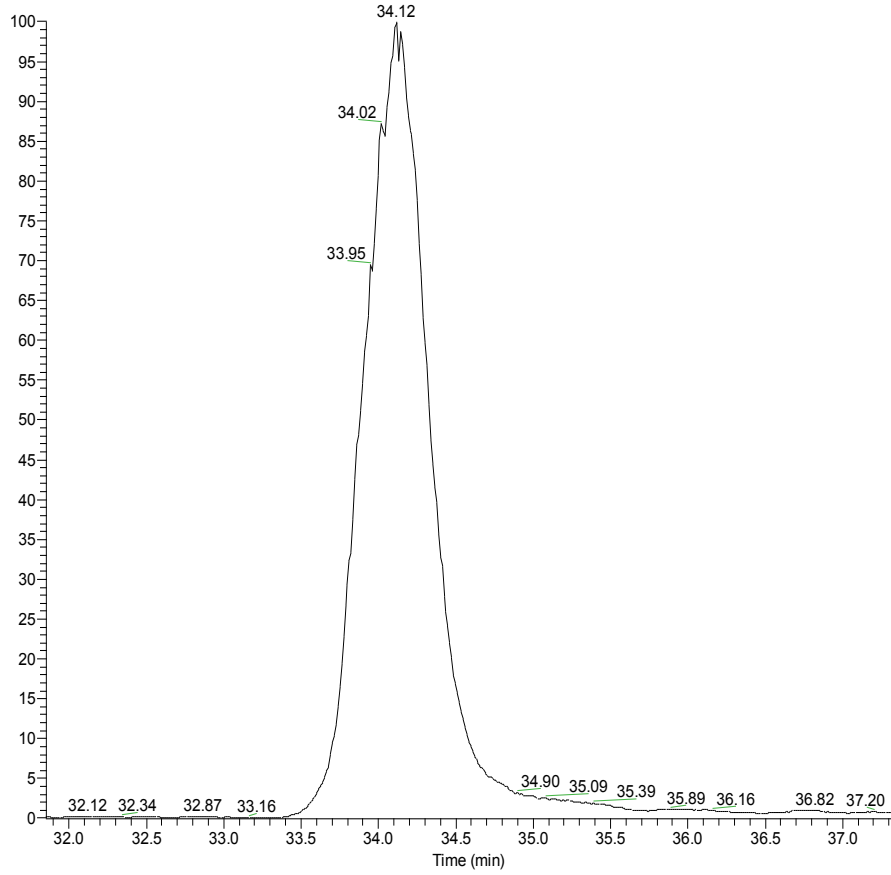
B)
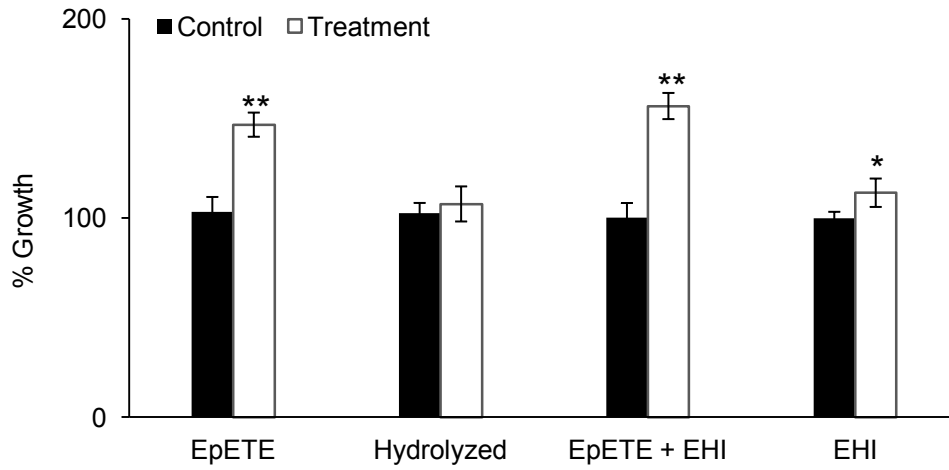
Figure IV.5. Quality control experiments.

(A) 17,18-EpETE purchased from Cayman Chemicals was validated by mass spectrometry. Show a representative spectrum of multiple experiments. (B) To confirm that the proliferative effects observed were specific to 17,18-EpETE treatment. MDA-MB-231 cells treated with either 3 µmol/L 17,18-EpETE, hydrolyzed 3 µmol/L 17,18-EpETE, or 3 µmol/L 17,18-EpETE +1 µmol/L EHI. Hydrolysis was performed at 37°C for 1 hour under acidic conditions (pH < 3.0). Cayman's 17,18-EpETE was utilized for this experiment. (n = 6-8, * p < 0.05, ** p < 0.001)

MDA-MB-231 cells
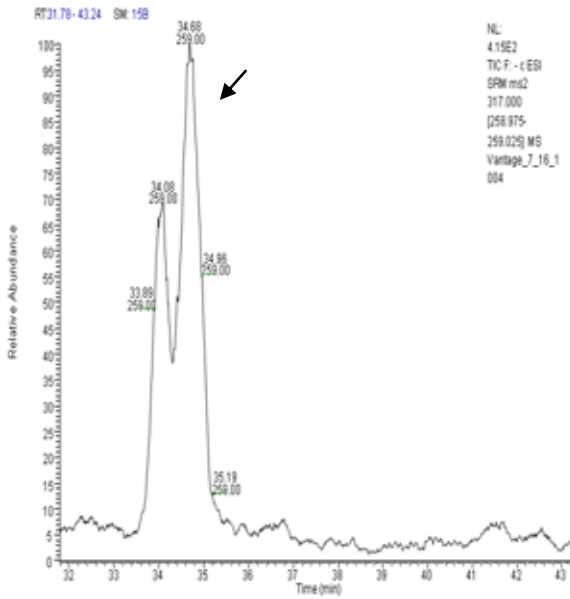
*EpETE standard
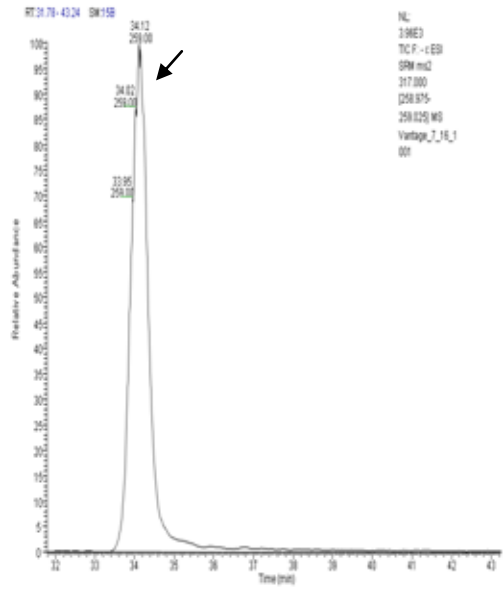
MCF7 cells
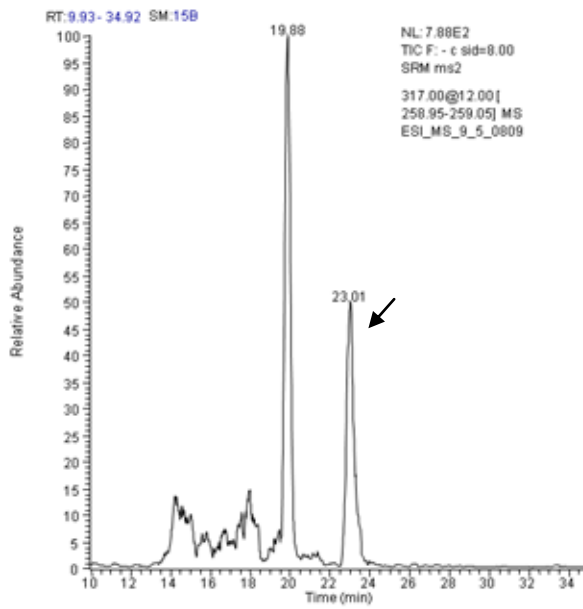
*EpETE standard
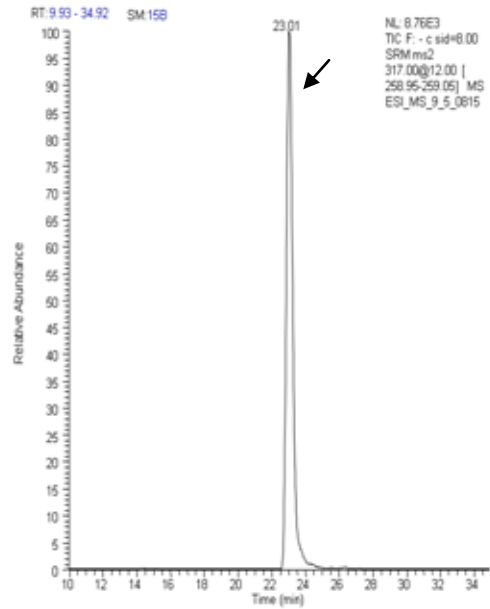
Figure IV.6. Breast cancer cells synthesize 17,18-EpETE.

Eicosanoids were extracted and 17,18-EpETE was detected by LC-ESI/SIM/MS. Shown are the 17,18-EpET peak (arrow) for (A) Standard of 17,18-EpETE (Cayman source), (B) MDA-MB-231 cells and (C) MCF7 cells.

A) MDA-MB-231: morphology

Complete medium	EtOH	EpETE
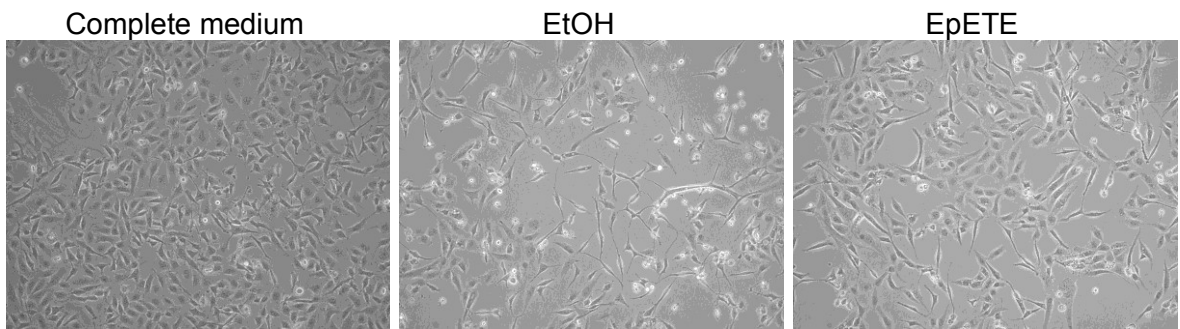
B) MDA-MB-231: proliferation
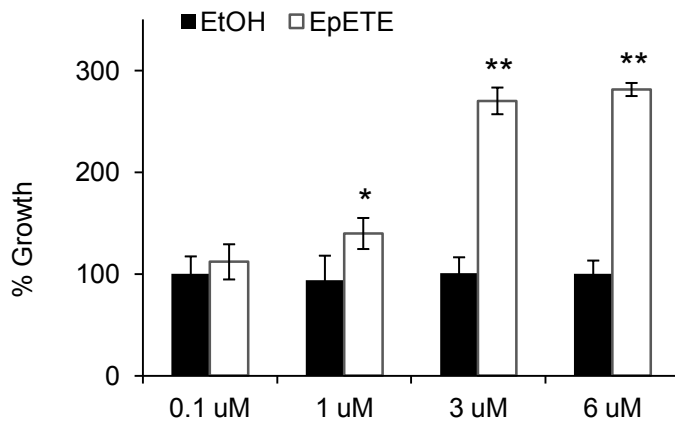
C) MDA-MB-231: clonogenicity

D) MCF7

E) MCF10A

113
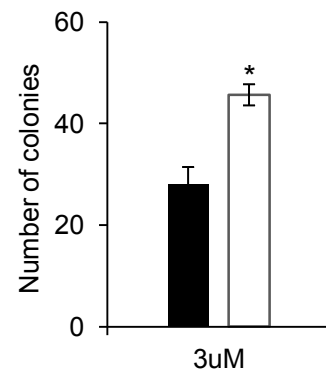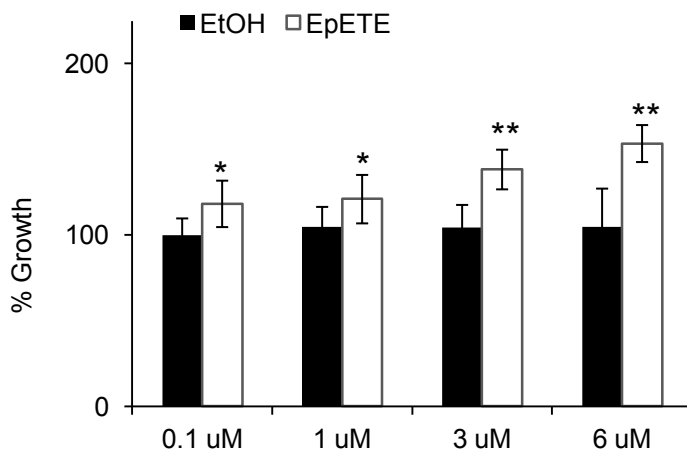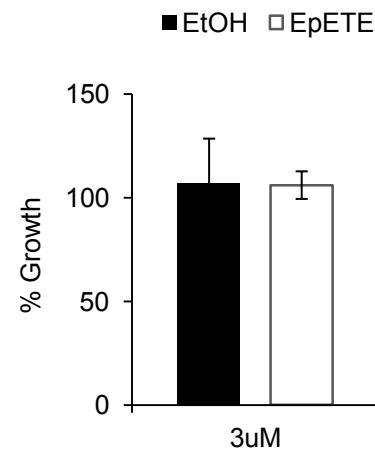
Figure IV.7. Effect of 17,18-EpETE treatment on breast cancer and epithelial cell proliferation.

Cells were plated, serum-starved for 24 hours, and treated with the indicated amounts of 17,18-EpETE. (A) Cells were treated with 3 µmol/L 17,18-EpETE and overall morphology and density was evaluated visually under phase contrast microscope. (B, D, E) Proliferation was measured by MTT assay (n = 6-8, * $p < 0.05$, ** $p < 0.001$). (C) MDA-MB-231 cells were seeded onto fibronectin-coated plates (200 cells/well), treated with 3 µmol/L 17,18-EpETE and grown for 14 days until visible colonies were formed. Due to the prolonged nature of the experiment 2% FBS medium was used through this clonogenic experiment. To maintain the supply of 17,18-EpETE, the treatment medium was replaced every other day. Colonies were counted manually (n = 3, $p = 0.002$).

A)
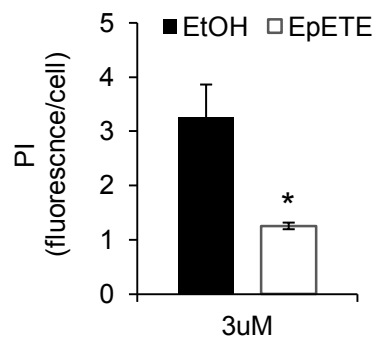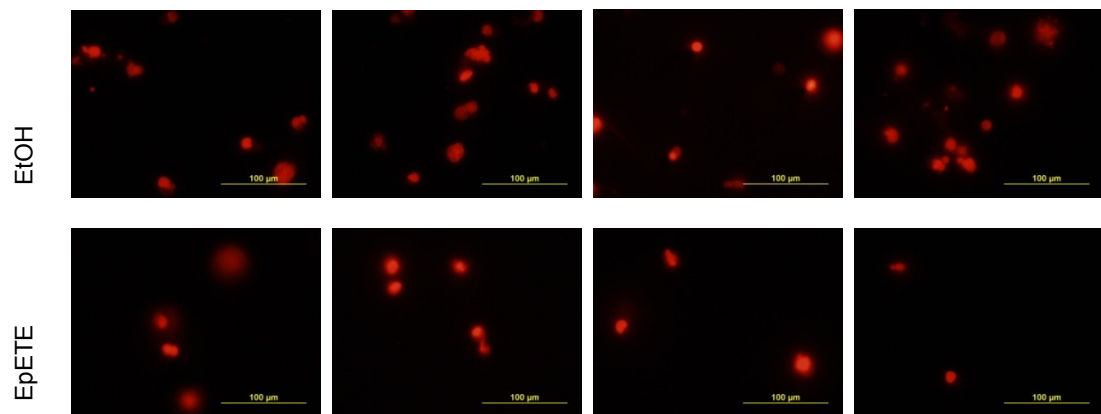
B)
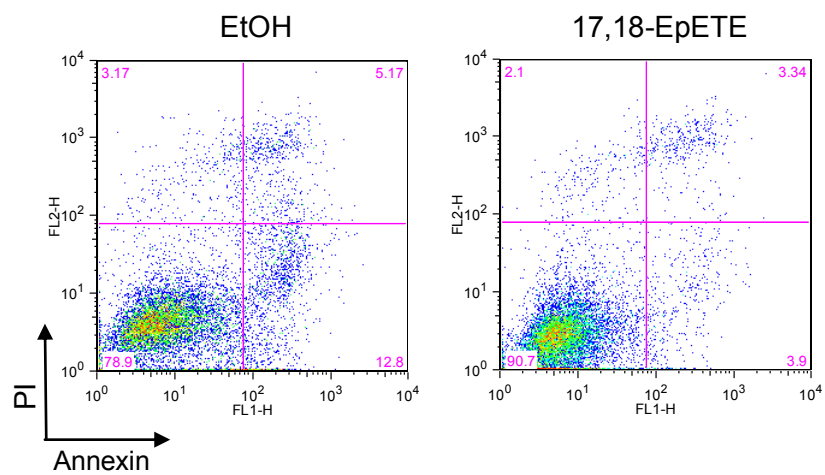
	Early	Late	Necrotic	Viable
EtOH	11.57	5.48	3.13	79.87
EpETE	4.13	4.35	2.16	89.37
p value	0.001	0.189	0.015	0.002

115

Figure IV.8. Effect of 17,18-EpETE treatment on MDA-MB-231 cell death.

(A) Overall cell death was assessed by measuring the amount of dead cells in the medium of MDA-MB-231 cells treated with 17,18-EpETE for 48 hours. The medium was then collected, centrifuged, and resuspended with propidium iodide in PBS. Propidium iodide fluorescence was assessed by plate reader at excitation of 540 ± 20 nm and emission of 600 ± 20 nm and results were normalized to total cultured cell number. (n = 3, p = 0.03). B) Apoptosis was assessed by flow cytometry of MDA-MB-231 treated with 3 µmol/L 17,18-EpETE for 48 hours and stained with propidium iodide and Annexin V-FITC. (n = 3, p value shown) Legend: Early, early apoptotic population in the lower right quadrant; Late, late apoptotic population in the upper right quadrant; Necrotic, necrotic population in the upper left quadrant; Viable, alive population in the lower left quadrant.

A) Mitotic index
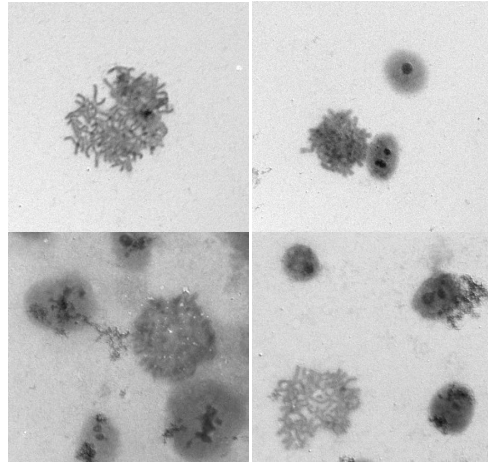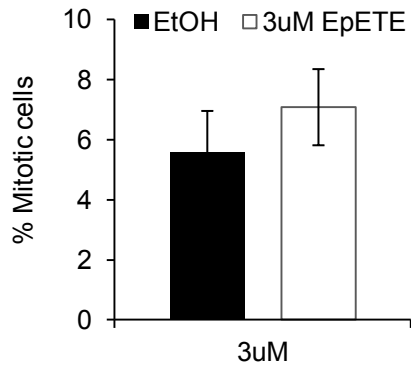
B) Cell cycle at 2 hours, 4 hours, and 8 hours
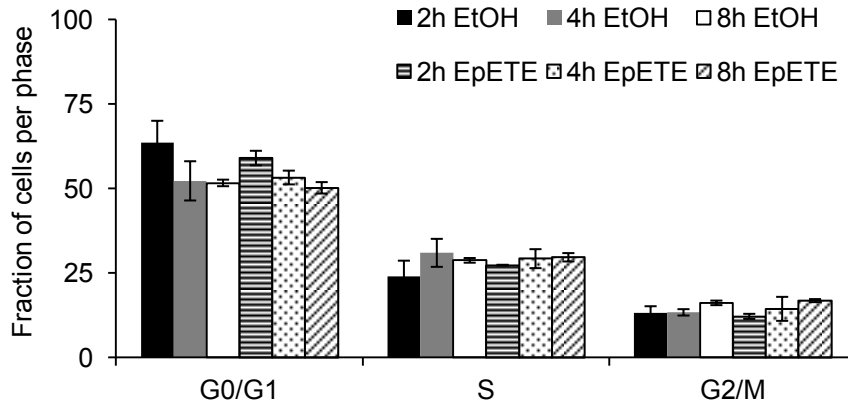
C) Cell cycle at 48 hours
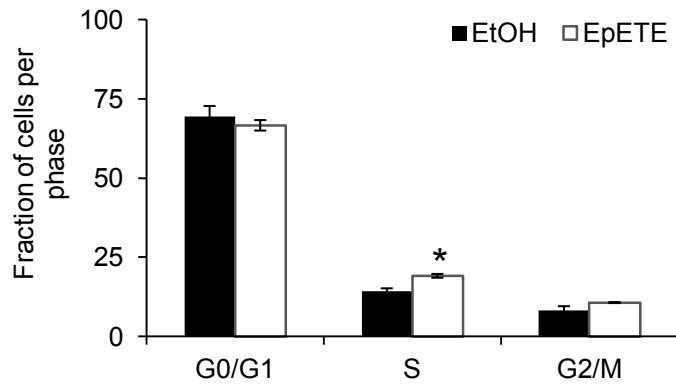
Figure IV.9. Effect of 17,18-EpETE treatment on MDA-MB-231 mitogenesis.

(A) MDA-MD-231 cells were treated with 3 μmol/L 17,18-EpETE for 48 hours, permeabilized, fixed, and stained with Giemsa to visualize chromosomes under 40X in a Zeiss AxioPlan II microscope. The mitotic index was calculated by dividing the number of cells undergoing mitosis by the total number of cells counted, representative images shown (350 cells/sample, n = 3, p = 0.237). (B-C) Cell cycle distribution was assessed by flow cytometry of MDA-MB-231 treated with 3 μmol/L 17,18-EpETE for the indicated times and stained with propidium iodide. (n = 3, * p < 0.05)

A) Boyden chamber assay
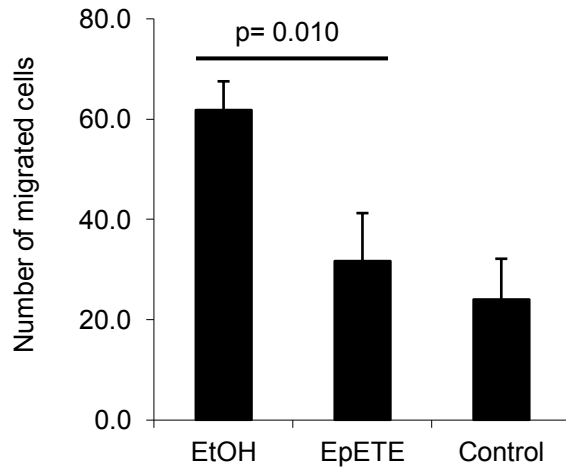
B) Scratch assay
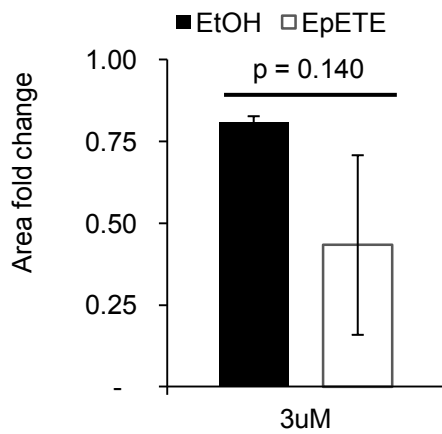
Treatment	Area fold change	AVG	STDEV	P value
EtOH 1	0.81			
EtOH 2	0.83	0.81	0.02	
EtOH 3	0.79			
EpETE 1	0.75			0.140
EpETE 2	0.23	0.43	0.27	
EpETE 3	0.32			

Figure IV.10. Effect of 17,18-EpETE treatment on MDA-MB-231 migration.

Cell migration was assessed by Boyden chamber (A) and scratch assay (B). For (A), cells were suspended in medium containing 17,18-EpETE or vehicle and placed on top portion of the chamber. 5%FBS medium was placed at the bottom portion of the chamber. Cells were incubated at $37^{\circ}C$, $5\%CO_2$ and allowed to migrate for 4-6h through a porous membrane. Amount of cells in the membrane were counted. (B) Cells were culture overnight, a scratch was made with a pipette tip and cells were immediately treated with 3 µmol/L 17,18-EpETE. The area of the scratch was measured at time 0 hours and 24 hours post treatment. (n = 3, p value shown)

	30min		4h		24h		48h-replicate 1		48h-replicate 2	
	Fold change	p value	Fold change	p value	Fold change	p value	Fold change	p value	Fold change	p value
p-p65NFKB	0.88	0.183	0.80	0.365						
IKBα	1.09	0.712	0.72	0.040						
p-FoxO1			1.12	0.778	0.79	0.451	2.59	0.027	0.90	0.402
p-GSK3β			0.90	0.249	1.25	0.082	2.12	0.023	2.00	0.006
p-AKT			1.13	0.057	1.33	0.067	4.59	0.002	0.81	0.035
t-AKT			0.52	0.230	0.63	0.090	1.13	0.126		
p-ERK1/2			0.57	0.083	0.64	0.172	1.05	0.679		
p-STAT3			1.02	0.937	0.80	0.147	1.19	0.079		
t-STAT3			0.79	0.206	0.63	0.021				
NM-23			1.41	0.086	0.74	0.536				
p-Src			0.97	0.944	1.12	0.758				
p-JNK					0.94	0.640				
t-JNK					1.69	0.113				
p-Jun					1.60	0.155				
t-Jun					0.89	0.327				
myc					1.43	0.058				
survivin			0.89	0.672					0.96	0.904
	2h		4h							
PDK4	1.50	0.026	0.45	2E-4						

Table IV.2. Effect of 17,18-EpETE treatment on MDA-MB-231 multiple pathways.

MDA-MB-231 cells were treated with 3 µmol/L 17,18-EpETE for the indicate amounts of times. Cells were collected, processed according to standard Western blot procedures, and probed with the indicated antibodies. (n = 3, p value shown)

	DHE		DCFDA	
Treatment time	Fold change	p value	Fold change	p value
2h	1.01	0.57	1.01	0.90
4h	0.96	0.23	1.26	0.01
24h	0.92	0.12	1.03	0.83

Table IV.3. Effect of 17,18-EpETE treatment on MDA-MB-231 on ROS production.

Cells were treated with 3 µmol/L 17,18-EpETE for the indicated times, collected and stained with 2µM DHE or 10µM DCFDA, and analyzed by flow cytometry. Cells treated with 250 µmol/L hydrogen peroxide for 2 hours served as positive control. (n = 3, p value shown)

CHAPTER V

Conclusions & Future Directions

One in eight women is at risk of developing breast cancer during their lifetime. The majority of new cases are diagnosed at an advanced stage when the probability of 5-year survival is only at 23% (BCF 2012). Because of this great burden of breast cancer incidence and mortality, there is an urgent unmet need for novel targeted therapeutics. Previous associations of cytochrome P450 (CYP) expressions in cancer, particularly of CYP1A1 in breast cancer, suggest that CYP1A1 plays a functional role in cancer biology (Murray et al. 2010; Vinothini and Nagini 2010). However, prior studies of CYP1A1 have focused primarily on metabolic activation of xenobiotics and on polymorphic variants of the gene that may alter the enzyme function. However, the roles of CYP1A1 in the absence of xenobiotic exposure are largely unknown. This motivated us to investigate the following research questions:

 (a) Is CYP1A1 <u>important</u> for the maintenance of breast cancer cells?

 (b) What are the <u>functional</u> roles of CYP1A1 in breast cancer biology?

 (c) What are the <u>mechanisms</u> by which CYP1A1 functions in breast cancer biology?

We initially hypothesized that CYP1A1 promotes the proliferation and survival of breast cancer cells and that this was mediated, in part, through the enzymatic activity of CYP1A1 in the metabolism of an endogenous substrate. However, in testing this hypothesis we were unable to identify putative endogenous substrates that would

explain the biological functions of CYP1A1 (**Chapter IV**). Therefore, we tested the

alternate **hypothesis** that CYP1A1 promotes the proliferation and survival of breast

cancer cells, in part, through signal transduction mechanisms (**Chapter III**).

Testing these hypotheses is important because it provides a better

understanding of the roles of CYP1A1 in breast cancer biology, thereby closing this

current gap in knowledge and giving way to improved therapeutic strategies. These

impacts are further discussed in this chapter and are divided into three subsections. The

first two sections deal with the impact of our studies in regards to cancer biology and the

third section deals with the clinical impact of our findings.

CYTOCHROME P450 1A1 IS IMPORTANT FOR BREAST CANCER PROLIFERATION AND SURVIVAL

Our first two aims were to determine whether CYP1A1 is important for the maintenance of breast cancer cells and, if so, to determine what these possible roles are. To this end we utilized a pool of four small interfering RNA (siRNA) to knockdown CYP1A1 in breast cancer lines MCF7 (ER+/PR+/HER2+) and MDA-MB-231 (ER-/PR-/HER2- or triple-negative). Reduction of CYP1A1 results in impaired proliferation and colony formation which indicates that CYP1A1 is important for the maintenance of breast cancer cells. Because proliferation depends on the balance between cell death, growth and division, we examined the effects of CYP1A1 knockdown on apoptosis and cell cycle. CYP1A1 knockdown blocks the cell cycle at G0/G1 associated with reduction of cyclin D1, and increases apoptosis associated with reduction of survivin. These results (see **Chapter III** for details) support the relevance of CYP1A1 in breast cancer biology and suggest that CYP1A1 plays a functional role in the progression of breast cancer through regulation of proliferation and survival mechanisms. It remains to be determined whether CYP1A1 is also important for the growth of tumors *in vivo*. Recommendations to understand the importance of CYP1A1 *in vivo* are discussed latter in this chapter.

POTENTIAL METABOLITE MECHANISMS OF CYTOCHROME P450 1A1 FUNCTION

Our thirds aim was to determine the mechanisms by which CYP1A1 promotes breast cancer proliferation and survival. First, we examined whether known CYP1A1 metabolites complement the growth-inhibitory effects of silencing this enzyme. We hypothesized that CYP1A1 could either synthesize a growth promoting metabolite or relieve the growth inhibition of a precursor molecule. With the goal of identifying a putative substrate, we investigated whether CYP1A1-mediated metabolism of retinoic acid, arachidonic acid, eicosapentaenoic acid, and pregnenolone may play a role in breast cancer progression. Surprisingly, in the context of our studies, we did not observe significant complementation of proliferation by any of these compounds (**Chapter IV**). These results differ from other CYPs exhibiting biological effects through synthesis of a bioactive metabolite. For example, CYP3A4 epoxygenases metabolize arachidonic acid into epoxide metabolites such as 14,15-EET which promotes breast cancer growth and survival through activation of STAT3 (Mitra et al. 2011). Additionally, CYP2J and CYP2C synthesize eicosanoids or steroidal products that promote cancer progression (Jiang et al. 2005; Pozzi et al. 2010). Other examples include, the synthesis of estrogen by CYP19 (aromatase) which promotes breast cancer progression and the synthesis of testosterone by CYP17 (17-lyase) which promotes prostate cancer progression (Sikka et al. 1985; Trachtenberg and Zadra 1988; Sasano et al. 1996; Yue et al. 1998). Our findings however, do not mean that CYP1A1 does not promote breast cancer

progression through metabolism of an endogenous substrate, but rather indicates that if such substrate exists, it remains to be identified.

We provide evidence that 17,18-EpETE may potentially be the sought after metabolite because (a) it is synthesized by breast cancer cells (**Figure IV.6**) and (b) the levels are affected by CYP1A1 knockdown (**Figure IV.4B**). This is the first time shown in cells that they are capable of synthesizing this metabolite and that CYP1A1 is major contributor of 17,18-EpETE. However, major limitations of our studies render many of results inconclusive. Therefore, whether 17,18-EpETE plays a functional role in the progression of breast cancer remains to be determined.

Although substrate metabolism may still be a possible mechanism of action of CYP1A1, the lack of complementation observed in our studies suggests that perhaps CYP1A1 regulates breast cancer progression through mechanisms distinct from substrate metabolism. Two independent evidence support this hypothesis. First, there is a differential targeting of CYP1A1 to the mitochondria versus the endoplasmic reticulum, which may be an indication of differing substrate specificities and functions (Avadhani et al. 2011). Secondly, polymorphic variants and potential phosphorylation may also affect the structure, function, and/or specificity of the protein (Landi et al. 1994; Bartsch et al. 2000). In any of these ways CYP1A1 may interact with homeostatic processes that regulate cell proliferation and survival. Whether CYP1A1 promotes breast cancer progression through its metabolic function or other mechanisms remains to be determined. Nonetheless, our studies provide evidence for one of several possible mechanisms: regulation of cell signal transduction.

CYTOCHROME P450 1A1 REGULATES CELL SIGNAL TRANSDUCTION

Since our results in regards to substrate metabolism do not explain the anti-proliferative effects of CYP1A1 silencing, we sought to determine whether CYP1A1 may promote these effects via regulation of signal transduction pathways. Analysis of growth and survival regulatory signaling pathways by Western blot revealed that CYP1A1 silencing impairs breast cancer cell proliferation and survival, at least in part, through induced phosphorylation of AMP-activated protein kinase (AMPK) and reduced phosphorylation of AKT, extracellular signal-regulated kinases 1 and 2 (ERK1/2), and 70kDa ribosomal protein S6 kinase (P70S6K). These pathways are interconnected and together regulate cell cycle progression, apoptosis, and protein translation (Lavoie et al. 1996; Diehl et al. 1998; Manning et al. 2002; Fornaro et al. 2003; Inoki et al. 2003; Kovacic et al. 2003; Corradetti et al. 2004; Fingar et al. 2004; Asanuma et al. 2005; Zhuang and Schnellmann 2006; Meloche and Pouyssegur 2007; Du et al. 2008; Zhuang and Miskimins 2008; Kim et al. 2010; Tao et al. 2010; Zhao et al. 2010). In this way we have shown for the first time that CYP1A1 is not only important for xenobiotic and endobiotic metabolism (see page 15), but also has its own role in cancer progression by interacting with cell signal transduction pathways. The signaling mechanisms identified in our studies differ from other CYPs, such as CYP3A4 which signals through STAT 3 (Mitra et al. 2011). Whether CYP1A1 regulates AKT, ERK1/2, AMPK and P70S6K signaling through protein-protein interactions, substrate metabolism, or other mechanisms remains to be elucidated.

CLINICAL IMPACT

The evidence showed here and by others strongly support that CYP1A1 is a potential target for breast cancer therapeutics. Below we discuss this supporting evidence.

(a) Because *CYP1a1* knockout mice is viable (Dalton et al. 2000) and CYP1A1 expression in hepatic and extrahepatic tissues is turned off in the absence of xenobiotic exposure (de Waziers et al. 1990; Galijatovic et al. 2004), we propose that targeting CYP1A1 will exhibit low systemic cytotoxicity. The next step would be to test this hypothesis in *in vivo* studies.

(b) The majority of breast cancers are estrogen receptor positive (70-80%) and a minority are triple-negative (15-20%). Independent of tumor type, about 10% of patients relapse (Abner et al. 1993; Bentzon et al. 2008; Arvold et al. 2011). Adjuvant hormone therapy has proven successful in receptor positive tumors (ER+, PR+). However, patients that relapse often develop resistance to hormone therapy (Dowsett et al. 2005). Triple-negative tumors do not respond to hormone therapy and current treatment options are limited. Therefore, an unmet need for targeted therapeutics exists for refractory and triple negative tumors (Dowsett et al. 2005). We show that CYP1A1 silencing significantly inhibits proliferation and survival of ER+ and triple-negative breast cancer lines (**Figure III.2**), suggesting that CYP1A1 targeting has therapeutic potential for breast cancer independent of ER status. In our studies, the effect of CYP1A1 knockdown on cell death appears to be greater in ER+ MCF7 line than in triple-negative MDA-MB-231 line, whereas both lines appear to be strongly inhibited at the G1-S

checkpoint. Whether strategies to inhibit CYP1A1 would be more effective in ER+ compared to triple-negative breast cancer remains to be determined. The therapeutic potential of CYP1A1 targeting should be tested in *in vivo* models of ER+ and triple-negative tumors as it would contribute to meet the need for triple-negative and recurrent metastatic disease.

(c) Consistent with CYP1A1siRNA results, pharmacologic reduction of CYP1A1 by the AhR inhibitor carnosol also impairs proliferation and induces AMPK phosphorylation. These results suggest that CYP1A1 silencing could be mediated by carnosol. Whether carnosol (Johnson et al. 2008) or other compounds are effective in reducing CYP1A1 levels and, more importantly, tumor growth in patients remains to be determined (Peterson and Barnes 1991; Kuffel et al. 2002; Androutsopoulos et al. 2009a; Pors et al. 2011; Sutherland et al. 2012). Of note, our results demonstrate that the therapeutic potential of CYP1A1 targeting lies in reduction of the protein levels and not just the inhibition of its activity. Our work points toward further pre-clinical development of carnosol for breast cancer therapeutics.

(d) The widespread expression of CYP1A1 in breast cancer has been exploited as a strategy to activate pro-drug compounds to cytotoxic intratumoral metabolites. For example, drugs of the 2-(4-aminophenyl)benzothiazole class such as 5F 203 (Phortress) exhibit potent anti-tumor properties in xenograft models and have been moved forward to clinical trials (Chua et al. 2000; Leong et al. 2003; Fichtner et al. 2004). The mechanism of action proposed is that these agents induce and are activated by CYP1A1 forming electrophilic metabolites that bind to and damage DNA, thus resulting in tumor growth arrest. It is noteworthy that while CYP1A1 activated pro-drugs exhibit promise,

induction of CYP1A1 expression with the intent of metabolically activating pro-drugs may be self-defeating. CYP1A1 may contribute to tumor progression if induction outstrips the inhibitory effects of a CYP1A1 activated drug, as may be the case when tumors acquire resistance to the drug (Bradshaw et al. 2000). Therefore, in light of this body of work it may be recommended that the ideal therapeutic candidate should inhibit the CYP1A1 already expressed in the tumor, but not result in further induction of the gene. All these possibilities should be further examined.

(e) Our findings implicate CYP1A1 upstream of ERK, AKT, AMPK, and P70S6K signaling. Inhibition of the PI3K/AKT and MEK/ERK pathways simultaneously with CYP1A1 silencing is important because cross talk between these pathways (ERK and AKT) display synergistic effects when combined inhibition is utilized for cancer therapeutics (She et al. 2010). In contrast to drugs that target the PI 3-kinase or ERK pathways independently, it is possible that novel drugs that target CYP1A1 may inhibit both pathways simultaneously, thus rendering CYP1A1 silencing as potentially more effective than independently inhibiting ERK or AKT (Halilovic et al. 2010) . Additionally, targeting CYP1A1 provides an alternative treatment strategy if drug resistance results from independently targeting the ERK and AKT pathways.

FUTURE DIRECTIONS

The exact mechanisms by which CYP1A1 regulates ERK, AKT, AMPK, and P70S6K signaling remain to be identified. Characterization of these mechanisms is important in order to develop drugs that appropriately target the levels of this enzyme. Below we make recommendations to further this research.

(a) Do microsomal versus mitochondrial CYP1A1 exhibit differential roles in breast cancer progression? Understanding the exact biological roles of these may assist in the development of better CYP1A1-targeting strategies.

(b) Are there polymorphic variants or post-translational modifications (e.g. phosphorylation sites), that render this enzyme more or less active? If so, these modifications could be considered in the development of anti-CYP1A1 therapy.

(c) What other possible functions may CYP1A1 have? Due to the difficulty in isolating shRNA clones, we propose examining the effects of CYP1A1 silencing on senescence. Current studies are underway to further understand this possibility. Also, the roles of CYP1A1 in cell migration should be examined.

(d) The present study has focuses on the impact of CYP1A1 *in vitro.* Whether these results translate *in vivo*, and most importantly in humans, remains to be determined. Toward this end several approaches may be undertaken: (1) *Xenograft mouse models* of stable CYP1A1 knockdowns (e.g. shRNA) can be developed to examine the effects of CYP1A1 silencing on tumor volume, burden (# of tumors), and metastasis. Additionally, establishing estrogen receptor positive and triple negative lines would assist in determining the clinical impact of CYP1A1 targeting in these types of

tumors. (2) Xenograft models of breast cancer tumors (no CYP1A1 knockdown) should be used to investigate the effects of carnosol *in vivo*. Furthermore, combination therapies should also be considered in order to find possible synergetic strategies. We suggest the combination of CYP1A1 reduction together with AKT and/or ERK inhibition. Alternatively, we recommend CYP1A1 reduction in combination with AMPK induction (e.g. metformin and AICAR). (3) It would be of value to establish a breast cancer-prone, CYP1A1 knockout mouse model. We would anticipate reduced tumor burden or tumor size in such mouse model.

(e) *Xenograft model for 17,18-EpETE studies.* Regarding the potential role of 17,18-EpETE in breast cancer, we propose utilizing several types of breast cancer xenograft models. First, we suggest examining the effects of 17,18-EpETE treatment in tumor volume and metastasis, similarly to previously studies of eicosanoids in tumor growth (Panigrahy et al. 2012). Such studies would involve systemic or localized treatment with 17,18-EpETE followed by evaluation of tumor size and burden. These studies could be extended by utilizing CYP1A1 knockdown xenograft models to determine whether CYP1A1 mediates breast cancer progression through synthesis of 17,18-EpETE. Furthermore, because our study suggests that 17,18-EpETE regulates PDK4, we recommend profiling the expression PDK4 upon treatment with 17,18-EpETE.

FINAL REMARKS

In this thesis we have provided *in vitro* evidence that CYP1A1 plays a functional role in the biology of breast cancer cell, in part through the regulation of proliferative and pro-survival cell signaling mechanisms (i.e. AKT, ERK, AMPK and P70S6K). To our knowledge this is the first study implicating CYP1A1 in cancer biology in the absence of xenobiotic exposure. More importantly, our studies support the development of therapeutic strategies that focus on reducing the levels of CYP1A1. We recommend that these findings be further investigated in *in vivo* models which will facilitate translation into clinical practice.

REFERENCES

Genome Browser website. Available: http://genome.ucsc.edu/.

Abdelrahim M, Smith R, 3rd, Safe S (2003) Aryl hydrocarbon receptor gene silencing with small inhibitory RNA differentially modulates Ah-responsiveness in MCF-7 and HepG2 cancer cells. Molecular pharmacology 63(6): 1373-1381.

Abner AL, Recht A, Eberlein T, Come S, Shulman L et al. (1993) Prognosis following salvage mastectomy for recurrence in the breast after conservative surgery and radiation therapy for early-stage breast cancer. J Clin Oncol 11(1): 44-48.

Abul-Hajj YJ, Iverson R, Kiang DT (1979) Metabolism of pregnenolone by human breast cancer. Evidence for 17 alpha-hydroxylase and 17,20-lyase. Steroids 34(7): 817-827.

ACS (2012) Breast Cancer Facts & Figures 2011-2012. Atlanta, Ga: American Cancer Society, Inc.

Addya S, Anandatheerthavarada HK, Biswas G, Bhagwat SV, Mullick J et al. (1997) Targeting of NH2-terminal-processed microsomal protein to mitochondria: a novel pathway for the biogenesis of hepatic mitochondrial P450MT2. The Journal of cell biology 139(3): 589-599.

Androutsopoulos VP, Li N, Arroo RR (2009a) The methoxylated flavones eupatorin and cirsiliol induce CYP1 enzyme expression in MCF7 cells. Journal of natural products 72(8): 1390-1394.

Androutsopoulos VP, Tsatsakis AM, Spandidos DA (2009b) Cytochrome P450 CYP1A1: wider roles in cancer progression and prevention. BMC cancer 9: 187.

Arvold ND, Taghian AG, Niemierko A, Abi Raad RF, Sreedhara M et al. (2011) Age, breast cancer subtype approximation, and local recurrence after breast-conserving therapy. J Clin Oncol 29(29): 3885-3891.

Asanuma H, Torigoe T, Kamiguchi K, Hirohashi Y, Ohmura T et al. (2005) Survivin expression is regulated by coexpression of human epidermal growth factor receptor 2 and epidermal growth factor receptor via phosphatidylinositol 3-kinase/AKT signaling pathway in breast cancer cells. Cancer research 65(23): 11018-11025.

Asokan P, Das M, Bik DP, Howard PC, McCoy GD et al. (1986) Comparative effects of topically applied nitrated arenes and their nonnitrated parent arenes on cutaneous and hepatic drug and carcinogen metabolism in neonatal rats. Toxicology and applied pharmacology 86(1): 33-43.

Avadhani NG, Sangar MC, Bansal S, Bajpai P (2011) Bimodal targeting of cytochrome P450s to endoplasmic reticulum and mitochondria: the concept of chimeric signals. The FEBS journal 278(22): 4218-4229.

Badawi AF, Cavalieri EL, Rogan EG (2001) Role of human cytochrome P450 1A1, 1A2, 1B1, and 3A4 in the 2-, 4-, and 16alpha-hydroxylation of 17beta-estradiol. Metabolism: clinical and experimental 50(9): 1001-1003.

Baertschi SW, Raney, K. D., Stone, M. P., and Harris, T. M. (1988) Preparation of the 8,9-epoxide of the mycotoxin aflatoxin B1: The ultimate carcinogenic species. J Am Chem Soc 110: 7929–7931.

Bartsch H, Nair U, Risch A, Rojas M, Wikman H et al. (2000) Genetic polymorphism of CYP genes, alone or in combination, as a risk modifier of tobacco-related cancers. Cancer Epidemiol Biomarkers Prev 9(1): 3-28.

Bentzon N, During M, Rasmussen BB, Mouridsen H, Kroman N (2008) Prognostic effect of estrogen receptor status across age in primary breast cancer. International journal of cancer 122(5): 1089-1094.

Boopathi E, Srinivasan S, Fang JK, Avadhani NG (2008) Bimodal protein targeting through activation of cryptic mitochondrial targeting signals by an inducible cytosolic endoprotease. Molecular cell 32(1): 32-42.

Boucher PD, Ruch RJ, Hines RN (1993) Specific nuclear protein binding to a negative regulatory element on the human CYP1A1 gene. The Journal of biological chemistry 268(23): 17384-17391.

Boucher PD, Piechocki MP, Hines RN (1995) Partial characterization of the human CYP1A1 negatively acting transcription factor and mutational analysis of its cognate DNA recognition sequence. Molecular and cellular biology 15(9): 5144-5151.

Bradshaw TD, Stevens MF, Westwell AD (2001) The discovery of the potent and selective antitumour agent 2-(4-amino-3-methylphenyl)benzothiazole (DF 203) and related compounds. Current medicinal chemistry 8(2): 203-210.

Bradshaw TD, Chua MS, Orr S, Matthews CS, Stevens MF (2000) Mechanisms of acquired resistance to 2-(4-aminophenyl)benzothiazole (CJM 126, NSC 34445). British journal of cancer 83(2): 270-277.

Brantley E, Trapani V, Alley MC, Hose CD, Bradshaw TD et al. (2004) Fluorinated 2-(4-amino-3-methylphenyl)benzothiazoles induce CYP1A1 expression, become metabolized, and bind to macromolecules in sensitive human cancer cells. Drug metabolism and disposition: the biological fate of chemicals 32(12): 1392-1401.

Bui P, Solaimani P, Wu X, Hankinson O (2011) 2,3,7,8-Tetrachlorodibenzo-p-dioxin treatment alters eicosanoid levels in several organs of the mouse in an aryl hydrocarbon receptor-dependent fashion. Toxicology and applied pharmacology 259(2): 143-151.

Carver LA, Bradfield CA (1997) Ligand-dependent interaction of the aryl hydrocarbon receptor with a novel immunophilin homolog in vivo. The Journal of biological chemistry 272(17): 11452-11456.

Chen H, Howald WN, Juchau MR (2000) Biosynthesis of all-trans-retinoic acid from all-trans-retinol: catalysis of all-trans-retinol oxidation by human P-450 cytochromes. Drug metabolism and disposition: the biological fate of chemicals 28(3): 315-322.

Chen JK, Falck JR, Reddy KM, Capdevila J, Harris RC (1998) Epoxyeicosatrienoic acids and their sulfonimide derivatives stimulate tyrosine phosphorylation and induce mitogenesis in renal epithelial cells. The Journal of biological chemistry 273(44): 29254-29261.

Chen JK, Wang DW, Falck JR, Capdevila J, Harris RC (1999) Transfection of an active cytochrome P450 arachidonic acid epoxygenase indicates that 14,15-epoxyeicosatrienoic acid functions as an intracellular second messenger in response to epidermal growth factor. The Journal of biological chemistry 274(8): 4764-4769.

Choi YM, An S, Lee EM, Kim K, Choi SJ et al. (2012) CYP1A1 is a target of miR-892a-mediated post-transcriptional repression. International journal of oncology 41(1): 331-336.

Choudhary D, Jansson I, Stoilov I, Sarfarazi M, Schenkman JB (2004) Metabolism of retinoids and arachidonic acid by human and mouse cytochrome P450 1b1. Drug metabolism and disposition: the biological fate of chemicals 32(8): 840-847.

Chua MS, Kashiyama E, Bradshaw TD, Stinson SF, Brantley E et al. (2000) Role of Cyp1A1 in modulation of antitumor properties of the novel agent 2-(4-amino-3-methylphenyl)benzothiazole (DF 203, NSC 674495) in human breast cancer cells. Cancer research 60(18): 5196-5203.

Chua MS, Shi DF, Wrigley S, Bradshaw TD, Hutchinson I et al. (1999) Antitumor benzothiazoles. 7. Synthesis of 2-(4-acylaminophenyl)benzothiazoles and investigations into the role of acetylation in the antitumor activities of the parent amines. Journal of medicinal chemistry 42(3): 381-392.

Ciolino HP, Wang TT, Yeh GC (1998) Diosmin and diosmetin are agonists of the aryl hydrocarbon receptor that differentially affect cytochrome P450 1A1 activity. Cancer research 58(13): 2754-2760.

Conney AH (1982) Induction of microsomal enzymes by foreign chemicals and carcinogenesis by polycyclic aromatic hydrocarbons: G. H. A. Clowes Memorial Lecture. Cancer research 42(12): 4875-4917.

Corchero J, Pimprale S, Kimura S, Gonzalez FJ (2001) Organization of the CYP1A cluster on human chromosome 15: implications for gene regulation. Pharmacogenetics 11(1): 1-6.

Corradetti MN, Inoki K, Bardeesy N, DePinho RA, Guan KL (2004) Regulation of the TSC pathway by LKB1: evidence of a molecular link between tuberous sclerosis complex and Peutz-Jeghers syndrome. Genes & development 18(13): 1533-1538.

Dalton TP, Dieter MZ, Matlib RS, Childs NL, Shertzer HG et al. (2000) Targeted knockout of Cyp1a1 gene does not alter hepatic constitutive expression of other genes in the mouse [Ah] battery. Biochemical and biophysical research communications 267(1): 184-189.

Das M, Asokan P, Don PS, Krueger GG, Bickers DR et al. (1986) Carcinogen metabolism in human skin grafted onto athymic nude mice: a model system for the study of human skin carcinogenesis. Biochemical and biophysical research communications 138(1): 33-39.

Dawling S, Hachey DL, Roodi N, Parl FF (2004) In vitro model of mammary estrogen metabolism: structural and kinetic differences between catechol estrogens 2- and 4-hydroxyestradiol. Chemical research in toxicology 17(9): 1258-1264.

de Waziers I, Cugnenc PH, Yang CS, Leroux JP, Beaune PH (1990) Cytochrome P 450 isoenzymes, epoxide hydrolase and glutathione transferases in rat and human hepatic and extrahepatic tissues. The Journal of pharmacology and experimental therapeutics 253(1): 387-394.

Dehal SS, Kupfer D (1997) CYP2D6 catalyzes tamoxifen 4-hydroxylation in human liver. Cancer research 57(16): 3402-3406.

Diamond L, Sardet C, Rothblat GH (1968) The metabolism of 7,12-dimethylbenz(a)anthracene in cell cultures. International journal of cancer 3(6): 838-849.

Diehl JA, Cheng M, Roussel MF, Sherr CJ (1998) Glycogen synthase kinase-3beta regulates cyclin D1 proteolysis and subcellular localization. Genes & development 12(22): 3499-3511.

Ding X, Kaminsky LS (2003) Human extrahepatic cytochromes P450: function in xenobiotic metabolism and tissue-selective chemical toxicity in the respiratory and gastrointestinal tracts. Annual review of pharmacology and toxicology 43: 149-173.

Dong H, Dalton TP, Miller ML, Chen Y, Uno S et al. (2009) Knock-in mouse lines expressing either mitochondrial or microsomal CYP1A1: differing responses to dietary benzo[a]pyrene as proof of principle. Molecular pharmacology 75(3): 555-567.

Dowsett M, Martin LA, Smith I, Johnston S (2005) Mechanisms of resistance to aromatase inhibitors. The Journal of steroid biochemistry and molecular biology 95(1-5): 167-172.

Dragin N, Uno S, Wang B, Dalton TP, Nebert DW (2007) Generation of 'humanized' hCYP1A1_1A2_Cyp1a1/1a2(-/-) mouse line. Biochemical and biophysical research communications 359(3): 635-642.

Dragin N, Shi Z, Madan R, Karp CL, Sartor MA et al. (2008) Phenotype of the Cyp1a1/1a2/1b1-/- triple-knockout mouse. Molecular pharmacology 73(6): 1844-1856.

Du J, Guan T, Zhang H, Xia Y, Liu F et al. (2008) Inhibitory crosstalk between ERK and AMPK in the growth and proliferation of cardiac fibroblasts. Biochemical and biophysical research communications 368(2): 402-407.

Dunnwald LK, Rossing MA, Li CI (2007) Hormone receptor status, tumor characteristics, and prognosis: a prospective cohort of breast cancer patients. Breast Cancer Res 9(1): R6.

Evans WE, Relling MV (1999) Pharmacogenomics: translating functional genomics into rational therapeutics. Science (New York, NY 286(5439): 487-491.

Fichtner I, Monks A, Hose C, Stevens MF, Bradshaw TD (2004) The experimental antitumor agents Phortress and doxorubicin are equiactive against human-derived breast carcinoma xenograft models. Breast cancer research and treatment 87(1): 97-107.

Fingar DC, Richardson CJ, Tee AR, Cheatham L, Tsou C et al. (2004) mTOR controls cell cycle progression through its cell growth effectors S6K1 and 4E-BP1/eukaryotic translation initiation factor 4E. Molecular and cellular biology 24(1): 200-216.

Fisher JM, Jones KW, Whitlock JP, Jr. (1989) Activation of transcription as a general mechanism of 2,3,7,8-tetrachlorodibenzo-p-dioxin action. Molecular carcinogenesis 1(4): 216-221.

Fonseca R, Hartmann LC, Petersen IA, Donohue JH, Crotty TB et al. (1997) Ductal carcinoma in situ of the breast. Annals of internal medicine 127(11): 1013-1022.

Fornaro M, Plescia J, Chheang S, Tallini G, Zhu YM et al. (2003) Fibronectin protects prostate cancer cells from tumor necrosis factor-alpha-induced apoptosis via the

AKT/survivin pathway. The Journal of biological chemistry 278(50): 50402-50411.

Fujita K, Kamataki T (2001) Predicting the mutagenicity of tobacco-related N-nitrosamines in humans using 11 strains of Salmonella typhimurium YG7108, each coexpressing a form of human cytochrome P450 along with NADPH-cytochrome P450 reductase. Environmental and molecular mutagenesis 38(4): 339-346.

Galijatovic A, Beaton D, Nguyen N, Chen S, Bonzo J et al. (2004) The human CYP1A1 gene is regulated in a developmental and tissue-specific fashion in transgenic mice. The Journal of biological chemistry 279(23): 23969-23976.

Galvez-Peralta M, Shi Z, Chen J, Miller ML, Nebert DW (2012) Oral benzo[a]pyrene in cyp1a1/1b1(-/-) double-knockout mice: Microarray analysis during squamous cell carcinoma formation in preputial gland duct. International journal of cancer.

Gelboin HV (1969) A microsome-dependent binding of benzo[a]pyrene to DNA. Cancer research 29(6): 1272-1276.

Gelboin HV, Huberman E, Sachs L (1969) Enzymatic hydroxylation of benzopyrene and its relationship to cytotoxicity. Proceedings of the National Academy of Sciences of the United States of America 64(4): 1188-1194.

Gennari A, Sormani MP, Pronzato P, Puntoni M, Colozza M et al. (2008) HER2 status and efficacy of adjuvant anthracyclines in early breast cancer: a pooled analysis of randomized trials. Journal of the National Cancer Institute 100(1): 14-20.

Gonzalez FJ, Tukey RH, Nebert DW (1984) Structural gene products of the Ah locus. Transcriptional regulation of cytochrome P1-450 and P3-450 mRNA levels by 3-methylcholanthrene. Molecular pharmacology 26(1): 117-121.

Guengerich FP (2008) Cytochrome p450 and chemical toxicology. Chemical research in toxicology 21(1): 70-83.

Haas S, Pierl C, Harth V, Pesch B, Rabstein S et al. (2006) Expression of xenobiotic and steroid hormone metabolizing enzymes in human breast carcinomas. International journal of cancer 119(8): 1785-1791.

Halilovic E, She QB, Ye Q, Pagliarini R, Sellers WR et al. (2010) PIK3CA mutation uncouples tumor growth and cyclin D1 regulation from MEK/ERK and mutant KRAS signaling. Cancer research 70(17): 6804-6814.

Hammons GJ, Milton D, Stepps K, Guengerich FP, Tukey RH et al. (1997) Metabolism of carcinogenic heterocyclic and aromatic amines by recombinant human cytochrome P450 enzymes. Carcinogenesis 18(4): 851-854.

Hanahan D, Weinberg RA (2000) The hallmarks of cancer. Cell 100(1): 57-70.

Hawley SA, Boudeau J, Reid JL, Mustard KJ, Udd L et al. (2003) Complexes between the LKB1 tumor suppressor, STRAD alpha/beta and MO25 alpha/beta are upstream kinases in the AMP-activated protein kinase cascade. Journal of biology 2(4): 28.

Hines RN, Mathis JM, Jacob CS (1988) Identification of multiple regulatory elements on the human cytochrome P450IA1 gene. Carcinogenesis 9(9): 1599-1605.

Hose CD, Hollingshead M, Sausville EA, Monks A (2003) Induction of CYP1A1 in tumor cells by the antitumor agent 2-[4-amino-3-methylphenyl]-5-fluoro-benzothiazole: a potential surrogate marker for patient sensitivity. Molecular cancer therapeutics 2(12): 1265-1272.

Howlader N NA, Krapcho M, Neyman N, Aminou R, Waldron W, Altekruse SF, Kosary CL, Ruhl J, Tatalovich Z, Cho H, Mariotto A, Eisner MP, Lewis DR, Chen HS, Feuer EJ, Cronin KA, Edwards BK (eds) (2010) SEER Cancer Statistics Review, 1975-2008, National Cancer Institute. Bethesda, MD: National Cancer Institute.

Huberman E, Sachs L, Yang SK, Gelboin V (1976) Identification of mutagenic metabolites of benzo(a)pyrene in mammalian cells. Proceedings of the National Academy of Sciences of the United States of America 73(2): 607-611.

Ingelman-Sundberg M (2004) Pharmacogenetics of cytochrome P450 and its applications in drug therapy: the past, present and future. Trends in pharmacological sciences 25(4): 193-200.

Inoki K, Zhu T, Guan KL (2003) TSC2 mediates cellular energy response to control cell growth and survival. Cell 115(5): 577-590.

Israel DI, Whitlock JP, Jr. (1984) Regulation of cytochrome P1-450 gene transcription by 2,3,7, 8-tetrachlorodibenzo-p-dioxin in wild type and variant mouse hepatoma cells. The Journal of biological chemistry 259(9): 5400-5402.

Jaiswal AK, Gonzalez FJ, Nebert DW (1985) Human P1-450 gene sequence and correlation of mRNA with genetic differences in benzo[a]pyrene metabolism. Nucleic acids research 13(12): 4503-4520.

Jaiswal AK, Nebert DW, McBride OW, Gonzalez FJ (1987) Human P(3)450: cDNA and complete protein sequence, repetitive Alu sequences in the 3' nontranslated region, and localization of gene to chromosome 15. Journal of experimental pathology 3(1): 1-17.

Jiang JG, Chen CL, Card JW, Yang S, Chen JX et al. (2005) Cytochrome P450 2J2 promotes the neoplastic phenotype of carcinoma cells and is up-regulated in human tumors. Cancer research 65(11): 4707-4715.

Jin J, Mullen TD, Hou Q, Bielawski J, Bielawska A et al. (2009) AMPK inhibitor Compound C stimulates ceramide production and promotes Bax redistribution and apoptosis in MCF7 breast carcinoma cells. Journal of lipid research 50(12): 2389-2397.

Johnson JJ, Syed DN, Heren CR, Suh Y, Adhami VM et al. (2008) Carnosol, a dietary diterpene, displays growth inhibitory effects in human prostate cancer PC3 cells leading to G2-phase cell cycle arrest and targets the 5'-AMP-activated protein kinase (AMPK) pathway. Pharmaceutical research 25(9): 2125-2134.

Johnson JJ, Syed DN, Suh Y, Heren CR, Saleem M et al. (2010) Disruption of androgen and estrogen receptor activity in prostate cancer by a novel dietary diterpene carnosol: implications for chemoprevention. Cancer prevention research (Philadelphia, Pa 3(9): 1112-1123.

Jouve C, Palmeirim I, Henrique D, Beckers J, Gossler A et al. (2000) Notch signalling is required for cyclic expression of the hairy-like gene HES1 in the presomitic mesoderm. Development (Cambridge, England) 127(7): 1421-1429.

Kaderlik KR, Minchin RF, Mulder GJ, Ilett KF, Daugaard-Jenson M et al. (1994) Metabolic activation pathway for the formation of DNA adducts of the carcinogen 2-amino-1-methyl-6-phenylimidazo[4,5-b]pyridine (PhIP) in rat extrahepatic tissues. Carcinogenesis 15(8): 1703-1709.

Kawajiri K, Watanabe J, Gotoh O, Tagashira Y, Sogawa K et al. (1986) Structure and drug inducibility of the human cytochrome P-450c gene. European journal of biochemistry / FEBS 159(2): 219-225.

Kellermann G, Shaw CR, Luyten-Kellerman M (1973) Aryl hydrocarbon hydroxylase inducibility and bronchogenic carcinoma. The New England journal of medicine 289(18): 934-937.

Kent WJ, Sugnet CW, Furey TS, Roskin KM, Pringle TH et al. (2002) The human genome browser at UCSC. Genome research 12(6): 996-1006.

Kiefer F, Arnold K, Kunzli M, Bordoli L, Schwede T (2009) The SWISS-MODEL Repository and associated resources. Nucleic acids research 37(Database issue): D387-392.

Kim MJ, Park IJ, Yun H, Kang I, Choe W et al. (2010) AMP-activated protein kinase antagonizes pro-apoptotic extracellular signal-regulated kinase activation by inducing dual-specificity protein phosphatases in response to glucose deprivation in HCT116 carcinoma. The Journal of biological chemistry 285(19): 14617-14627.

Kinoshita N, Gelboin HV (1972) Aryl hydrocarbon hydroxylase and polycyclic hydrocarbon tumorigenesis: effect of the enzyme inhibitor 7,8-benzoflavone on tumorigenesis and macromolecule binding. Proceedings of the National Academy of Sciences of the United States of America 69(4): 824-828.

Kopp J, Schwede T (2004) The SWISS-MODEL Repository of annotated three-dimensional protein structure homology models. Nucleic acids research 32(Database issue): D230-234.

Kovacic S, Soltys CL, Barr AJ, Shiojima I, Walsh K et al. (2003) Akt activity negatively regulates phosphorylation of AMP-activated protein kinase in the heart. The Journal of biological chemistry 278(41): 39422-39427.

Kress S, Reichert J, Schwarz M (1998) Functional analysis of the human cytochrome P4501A1 (CYP1A1) gene enhancer. European journal of biochemistry / FEBS 258(2): 803-812.

Kuffel MJ, Schroeder JC, Pobst LJ, Naylor S, Reid JM et al. (2002) Activation of the antitumor agent aminoflavone (NSC 686288) is mediated by induction of tumor cell cytochrome P450 1A1/1A2. Molecular pharmacology 62(1): 143-153.

Kuhn NJ, Briley MS (1970) The roles of pregn-5-ene-3 beta, 20 alpha-diol and 20 alpha-hydroxy steroid dehydrogenase in the control of progesterone synthesis preceding parturition and lactogenesis in the rat. The Biochemical journal 117(2): 193-201.

Kupchan SM, Knox JR, Udayamurthy MS (1965) Tumor inhibitors. 8. Eupatorin, new cytotoxic flavone from Eupatorium semiserratum. Journal of pharmaceutical sciences 54(6): 929-930.

Landi MT, Bertazzi PA, Shields PG, Clark G, Lucier GW et al. (1994) Association between CYP1A1 genotype, mRNA expression and enzymatic activity in humans. Pharmacogenetics 4(5): 242-246.

Lavoie JN, L'Allemain G, Brunet A, Muller R, Pouyssegur J (1996) Cyclin D1 expression is regulated positively by the p42/p44MAPK and negatively by the p38/HOGMAPK pathway. The Journal of biological chemistry 271(34): 20608-20616.

Lekas P, Tin KL, Lee C, Prokipcak RD (2000) The human cytochrome P450 1A1 mRNA is rapidly degraded in HepG2 cells. Archives of biochemistry and biophysics 384(2): 311-318.

Lemon HM, Heidel JW, Rodriguez-Sierra JF (1992) Increased catechol estrogen metabolism as a risk factor for nonfamilial breast cancer. Cancer 69(2): 457-465.

Leong CO, Gaskell M, Martin EA, Heydon RT, Farmer PB et al. (2003) Antitumour 2-(4-aminophenyl)benzothiazoles generate DNA adducts in sensitive tumour cells in vitro and in vivo. British journal of cancer 88(3): 470-477.

Leung YK, Lau KM, Mobley J, Jiang Z, Ho SM (2005) Overexpression of cytochrome P450 1A1 and its novel spliced variant in ovarian cancer cells: alternative subcellular enzyme compartmentation may contribute to carcinogenesis. Cancer research 65(9): 3726-3734.

Lewis BC, Mackenzie PI, Miners JO (2007) Comparative homology modeling of human cytochrome P4501A1 (CYP1A1) and confirmation of residues involved in 7-ethoxyresorufin O-deethylation by site-directed mutagenesis and enzyme kinetic analysis. Archives of biochemistry and biophysics 468(1): 58-69.

Li G, Siddiqui H, Teng Y, Lin R, Wan XY et al. (2011) Coordinated transcriptional regulation underlying the circadian clock in Arabidopsis. Nature cell biology 13(5): 616-622.

Liang CJ, Ives HE, Yang CM, Ma YH (2008) 20-HETE inhibits the proliferation of vascular smooth muscle cells via transforming growth factor-beta. Journal of lipid research 49(1): 66-73.

Liehr JG, Ricci MJ (1996) 4-Hydroxylation of estrogens as marker of human mammary tumors. Proceedings of the National Academy of Sciences of the United States of America 93(8): 3294-3296.

Lin F, Rios A, Falck JR, Belosludtsev Y, Schwartzman ML (1995) 20-Hydroxyeicosatetraenoic acid is formed in response to EGF and is a mitogen in rat proximal tubule. The American journal of physiology 269(6 Pt 2): F806-816.

Liu L, Chen C, Gong W, Li Y, Edin ML et al. (2011) Epoxyeicosatrienoic acids attenuate reactive oxygen species level, mitochondrial dysfunction, caspase activation, and apoptosis in carcinoma cells treated with arsenic trioxide. The Journal of pharmacology and experimental therapeutics 339(2): 451-463.

Loeper J, Descatoire V, Maurice M, Beaune P, Belghiti J et al. (1993) Cytochromes P-450 in human hepatocyte plasma membrane: recognition by several autoantibodies. Gastroenterology 104(1): 203-216.

Lukas J, Bartkova J, Bartek J (1996) Convergence of mitogenic signalling cascades from diverse classes of receptors at the cyclin D-cyclin-dependent kinase-pRb-controlled G1 checkpoint. Molecular and cellular biology 16(12): 6917-6925.

Luo Z, Zang M, Guo W (2010) AMPK as a metabolic tumor suppressor: control of metabolism and cell growth. Future oncology (London, England) 6(3): 457-470.

Lusska A, Shen E, Whitlock JP, Jr. (1993) Protein-DNA interactions at a dioxin-responsive enhancer. Analysis of six bona fide DNA-binding sites for the liganded Ah receptor. The Journal of biological chemistry 268(9): 6575-6580.

Ma Q, Whitlock JP, Jr. (1997) A novel cytoplasmic protein that interacts with the Ah receptor, contains tetratricopeptide repeat motifs, and augments the

transcriptional response to 2,3,7,8-tetrachlorodibenzo-p-dioxin. The Journal of biological chemistry 272(14): 8878-8884.

Madra S, Mann F, Francis JE, Manson MM, Smith AG (1996) Modulation by iron of hepatic microsomal and nuclear cytochrome P450, and cytosolic glutathione S-transferase and peroxidase in C57BL/10ScSn mice induced with polychlorinated biphenyls (Aroclor 1254). Toxicology and applied pharmacology 136(1): 79-86.

Manning BD, Tee AR, Logsdon MN, Blenis J, Cantley LC (2002) Identification of the tuberous sclerosis complex-2 tumor suppressor gene product tuberin as a target of the phosphoinositide 3-kinase/akt pathway. Molecular cell 10(1): 151-162.

McLean L, Soto U, Agama K, Francis J, Jimenez R et al. (2008) Aminoflavone induces oxidative DNA damage and reactive oxidative species-mediated apoptosis in breast cancer cells. International journal of cancer 122(7): 1665-1674.

McLemore TL, Adelberg S, Czerwinski M, Hubbard WC, Yu SJ et al. (1989) Altered regulation of the cytochrome P4501A1 gene: novel inducer-independent gene expression in pulmonary carcinoma cell lines. Journal of the National Cancer Institute 81(23): 1787-1794.

McLemore TL, Adelberg S, Liu MC, McMahon NA, Yu SJ et al. (1990) Expression of CYP1A1 gene in patients with lung cancer: evidence for cigarette smoke-induced gene expression in normal lung tissue and for altered gene regulation in primary pulmonary carcinomas. Journal of the National Cancer Institute 82(16): 1333-1339.

McSorley LC, Daly AK (2000) Identification of human cytochrome P450 isoforms that contribute to all-trans-retinoic acid 4-hydroxylation. Biochemical pharmacology 60(4): 517-526.

Meloche S, Pouyssegur J (2007) The ERK1/2 mitogen-activated protein kinase pathway as a master regulator of the G1- to S-phase transition. Oncogene 26(22): 3227-3239.

Mitra R, Guo Z, Milani M, Mesaros C, Rodriguez M et al. (2011) CYP3A4 mediates growth of estrogen receptor-positive breast cancer cells in part by inducing nuclear translocation of phospho-Stat3 through biosynthesis of (+/-)-14,15-epoxyeicosatrienoic acid (EET). The Journal of biological chemistry 286(20): 17543-17559.

Mohebati A, Guttenplan JB, Kochhar A, Zhao ZL, Kosinska W et al. (2012) Carnosol, a constituent of Zyflamend, inhibits aryl hydrocarbon receptor-mediated activation of CYP1A1 and CYP1B1 transcription and mutagenesis. Cancer prevention research (Philadelphia, Pa 5(4): 593-602.

Monks A, Harris E, Hose C, Connelly J, Sausville EA (2003) Genotoxic profiling of MCF-7 breast cancer cell line elucidates gene expression modifications underlying toxicity of the anticancer drug 2-(4-amino-3-methylphenyl)-5-fluorobenzothiazole. Molecular pharmacology 63(3): 766-772.

Morin C, Sirois M, Echave V, Rizcallah E, Rousseau E (2009) Relaxing effects of 17(18)-EpETE on arterial and airway smooth muscles in human lung. American journal of physiology 296(1): L130-139.

Murray GI, Patimalla S, Stewart KN, Miller ID, Heys SD (2010) Profiling the expression of cytochrome P450 in breast cancer. Histopathology 57(2): 202-211.

Murray GI, Shaw D, Weaver RJ, McKay JA, Ewen SW et al. (1994) Cytochrome P450 expression in oesophageal cancer. Gut 35(5): 599-603.

Murray GI, Taylor VE, McKay JA, Weaver RJ, Ewen SW et al. (1995) Expression of xenobiotic metabolizing enzymes in tumours of the urinary bladder. International journal of experimental pathology 76(4): 271-276.

Nandekar PP, Sangamwar AT (2012) Cytochrome P450 1A1-mediated anticancer drug discovery: in silico findings. Expert opinion on drug discovery 7(9): 771-789.

Nebert DW, Dalton TP, Okey AB, Gonzalez FJ (2004) Role of aryl hydrocarbon receptor-mediated induction of the CYP1 enzymes in environmental toxicity and cancer. The Journal of biological chemistry 279(23): 23847-23850.

Nebert DW, Roe AL, Dieter MZ, Solis WA, Yang Y et al. (2000) Role of the aromatic hydrocarbon receptor and [Ah] gene battery in the oxidative stress response, cell cycle control, and apoptosis. Biochemical pharmacology 59(1): 65-85.

Neher R, Wettstein A (1960) Occurence of Delta5-3beta-hydroxy-steroids in adrenal and testicular tissue. Acta endocrinologica 35: 1-7.

Nelson DR, Zeldin DC, Hoffman SM, Maltais LJ, Wain HM et al. (2004) Comparison of cytochrome P450 (CYP) genes from the mouse and human genomes, including nomenclature recommendations for genes, pseudogenes and alternative-splice variants. Pharmacogenetics 14(1): 1-18.

Niranjan BG, Avadhani NG, DiGiovanni J (1985) Formation of benzo(alpha)pyrene metabolites and DNA adducts catalyzed by a rat liver mitochondrial monooxygenase system. Biochemical and biophysical research communications 131(2): 935-942.

Niwa T, Murayama N, Yamazaki H (2009) Oxidation of endobiotics mediated by xenobiotic-metabolizing forms of human cytochrome. Current drug metabolism 10(7): 700-712.

Niwa T, Yabusaki Y, Honma K, Matsuo N, Tatsuta K et al. (1998) Contribution of human hepatic cytochrome P450 isoforms to regioselective hydroxylation of steroid hormones. Xenobiotica; the fate of foreign compounds in biological systems 28(6): 539-547.

Offord EA, Mace K, Ruffieux C, Malnoe A, Pfeifer AM (1995) Rosemary components inhibit benzo[a]pyrene-induced genotoxicity in human bronchial cells. Carcinogenesis 16(9): 2057-2062.

Omura T (2006) Mitochondrial P450s. Chemico-biological interactions 163(1-2): 86-93.

Onitilo AA, Engel JM, Greenlee RT, Mukesh BN (2009) Breast cancer subtypes based on ER/PR and Her2 expression: comparison of clinicopathologic features and survival. Clinical medicine & research 7(1-2): 4-13.

Ortiz de Montellano PR (2005) Cytochrome P450 : structure, mechanism, and biochemistry. New York: Kluwer Academic/Plenum Publishers. xx, 689 p. p.

Osanai M, Sawada N, Lee GH (2010) Oncogenic and cell survival properties of the retinoic acid metabolizing enzyme, CYP26A1. Oncogene 29(8): 1135-1144.

Panigrahy D, Edin ML, Lee CR, Huang S, Bielenberg DR et al. (2012) Epoxyeicosanoids stimulate multiorgan metastasis and tumor dormancy escape in mice. The Journal of clinical investigation 122(1): 178-191.

Perdew GH, Whitelaw ML (1991) Evidence that the 90-kDa heat shock protein (HSP90) exists in cytosol in heteromeric complexes containing HSP70 and three other

proteins with Mr of 63,000, 56,000, and 50,000. The Journal of biological chemistry 266(11): 6708-6713.

Peterson G, Barnes S (1991) Genistein inhibition of the growth of human breast cancer cells: independence from estrogen receptors and the multi-drug resistance gene. Biochemical and biophysical research communications 179(1): 661-667.

Pollenz RS, Sattler CA, Poland A (1994) The aryl hydrocarbon receptor and aryl hydrocarbon receptor nuclear translocator protein show distinct subcellular localizations in Hepa 1c1c7 cells by immunofluorescence microscopy. Molecular pharmacology 45(3): 428-438.

Pors K, Loadman PM, Shnyder SD, Sutherland M, Sheldrake HM et al. (2011) Modification of the duocarmycin pharmacophore enables CYP1A1 targeting for biological activity. Chemical communications (Cambridge, England) 47(44): 12062-12064.

Pozzi A, Popescu V, Yang S, Mei S, Shi M et al. (2010) The anti-tumorigenic properties of peroxisomal proliferator-activated receptor alpha are arachidonic acid epoxygenase-mediated. The Journal of biological chemistry 285(17): 12840-12850.

Raza H, Avadhani NG (1988) Hepatic mitochondrial cytochrome P-450 system. Purification and characterization of two distinct forms of mitochondrial cytochrome P-450 from beta-naphthoflavone-induced rat liver. The Journal of biological chemistry 263(19): 9533-9541.

Rodriguez M, Potter DA (2013) Cytochrome P450 1A1 Regulates Breast Cancer Cell Proliferation and Survival. Mol Cancer Res.

Ryan KJ, Engel LL (1957) Hydroxylation of steroids at carbon 21. The Journal of biological chemistry 225(1): 103-114.

Sangamwar AT, Labhsetwar LB, Kuberkar SV (2008) Exploring CYP1A1 as anticancer target: homology modeling and in silico inhibitor design. Journal of molecular modeling 14(11): 1101-1109.

Sasano H, Frost AR, Saitoh R, Harada N, Poutanen M et al. (1996) Aromatase and 17 beta-hydroxysteroid dehydrogenase type 1 in human breast carcinoma. The Journal of clinical endocrinology and metabolism 81(11): 4042-4046.

Schmelzle M, Felix SB, Staudt A, Herda LR (2011) Cardioprotection of 17,18-epoxyeicosatetraenoic acid in ischemia/reperfusion is mediated by cyclooxygenase-2: a study in a rat model. Transplantation proceedings 43(5): 1515-1519.

Schmittgen TD, Livak KJ (2008) Analyzing real-time PCR data by the comparative C(T) method. Nature protocols 3(6): 1101-1108.

Schwarz D, Kisselev P, Ericksen SS, Szklarz GD, Chernogolov A et al. (2004) Arachidonic and eicosapentaenoic acid metabolism by human CYP1A1: highly stereoselective formation of 17(R),18(S)-epoxyeicosatetraenoic acid. Biochemical pharmacology 67(8): 1445-1457.

Seewaldt VL, Johnson BS, Parker MB, Collins SJ, Swisshelm K (1995) Expression of retinoic acid receptor beta mediates retinoic acid-induced growth arrest and apoptosis in breast cancer cells. Cell Growth Differ 6(9): 1077-1088.

Sergentanis TN, Economopoulos KP (2010) Four polymorphisms in cytochrome P450 1A1 (CYP1A1) gene and breast cancer risk: a meta-analysis. Breast cancer research and treatment 122(2): 459-469.

She QB, Halilovic E, Ye Q, Zhen W, Shirasawa S et al. (2010) 4E-BP1 is a key effector of the oncogenic activation of the AKT and ERK signaling pathways that integrates their function in tumors. Cancer cell 18(1): 39-51.

Shen ES, Whitlock JP, Jr. (1992) Protein-DNA interactions at a dioxin-responsive enhancer. Mutational analysis of the DNA-binding site for the liganded Ah receptor. The Journal of biological chemistry 267(10): 6815-6819.

Sikka SC, Swerdloff RS, Rajfer J (1985) In vitro inhibition of testosterone biosynthesis by ketoconazole. Endocrinology 116(5): 1920-1925.

Silver G, Krauter KS (1988) Expression of cytochromes P-450c and P-450d mRNAs in cultured rat hepatocytes. 3-Methylcholanthrene induction is regulated primarily at the post-transcriptional level. The Journal of biological chemistry 263(24): 11802-11807.

Sim SC, Ingelman-Sundberg M (2010) The Human Cytochrome P450 (CYP) Allele Nomenclature website: a peer-reviewed database of CYP variants and their associated effects. Human genomics 4(4): 278-281.

Sinal CJ, Bend JR (1997) Aryl hydrocarbon receptor-dependent induction of cyp1a1 by bilirubin in mouse hepatoma hepa 1c1c7 cells. Molecular pharmacology 52(4): 590-599.

Singh V, Parmar D, Singh MP (2008) Do single nucleotide polymorphisms in xenobiotic metabolizing genes determine breast cancer susceptibility and treatment outcomes? Cancer investigation 26(8): 769-783.

Sinz M, Wallace G, Sahi J (2008) Current industrial practices in assessing CYP450 enzyme induction: preclinical and clinical. The AAPS journal 10(2): 391-400.

Sivaraman VS, Wang H, Nuovo GJ, Malbon CC (1997) Hyperexpression of mitogen-activated protein kinase in human breast cancer. The Journal of clinical investigation 99(7): 1478-1483.

Soderkvist P, Busk L, Toftgard R, Gustafsson JA (1983) Metabolic activation of promutagens, detectable in Ames' Salmonella assay, by 5000 X g supernatant of rat ventral prostate. Chemico-biological interactions 46(2): 151-163.

Sonneveld E, van den Brink CE, van der Leede BM, Schulkes RK, Petkovich M et al. (1998) Human retinoic acid (RA) 4-hydroxylase (CYP26) is highly specific for all-trans-RA and can be induced through RA receptors in human breast and colon carcinoma cells. Cell Growth Differ 9(8): 629-637.

Spink DC, Eugster HP, Lincoln DW, 2nd, Schuetz JD, Schuetz EG et al. (1992) 17 beta-estradiol hydroxylation catalyzed by human cytochrome P450 1A1: a comparison of the activities induced by 2,3,7,8-tetrachlorodibenzo-p-dioxin in MCF-7 cells with those from heterologous expression of the cDNA. Archives of biochemistry and biophysics 293(2): 342-348.

Sporn MB (1996) The war on cancer. Lancet 347(9012): 1377-1381.

Sun M, Paciga JE, Feldman RI, Yuan Z, Coppola D et al. (2001a) Phosphatidylinositol-3-OH Kinase (PI3K)/AKT2, activated in breast cancer, regulates and is induced by estrogen receptor alpha (ERalpha) via interaction between ERalpha and PI3K. Cancer research 61(16): 5985-5991.

Sun M, Wang G, Paciga JE, Feldman RI, Yuan ZQ et al. (2001b) AKT1/PKBalpha kinase is frequently elevated in human cancers and its constitutive activation is required for oncogenic transformation in NIH3T3 cells. The American journal of pathology 159(2): 431-437.

Sutherland M, Gill JH, Loadman PM, Laye JP, Sheldrake HM et al. (2012) Antitumor Activity of a Duocarmycin Analogue Rationalised to Be Metabolically Activated by Cytochrome P450 1a1 in Human Transitional Cell Carcinoma of the Bladder. Molecular cancer therapeutics.

Tanaka K, Iwamoto S, Gon G, Nohara T, Iwamoto M et al. (2000) Expression of survivin and its relationship to loss of apoptosis in breast carcinomas. Clin Cancer Res 6(1): 127-134.

Tang XH, Gudas LJ (2011) Retinoids, retinoic acid receptors, and cancer. Annual review of pathology 6: 345-364.

Tao R, Gong J, Luo X, Zang M, Guo W et al. (2010) AMPK exerts dual regulatory effects on the PI3K pathway. Journal of molecular signaling 5(1): 1.

Thibier-Fouchet C, Mulner O, Ozon R (1976) Progesterone biosynthesis and metabolism by ovarian follicles and isolated oocytes Xenopus laevis. Biology of reproduction 14(3): 317-326.

Trachtenberg J, Zadra J (1988) Steroid synthesis inhibition by ketoconazole: sites of action. Clinical and investigative medicine 11(1): 1-5.

Trapani V, Patel V, Leong CO, Ciolino HP, Yeh GC et al. (2003) DNA damage and cell cycle arrest induced by 2-(4-amino-3-methylphenyl)-5-fluorobenzothiazole (5F 203, NSC 703786) is attenuated in aryl hydrocarbon receptor deficient MCF-7 cells. British journal of cancer 88(4): 599-605.

Uno S, Dalton TP, Derkenne S, Curran CP, Miller ML et al. (2004) Oral exposure to benzo[a]pyrene in the mouse: detoxication by inducible cytochrome P450 is more important than metabolic activation. Molecular pharmacology 65(5): 1225-1237.

Uno S, Dalton TP, Dragin N, Curran CP, Derkenne S et al. (2006) Oral benzo[a]pyrene in Cyp1 knockout mouse lines: CYP1A1 important in detoxication, CYP1B1 metabolism required for immune damage independent of total-body burden and clearance rate. Molecular pharmacology 69(4): 1103-1114.

van Cantfort J, Gielen JE (1981) Ontogenetic variation in rat liver, lung and kidney monooxygenase induction by low doses of benzo(A)pyrene and cigarette-smoke condensate. British journal of cancer 44(6): 902-910.

Van heusden J, Wouters W, Ramaekers FC, Krekels MD, Dillen L et al. (1998) All-trans-retinoic acid metabolites significantly inhibit the proliferation of MCF-7 human breast cancer cells in vitro. British journal of cancer 77(1): 26-32.

Vinothini G, Nagini S (2010) Correlation of xenobiotic-metabolizing enzymes, oxidative stress and NFkappaB signaling with histological grade and menopausal status in patients with adenocarcinoma of the breast. Clinica chimica acta; international journal of clinical chemistry 411(5-6): 368-374.

Walsh AA, Szklarz GD, Scott EE (2013) Human Cytochrome P450 1A1 Structure and Utility In Understanding Drug and Xenobiotic Metabolism. The Journal of biological chemistry Epub. DOI: 10.1074/jbc.M113.452953.

Werlinder V, Backlund M, Zhukov A, Ingelman-Sundberg M (2001) Transcriptional and post-translational regulation of CYP1A1 by primaquine. The Journal of pharmacology and experimental therapeutics 297(1): 206-214.

West CD, Naville AH (1962) The in vitro conversion of dehydroepiandrosterone-4-C14 to estrogens by ovarian tissue. Biochemistry 1: 645-651.

White JA, Guo YD, Baetz K, Beckett-Jones B, Bonasoro J et al. (1996) Identification of the retinoic acid-inducible all-trans-retinoic acid 4-hydroxylase. The Journal of biological chemistry 271(47): 29922-29927.

Williams JA, Hyland R, Jones BC, Smith DA, Hurst S et al. (2004) Drug-drug interactions for UDP-glucuronosyltransferase substrates: a pharmacokinetic explanation for typically observed low exposure (AUCi/AUC) ratios. Drug metabolism and disposition: the biological fate of chemicals 32(11): 1201-1208.

Xing C, Imagawa W (1999) Altered MAP kinase (ERK1,2) regulation in primary cultures of mammary tumor cells: elevated basal activity and sustained response to EGF. Carcinogenesis 20(7): 1201-1208.

Xu LC, Sinclair PR, Bresnick E (1993) Induction of cytochrome P450IA1 and its recombinant construct in H4IIE rat hepatoma cells. The International journal of biochemistry 25(1): 13-21.

Yang L, Cao Z, Yan H, Wood WC (2003) Coexistence of high levels of apoptotic signaling and inhibitor of apoptosis proteins in human tumor cells: implication for cancer specific therapy. Cancer research 63(20): 6815-6824.

Yao EF, Denison MS (1992) DNA sequence determinants for binding of transformed Ah receptor to a dioxin-responsive enhancer. Biochemistry 31(21): 5060-5067.

Yu W, Chai H, Li Y, Zhao H, Xie X et al. (2012) Increased expression of CYP4Z1 promotes tumor angiogenesis and growth in human breast cancer. Toxicology and applied pharmacology 264(1): 73-83.

Yu Z, Hu D, Li Y (2004) Effects of zearalenone on mRNA expression and activity of cytochrome P450 1A1 and 1B1 in MCF-7 cells. Ecotoxicology and environmental safety 58(2): 187-193.

Yue W, Wang JP, Hamilton CJ, Demers LM, Santen RJ (1998) In situ aromatization enhances breast tumor estradiol levels and cellular proliferation. Cancer research 58(5): 927-932.

Zhang QY, Dunbar D, Kaminsky L (2000) Human cytochrome P-450 metabolism of retinals to retinoic acids. Drug metabolism and disposition: the biological fate of chemicals 28(3): 292-297.

Zhao P, Meng Q, Liu LZ, You YP, Liu N et al. (2010) Regulation of survivin by PI3K/Akt/p70S6K1 pathway. Biochemical and biophysical research communications 395(2): 219-224.

Zhuang S, Schnellmann RG (2006) A death-promoting role for extracellular signal-regulated kinase. The Journal of pharmacology and experimental therapeutics 319(3): 991-997.

Zhuang Y, Miskimins WK (2008) Cell cycle arrest in Metformin treated breast cancer cells involves activation of AMPK, downregulation of cyclin D1, and requires p27Kip1 or p21Cip1. Journal of molecular signaling 3: 18.

APPENDIX I

siRNA Transfection Protocol

The protocol described here was optimized by Dr. Ranjana Mitra for the transfection of MCF7 line with siRNA against cytochrome P450s. This protocol has been successfully utilized for transfection of CYP1A1siRNA in MCF7 and MDA-MB-231 lines.

1) Plate 13,000 cells/well cells onto a 24-well plate or 65-75,000cells/well onto a 6-well plate using phenol-red free, antibiotic-free medium. Incubate overnight at 37^oC, 5% CO_2. *Note*: To improve transfection efficiency, passage the cells at least once in phenol-red-free medium without antibiotics. See **Chapter II** for cell-specific medium.

2) Prepare transfection solution in eppendorf tubes or in 96-well plates. Throughout the experiment use RNase/DNase free tubes and pipette tips.

   a. Mix A: To 195uL of OptiMeM medium, gently and evenly add 39uL of oligofectamine. Do not pipette or mix, proper micelles will be obtained if left undisturbed. These amounts are sufficient for 12 wells of a 6-well plate or for 48 wells of a 24-well plate. Because these conditions have been optimized, instead of scaling (up or down) make as many of these "Mix A" as needed. Cover Mix A and allow resting for exactly 5min at room temperature.

   b. Mix B: To 175uL OptiMeM medium, add 3uL of 20 µmol/L siRNA and mix gently with the pipette tip. Gently and evenly add 18uL of Mix A (already

incubated for 5min) to the surface of this solution. Do not pipette or mix, incubate for exactly 20min at room temperature.

3) Wash the cells twice with phenol-red free MEM. To each well add 800uL of OptiMeM to a 6-well plate or 300uL to a 24-well plate.

4) After the 20min incubation (Step 2b), transfect the cells as follow. Gently add the indicated amounts of Mix B to each well, gently, from about 0.5-1inch from above the well, distributing it systematically around the well.

   a. 6-well plate: to each well add the entire content of Mix B (~196uL).

   b. 24-well plate: to each well add 46uL of Mix B.

   After adding Mix B to all wells, mix gently by rocking the plate with your hand in circular motions and to each side. Incubate cells at 37°C, 5% CO_2 for at least 5h and preferably overnight.

5) After overnight incubation with the transfection reaction, add phenol-red free, antibiotic-free media to the cells to a final serum concentration of 5-10%. Do not need to remove the transfection solution for these lines. Incubate for the desired amount of time (48-120 hours recommended depending on the siRNA) and use cells for desired assay.

APPENDIX II

Eicosanoid Extraction for
Mass Spectrometry Analysis

The protocol described here was optimized by Dr. Zhijun Guo to extract EETs from breast cancer lines. It is recommended that all reagents are prepared fresh prior to performing the experiment. Care should be taken to avoid oxidation of eicosanoids.

1) Plate cells and treat as desired. Three 100mm confluent (80-90% confluence) plates are recommended per sample. Alternatively one 150mm plate/sample can be used.

2) Wash plates twice with 5mL of 1X PBS, add 1mL of ice-cold 1 μmol/L epoxide hydrolase inhibitor in PBS (1 μmol/L EHI-1471/PBS), and detach cells from the plate with a cell scraper. Collect cells in 12 mL disposable glass tubes and make sure to label tube appropriately and cover with clear tape to avoid the ink from erasing by organic solvents. Centrifuge cells for 10min at 3,000rpm.

3) Discard supernatant and resuspend the pellet in 1 mL 1 μmol/L EHI/PBS. Pipette pellet vigorously to ensure cells are in uniform suspension.

4) For normalization purposes aliquot 100uL of the cell suspension and keep in a equally labeled microtube. Store at -80°C immediately for future microBCA assay to be performed as follow:

a. Centrifuge cells and resuspend in 50uL of RIPA buffer.

b. Rotate tubes at 4°C for 20 minutes.

c. Centrifuge at 1,300rpm for 15 minutes.

d. Save the supernatant and put into a clean microtube.

e. Perform a Bradford's micro-BCA protein quantification assay.

f. Using Standard Curve equation, calculate the protein concentration of each sample and normalize eicosanoids levels to total protein content.

5) In clean glass tubes prepare samples for extraction by adding the same volume of sample (from step 3) and complete with 1 µmol/L EHI/PBS to a final volume of 1mL. For internal quality control purposes (e.g. eicosanoids loss due to sample handling) add 10ul internal standards (2.5ng of ^{13}C-labeled eicosanoid STD mixture).

6) Prepare 6mL/sample of a chloroform/methanol extraction mix (CH$_3$Cl/MeOH; 2:1). Extract with CH$_3$Cl/MeOH by adding 3mL of CH$_3$Cl/MeOH per sample and vortex thoroughly for 10sec. Centrifuge for 10 minutes at 4,000rpm.

7) Using a Pasteur pipette with rubber bulb transfer the organic phase (bottom portion of the tube) into a new tube and label as the initial tube.

8) Repeat CH$_3$Cl/MeOH extraction (step 6). While the samples are being centrifuged, start to dry the first extraction. Upon completion of centrifugation combine the two organic phases and continue to dry. If needed, the procedure can be stopped after completion of this step. Flush the dried tubes with N$_2$ and store samples at -80°C. Drying conditions: place tubes under N$_2$ using Organomation N-EVAP under pressure 10-LPM.

9) Prepare 10mL of 0.4N potassium hydroxide in 80% methanol (KOH/MeOH). To perform the alkaline hydrolysis to cleave the eicosanoids from the glycerol backbone add 0.5mL of 0.4N KOH/MeOH to each tube. Incubate 60 minutes at 50°C (preferably in a water bath shaker gently shaking mode 50-100rpm/min).

10) Add 2mLof water to each tube and 50ul of 3N HCl. Check the pH using pH paper and keep adding 2uL at-a-time of 3N HCl until pH comes down to pH of 5.0. Avoid bringing down pH 3.0. Work carefully but quickly to avoid oxidation.

11) Perform an ether (Et_2O) extraction by adding 3ml of Et_2O to each sample, briefly vortex and centrifuge for 10 minutes at 3,000rpm. Collect upper organic phase and transfer into a new, labeled glass tube. Avoid mixing with the aqueous phase (bottom) as this will delay the drying step.

12) Repeat Et_2O extraction (Step 12). While the samples are being centrifuged, start to dry under N_2 the first Et_2O extraction as described above. Combine the two organic phases and dry completely under N_2.

13) Resuspend in ~200uL ethanol, rinsing the walls carefully, transfer to a small mass spectrometry conical glass vial and dry overnight under vacuum.

14) Resuspend dried samples in 20uL of methanol. Analyze by mass spectrometry as described in **Chapter II** (page 36).

APPENDIX III

*Microarray of *EpETE-treated MDA-MB-231 Cells*

To determine early signaling effects of *EpETE treatment, MDA-MB-231 cells were serum-starved overnight and treated for 1 hour with vehicle or 3 µmol/L *EpETE (catalog no. 50861, lot no. 0400015-17, Cayman Chemical Company, MI). Following treatment, total RNA was collected in RLT buffer and beta-mercaptoethanol, passed through a QiaShredder column, and purified using the RNeasy Mini Kit according to the manufacturer's protocol (Qiagen). The samples were processed by the BioMedical Genomics Center at the University of Minnesota for microarray analysis using an Illumina Human WG-6 Expression Bead Chip HT12v3 format. The table attached summarizes the microarray analysis done by Aaron Becker.

SYMBOL	17,18-EpETE (n = 3)			EtOH (n=3)			DiffScore (rel. to EtOH)	Fold change	DEFINITION
	AVG	STDEV	Detection Pval	AVG	STDEV	Detection Pval			
Sorted by Fold Change, 1.3-fold change cut off.									
HBB	720.06	1019.06	0.0E+00	73.23	16.32	6.5E-02	-7.5E-05	9.8	Homo sapiens hemoglobin, beta (HBB), mRNA.
HBA2	357.08	448.20	0.0E+00	70.07	6.53	1.8E-02	-7.5E-05	5.1	Homo sapiens hemoglobin, alpha 2 (HBA2), mRNA.
S100A8	386.03	452.83	0.0E+00	81.43	27.63	3.6E-02	-7.5E-05	4.7	Homo sapiens S100 calcium binding protein A8 (S100A8), mRNA.
S100A9	269.24	290.59	0.0E+00	70.73	14.65	8.7E-02	-7.5E-05	3.8	Homo sapiens S100 calcium binding protein A9 (calgranulin B) (S100A9), mRNA.
KRT13	194.95	178.06	0.0E+00	76.33	5.34	5.4E-02	-7.5E-05	2.6	Homo sapiens keratin 13 (KRT13), transcript variant 2, mRNA.
LOR	154.22	140.01	2.6E-03	71.05	26.00	8.2E-02	-7.5E-05	2.2	Homo sapiens loricrin (LOR), mRNA.
FOS	318.95	125.66	0.0E+00	149.04	23.57	2.6E-03	-7.5E-05	2.1	Homo sapiens v-fos FBJ murine osteosarcoma viral oncogene homolog (FOS), mRNA.
PI3	176.04	139.46	1.3E-03	83.11	11.69	3.2E-02	-7.5E-05	2.1	Homo sapiens peptidase inhibitor 3, skin-derived (SKALP) (PI3), mRNA.
KRT6A	147.60	138.83	2.6E-03	71.41	2.49	7.9E-02	-7.5E-05	2.1	Homo sapiens keratin 6A (KRT6A), mRNA.
KRTDAP	183.17	141.41	0.0E+00	89.77	20.20	2.1E-02	-7.5E-05	2.0	Homo sapiens keratinocyte differentiation-associated protein (KRTDAP), mRNA.
PDK4	**155.79**	**15.29**	**2.6E-03**	**77.85**	**8.36**	**5.1E-02**	**-3.5E+01**	**2.0**	**Homo sapiens pyruvate dehydrogenase kinase, isozyme 4 (PDK4), mRNA.**
KRT1	117.58	86.94	7.9E-03	58.91	7.70	4.1E-01	-7.5E-05	2.0	Homo sapiens keratin 1 (KRT1), mRNA.

155

	17,18-EpETE (n=3)			EtOH (n=3)			DiffScore (rel. to EtOH)	Fold change	DEFINITION
SYMBOL	AVG	STDEV	Detection Pval	AVG	STDEV	Detection Pval			
Sorted by Fold Ghange, 1.3-fold change cut off.									
S100A7	89.96	54.03	2.2E-02	50.95	1.96	8.8E-01	-7.5E-05	1.8	Homo sapiens S100 calcium binding protein A7 (S100A7), mRNA.
EGR1	532.80	104.21	0.0E+00	301.90	24.75	0.0E+00	-7.3E+00	1.8	Homo sapiens early growth response 1 (EGR1), mRNA.
FOSB	497.06	147.88	0.0E+00	322.80	45.74	0.0E+00	-7.5E-05	1.5	Homo sapiens FBJ murine osteosarcoma viral oncogene homolog B (FOSB), mRNA.
DUSP1	1401.53	54.42	0.0E+00	974.56	19.77	0.0E+00	-2.2E+02	1.4	Homo sapiens dual specificity phosphatase 1 (DUSP1), mRNA.
LOC728910	98.62	34.71	1.6E-02	70.79	3.55	8.3E-02	-7.5E-05	1.4	PREDICTED: Homo sapiens similar to Galectin-7 (Gal-7) (HKL-14) (PI7) (p53-induced protein 1) (LOC728910), mRNA.
SPRR3	93.56	25.33	1.8E-02	68.37	5.84	1.1E-01	-7.5E-05	1.4	Homo sapiens small proline-rich protein 3 (SPRR3), transcript variant 1, mRNA.
ANGPTL4	155.15	6.17	1.1E-04	115.64	11.56	6.4E-04	-6.9E+00	1.3	Homo sapiens angiopoietin-like 4 (ANGPTL4), transcript variant 3, mRNA.
SPRR2A	78.44	21.72	4.1E-02	58.95	2.34	4.0E-01	-7.5E-05	1.3	Homo sapiens small proline-rich protein 2A (SPRR2A), mRNA.
KRT6C	68.99	27.93	1.2E-01	51.94	2.08	8.3E-01	-7.5E-05	1.3	Homo sapiens keratin 6C (KRT6C), mRNA.
CSF2	1296.49	69.49	0.0E+00	978.25	61.58	0.0E+00	-4.2E+01	1.3	Homo sapiens colony stimulating factor 2 (granulocyte-macrophage) (CSF2), mRNA.

	17,18-EpETE (n=3)			EtOH (n=3)			DiffScore (rel. to EtOH)	Fold change	DEFINITION
SYMBOL	AVG	STDEV	Detection Pval	AVG	STDEV	Detection Pval			
Sorted by Fold Ghange, 1.3-fold change cut off.									
	74.52	3.42	6.1E-02	56.53	4.07	5.6E-01	-7.5E-05	1.3	xl15d01.x1 NCI_CGAP_Ut4 Homo sapiens cDNA clone IMAGE:2676289 3, mRNA sequence
	217.98	54.22	0.0E+00	166.78	30.93	2.6E-03	-7.5E-05	1.3	AGENCOURT_10229596 NIH_MGC_141 Homo sapiens cDNA clone IMAGE:6563923 5, mRNA sequence
	143.16	7.03	2.6E-03	109.70	8.21	9.2E-03	-7.5E-05	1.3	Homo sapiens cDNA FLJ34428 fis, clone HLUNG2000761
SBSN	72.19	20.99	7.6E-02	56.11	1.99	5.8E-01	-7.5E-05	1.3	Homo sapiens suprabasin (SBSN), mRNA.
LOC652251	66.78	2.28	1.5E-01	52.15	2.18	8.1E-01	-7.5E-05	1.3	PREDICTED: Homo sapiens similar to G-protein signalling modulator 1 (AGS3-like, C. elegans) (LOC652251), mRNA.
PTMA	2177.14	281.19	0.0E+00	1702.52	325.53	0.0E+00	-7.5E-05	1.3	Homo sapiens prothymosin, alpha (PTMA), transcript variant 1, mRNA.
	243.91	30.69	0.0E+00	191.37	7.55	0.0E+00	-7.5E-05	1.3	MR1-GN0172-061100-005-h03 GN0172 Homo sapiens cDNA, mRNA sequence
	177.63	6.04	1.3E-03	139.50	22.06	2.6E-03	-7.5E-05	1.3	EST366269 MAGE resequences, MAGC Homo sapiens cDNA, mRNA sequence
LGALS7	85.83	26.85	2.4E-02	67.83	7.21	1.2E-01	-7.5E-05	1.3	Homo sapiens lectin, galactoside-binding, soluble, 7 (galectin 7) (LGALS7), mRNA.

	17,18-EpETE (n=3)			EtOH (n=3)			DiffScore (rel. to EtOH)	Fold change	DEFINITION
SYMBOL	AVG	STDEV	Detection Pval	AVG	STDEV	Detection Pval			
Sorted by Fold Ghange, 1.3-fold change cut off.									
HYPK	850.59	51.68	8.9E-04	672.75	65.79	1.4E-03	-3.3E+00	1.3	Homo sapiens Huntingtin interacting protein K (HYPK), mRNA.
LOC653499	80.09	26.74	3.3E-02	63.68	3.97	2.0E-01	-7.5E-05	1.3	Homo sapiens similar to Galectin-7 (Gal-7) (HKL-14) (PI7) (p53-induced protein 1) (LOC653499), mRNA.
Sorted by Differential Score, top negative Diff Score values shown									
DUSP1	1401.53	54.42	0.0E+00	974.56	19.77	0.0E+00	-216.01	1.4	Homo sapiens dual specificity phosphatase 1 (DUSP1), mRNA.
CSF2	1296.49	69.49	0.0E+00	978.25	61.58	0.0E+00	-41.84	1.3	Homo sapiens colony stimulating factor 2 (granulocyte-macrophage) (CSF2), mRNA.
PDK4	**155.79**	**15.29**	**2.6E-03**	**77.85**	**8.36**	**5.1E-02**	**-34.76**	**2.0**	**Homo sapiens pyruvate dehydrogenase kinase, isozyme 4 (PDK4), mRNA.**
LOC441087	6130.12	260.23	0.0E+00	5121.73	194.06	0.0E+00	-33.24	1.2	Homo sapiens hypothetical gene supported by AK125735 (LOC441087), mRNA.
PNN	1298.74	68.82	0.0E+00	1071.32	40.49	0.0E+00	-21.79	1.2	Homo sapiens pinin, desmosome associated protein (PNN), mRNA.
COX6C	9128.53	140.93	0.0E+00	7784.54	333.86	0.0E+00	-21.63	1.2	Homo sapiens cytochrome c oxidase subunit VIc (COX6C), mRNA.
LOC90586	536.14	10.53	1.0E-01	441.06	11.67	2.3E-01	-21.35	1.2	PREDICTED: Homo sapiens AOC3 pseudogene (LOC90586), misc RNA.
JUN	1348.13	54.73	0.0E+00	1145.77	51.05	0.0E+00	-19.30	1.2	Homo sapiens jun oncogene (JUN), mRNA.

	17,18-EpETE (n=3)			EtOH (n=3)			DiffScore (rel. to EtOH)	Fold change	DEFINITION
SYMBOL	AVG	STDEV	Detection Pval	AVG	STDEV	Detection Pval			
Sorted by Differential Score, top negative Diff Score values shown									
MAGT1	830.07	29.03	0.0E+00	709.03	4.47	0.0E+00	-18.85	1.2	Homo sapiens magnesium transporter 1 (MAGT1), mRNA.
KLF4	816.17	16.10	8.7E-05	684.67	22.72	1.7E-04	-17.38	1.2	Homo sapiens Kruppel-like factor 4 (gut) (KLF4), mRNA.
XPNPEP3	3903.57	108.69	2.9E-03	3310.22	46.89	4.1E-03	-16.11	1.2	Homo sapiens X-prolyl aminopeptidase (aminopeptidase P) 3, putative (XPNPEP3), mRNA.
TDP1	397.91	3.24	0.0E+00	354.25	15.06	0.0E+00	-13.95	1.1	Homo sapiens tyrosyl-DNA phosphodiesterase 1 (TDP1), transcript variant 1, mRNA.
LRAP	3686.65	185.20	0.0E+00	3124.62	140.97	0.0E+00	-13.48	1.2	Homo sapiens leukocyte-derived arginine aminopeptidase (LRAP), mRNA.
RABAC1	1189.34	31.41	0.0E+00	1036.40	40.87	0.0E+00	-12.43	1.1	Homo sapiens Rab acceptor 1 (prenylated) (RABAC1), mRNA.
LOC613037	543.02	21.57	0.0E+00	452.94	21.22	0.0E+00	-11.54	1.2	Homo sapiens nuclear pore complex interacting protein pseudogene (LOC613037), non-coding RNA.
LOC440589	24143.93	180.24	0.0E+00	22020.98	431.64	0.0E+00	-10.41	1.1	PREDICTED: Homo sapiens similar to ribosomal protein S2, transcript variant 3 (LOC440589), mRNA.
NLRP8	769.19	26.04	3.2E-01	664.73	26.58	6.2E-02	-10.41	1.2	Homo sapiens NLR family, pyrin domain containing 8 (NLRP8), mRNA.
CHRNA5	443.27	18.28	1.4E-05	372.89	13.63	2.2E-05	-10.30	1.2	Homo sapiens cholinergic receptor, nicotinic, alpha 5 (CHRNA5), mRNA.

	17,18-EpETE (n=3)			EtOH (n=3)			DiffScore (rel. to EtOH)	Fold change	DEFINITION
SYMBOL	AVG	STDEV	Detection Pval	AVG	STDEV	Detection Pval			
Sorted by Differential Score, top negative Diff Score values shown									
YRDC	1318.34	10.45	0.0E+00	1151.10	61.01	0.0E+00	-10.13	1.1	Homo sapiens yrdC domain containing (E. coli) (YRDC), mRNA.
Sorted by Differential Score, top positive Diff Score values shown.									
FAM53C	683.78	11.59	0	824.20	41.39	0.0E+00	20.26	0.8	Homo sapiens family with sequence similarity 53, member C (FAM53C), mRNA.
PARP4	1926.05	46.63	0	2190.55	79.45	0.0E+00	11.99	0.9	Homo sapiens poly (ADP-ribose) polymerase family, member 4 (PARP4), mRNA.
PCNT	701.61	34.46	0	814.22	11.77	0.0E+00	10.34	0.9	Homo sapiens pericentrin (PCNT), mRNA.
FBXO5	574.59	10.09	0	644.96	8.53	0.0E+00	7.82	0.9	Homo sapiens F-box protein 5 (FBXO5), mRNA.
EIF4B	3608.91	163.07	0	4092.36	40.81	0.0E+00	7.66	0.9	Homo sapiens eukaryotic translation initiation factor 4B (EIF4B), mRNA.
MAMLD1	509.82	20.54	0	585.09	19.11	0.0E+00	7.34	0.9	Homo sapiens mastermind-like domain containing 1 (MAMLD1), mRNA.
C6orf130	1342.72	51.08	0	1508.34	34.04	0.0E+00	6.51	0.9	Homo sapiens chromosome 6 open reading frame 130 (C6orf130), mRNA.
MED19	912.81	12.34	0	1028.41	25.01	0.0E+00	6.10	0.9	Homo sapiens mediator complex subunit 19 (MED19), mRNA.
PDCD6	2360.64	68.38	0	2639.34	26.05	0.0E+00	5.91	0.9	Homo sapiens programmed cell death 6 (PDCD6), mRNA.
DCLRE1A	348.27	11.23	0	406.03	17.01	0.0E+00	5.91	0.9	Homo sapiens DNA cross-link repair 1A (PSO2 homolog, S. cerevisiae) (DCLRE1A), mRNA.

	17,18-EpETE (n=3)			EtOH (n=3)			DiffScore (rel. to EtOH)	Fold change	DEFINITION
SYMBOL	AVG	STDEV	Detection Pval	AVG	STDEV	Detection Pval			
Sorted by Differential Score, top positive Diff Score values shown.									
ARID1A	583.48	9.88	0.12533	660.55	3.00	1.7E-01	5.68	0.9	Homo sapiens AT rich interactive domain 1A (SWI-like) (ARID1A), transcript variant 1, mRNA.
ATP2C1	304.42	4.33	3.05E-09	330.81	3.99	3.0E-09	4.96	0.9	Homo sapiens ATPase, Ca++ transporting, type 2C, member 1 (ATP2C1), transcript variant 1, mRNA.
BAG5	396.39	7.79	0.01457	444.45	11.99	1.7E-02	4.71	0.9	Homo sapiens BCL2-associated athanogene 5 (BAG5), transcript variant 2, mRNA.
TOR1B	480.63	2.94	0	544.00	19.73	0.0E+00	3.15	0.9	Homo sapiens torsin family 1, member B (torsin B) (TOR1B), mRNA.
IRX5	324.64	9.69	0	371.92	13.88	0.0E+00	2.60	0.9	Homo sapiens iroquois homeobox 5 (IRX5), mRNA.
TMEM97	969.13	20.16	0	1019.04	17.86	0.0E+00	2.50	1.0	Homo sapiens transmembrane protein 97 (TMEM97), mRNA.
FAM133B	422.53	22.46	0	487.99	13.13	0.0E+00	2.33	0.9	Homo sapiens family with sequence similarity 133, member B (FAM133B), transcript variant 2, mRNA.
ZFYVE26	403.22	12.85	0	458.52	18.76	0.0E+00	2.18	0.9	Homo sapiens zinc finger, FYVE domain containing 26 (ZFYVE26), mRNA.
LPIN1	1044.68	19.91	0	1157.58	42.51	0.0E+00	1.95	0.9	Homo sapiens lipin 1 (LPIN1), mRNA.
EPDR1	1459.37	17.72	0	1611.71	44.76	0.0E+00	1.79	0.9	Homo sapiens ependymin related protein 1 (zebrafish) (EPDR1), mRNA.

	17,18-EpETE (n=3)			EtOH (n=3)			DiffScore (rel. to EtOH)	Fold change	DEFINITION
SYMBOL	AVG	STDEV	Detection Pval	AVG	STDEV	Detection Pval			
Sorted by Differential Score, top positive Diff Score values shown.									
GLTP	4372.39	154.78	0	4839.92	198.87	0.0E+00	1.79	0.9	Homo sapiens glycolipid transfer protein (GLTP), mRNA.
TEX2	464.50	22.94	0	526.79	5.12	0.0E+00	1.43	0.9	Homo sapiens testis expressed 2 (TEX2), mRNA.
USP33	204.51	11.43	8.68E-05	237.66	5.91	2.2E-05	1.39	0.9	Homo sapiens ubiquitin specific peptidase 33 (USP33), transcript variant 1, mRNA.
TOMM22	861.39	27.14	0	953.77	30.76	0.0E+00	1.20	0.9	Homo sapiens translocase of outer mitochondrial membrane 22 homolog (yeast) (TOMM22), nuclear gene encoding mitochondrial protein, mRNA.
SMAP2	421.48	15.57	3.47E-06	467.56	18.17	3.5E-06	1.14	0.9	Homo sapiens small ArfGAP2 (SMAP2), mRNA.
SMS	2606.36	111.68	0	2756.49	176.31	0.0E+00	1.06	0.9	Homo sapiens spermine synthase (SMS), mRNA.